A proteomic investigation into the bacteriostatic mechanism of glycocin F, secreted by *Lactiplantibacillus plantarum* KW30

A thesis presented in partial fulfilment of the requirements for the degree of

Master of Science

in

Biochemistry

at Massey University, Manawatū, New Zealand.

Teiarere Te Horomai Stephens

2021

Abstract

Antimicrobial resistance to clinical antibiotics has increased significantly over the past decade and continues to pose a serious public health concern worldwide. Due to this rise in antimicrobial resistance, clinical health professionals and scientific researchers alike have been eager to explore alternative options in place of traditional treatments (*e.g.* antibiotics). Bacteriocins are antimicrobial polypeptides secreted by bacteria. The therapeutic potential of these diverse natural products is largely unexplored and, as such, they constitute a novel source of potentially viable treatment options in the fight against resistant strains of pathogenic bacteria. At the most basic level, bacteriocins can be divided into two groups, those that are modified and those that are not. Glycocins fall into the former group as they are post-translationally modified by one or more monosaccharide moieties. These monosaccharides can be *O*-linked to the hydroxyl group of serine or threonine residues, or *S*-linked to the sidechain thiol group of cysteine residues. Glycocin F (GccF) is a doubly glycosylated bacteriocin secreted by the lactic acid bacterium *Lactiplantibacillus plantarum* (*Lb. plantarum*) KW30 that inhibits the growth of its bacterial targets. Although it is known that GccF is bacteriostatic, the exact mechanism by which it inhibits cell growth within two minutes, at nanomolar (nM) concentrations, remains unknown. Previous bacterial genomics, nuclear magnetic resonance (NMR) spectroscopy, total chemical synthesis and analysis of synthetic peptides, and transcriptomic studies have provided the framework for this present research. Collectively, these studies led to the proposal that GccF binds to the transmembrane domain of a specific *N*-acetylglucosamine (GlcNAc) phosphotransferase system (PTS) transporter on the surface of targeted bacterial cells, causing the amplification of a signal that results in the rapid onset of bacteriostasis. This project used proteomic methods to investigate changes that occurred in the proteome of susceptible cells when treated with GccF. Cultures were sampled immediately before, and then at specific timepoints after the addition of GccF. Sampled cells were separated into membrane and cytosol fractions, then analysed for changes in their proteomes. Changes in the abundances of specific target cell proteins were linked to biochemical pathways that may be affected by treatment with GccF, providing clues to its mechanism of action. The results showed clear changes in the abundance of proteins involved in cell wall metabolism and protein translation in GccF-treated *Lb. plantarum* ATCC 8014 cells.

He mihi

Waikato Taniwharau - He piko, he taniwha
Ko Maungatautari te maunga
Ko Waikato te awa
Ko Raukawa te iwi
Ko Werohoko, Waenganui, Ngāti Roro
Ngāti Haua, Ngāti Mahanga ngā hapū
Ko Te Taumata (ki Pārāwera) te marae
Ko Tāne I Rangi Kapua te whare
Ko Te Ure Pārāwera tenei
Ko Tainui te waka

Ko Tarawera te maunga
Ko Puarenga te awa
Ko Te Arawa te iwi
Ko Tuhourangi - Ngāti Wahiao tōku hapū
Ko Te Pakira te marae
Ko Te Arawa te waka

Te Arawa Māngai nui
Ko Matawhaura te maunga
Ko Te Rotoiti-i-kite-ai-a-Ihenga te moana
Ko Ngāti Pikiao te iwi
Ko Ngāti Hinekura te hapū
Ko Pounamunui te marae
Ko Houmaitawhiti te whare
Ko Te Arawa te waka

Taranaki Maunga – Taranaki Tangata
Ko Taranaki te maunga
Ko Hangātahua me Matanehunehu ngā awa
Ko Taranaki tūturu te iwi
Ko Ngā Māhanga-a-Tairi te hapū
Ko Tarawainuku (ki Puniho) te marae
Ko Pauna te Tupuna te whare
Ko Kurahaupo te waka

Acknowledgments

Associate Professor Gillian Norris and Dr Mark Patchett

For your guidance, support, patience and for believing in me throughout this entire journey.

Mr Trevor Loo

For your unmatched technical expertise, knowledge and skills, as well as your advice and difference of opinion.

To my friends in the X-Lab

For being a necessary distraction, a source of discussion, a helping hand and allowing me to bounce ideas off you.

The School of Fundamental Sciences

For providing the facilities, equipment and funding for my research.

To my Īwi and Hapū

For providing me with financial support throughout my years of study

To my Whānau and friends

For your unwavering love and support through all my life's endeavours. This is for you.

Contents

List of Abbreviations

1D	One-dimensional
2D	Two-dimensional
3D	Three-dimensional
ABC	Adenosine triphosphate-binding cassette
ADP	Adenosine diphosphate
Ala	Alanine
AMBIC	Ammonium bicarbonate
AMR	Antimicrobial resistance
APS	Ammonium persulfate
ATCC	American Type Culture Collection
ATP	Adenosine triphosphate
BCA	Bicinchoninic acid
BSA	Bovine serum albumin
$CaCl_2$	Calcium chloride
CCR	Carbon catabolite repression
CDS	Coding sequence
CHAPS	3-[(3-Cholamidopropyl)dimethylammonio]-1-propanesulfonate
cm	Centimetre
CO_2	Carbon dioxide
Cys	Cysteine
Da	Dalton
DAP	Diaminopimelate
DF	Dilution factor
DNA	Deoxyribonucleic acid
DNase I	Deoxyribonuclease I
DTT	Dithiothreitol
DUF	Domain of unknown function
ECF	Extracytoplasmic function
EDTA	Ethylenediaminetetraacetic acid
EtOH	Ethanol
FA	Formic acid

FDR	False discovery rate
g	Gram
G+ve	Gram-positive
GccF	Glycocin F
GFP	Green fluorescent protein
GI	Gastrointestinal
GlcNAc	*N*-acetylglucosamine
GlpF	Glycerol uptake facilitator protein
GO	Gene ontology
GRAS	Generally regarded as safe
HCD	Higher-energy collision-induced dissociation
HCl	Hydrochloric acid
HCOONa	Sodium formate
His	Histidine
HK	Histidine kinase
HPLC	High-pressure liquid chromatography
HTPA	Hydroxytetrahydrodipicolinate
IC_{50}	Bacteriocin concentration that results in 50 % growth inhibition of target cells
KEGG	Kyoto Encyclopedia of Genes and Genomes
kDa	Kilodalton
L	Litre
LAB	Lactic acid bacteria
LCMS	Liquid chromatography mass spectrometry
LTA	Lipoteichoic acid
Ltd.	Limited
M	Molar
ManNAc	*N*-acetylmannosamine
MeCN	Acetonitrile
MeOH	Methanol
MFS	Major facilitator superfamily
mg	Milligram
$MgCl_2$	Magnesium chloride
MIC	Minimum inhibitory concentration
mL	Millilitre
mM	Millimolar
MOPS	3-Morpholinopropapne-1-sulfonic acid

mRNA	Messenger RNA
MRS	De Man, Rogosa and Sharpe medium
MS	Mass spectrometry
Msc	Mechanosensitive channel
MurNAc	*N*-acetylmuramic acid
MW	Molecular weight
μg	Microgram
μL	Microlitre
μM	Micromolar
N (*liq*.)	Liquid nitrogen
NaCl	Sodium chloride
NAD(P)H	Nicotinamide adenine dinucleotide phosphate
NaOH	Sodium hydroxide
NCBI	National Center for Biotechnology Information
nM	Nanomolar
NMR	Nuclear magnetic resonance
NO	Nitric oxide
O_2	Oxygen
OD_{600}	Optical density at 600 nm
PASTA	Penicillin-binding and serine/threonine kinase-associated
PBP	Penicillin-binding protein
PD	Proteome Discoverer
PDB	Protein data bank
PEP	Phosphoenolpyruvate
PIN	PilT N-terminus
pN	Pico-Newton
ppm	Parts per million
Psi	Phosphate starvation-inducible
PSM	Peptide spectrum matches
PTM	Post-translational modification
PTS	Phosphoenolpyruvate phosphotransferase system
RiPPs	Ribosomally synthesised and post-translationally modified peptides
RNA	Ribonucleic acid
RNase	RNA specific endoribonuclease
RR	Response regulator
rRNA	Ribosomal RNA

SDS	Sodium dodecyl sulfate
SDS-PAGE	SDS-polyacrylamide gel electrophoresis
Sec	Secretory
Ser	Serine
SP	Sulfopropyl
sRNA	Small RNA
SRP	Signal recognition particle
TA	Teichoic acid
Tag	Teichoic acid glycerol
TBS	Tris-buffered saline
TCA	Trichloroacetic acid
TCEP	Tris(2-carboxyethyl)phosphine
TEMED	N,N,N′,N′-Tetramethylethane-1,2-diamine
TFA	Trifluoroacetic acid
THDPA	Tetrahydrodipicolinate
Thr	Threonine
TIC	Total ion count
TRAM	TRM2 and MiaB
Tris-HCl	Tris hydrochloride
tRNA	Transfer RNA
UDP	Uridine diphosphate
UK	The United Kingdom
UndP	Undecaprenyl phosphate
USA	The United States of America
UV	Ultraviolet
V	Volts
v/v	Volume/volume
w/v	Weight/volume
WT	Wild-type
WTA	Wall teichoic acid
× *g*	Multiple of earth's gravitational force
°C	Degrees Celsius

List of Consumables

Acetone	Fisher Chemical
Acetic acid	Merck (Sigma-Aldrich)
Acetonitrile	Thermo Fisher
Acrylamide	Merck (Sigma-Aldrich)
Agar	BioRad
AMBIC	Fisher Scientific
APS	Sigma Aldrich
BCA protein assay kit	Thermo Fisher
Bead tubes	Sigma Aldrich
BSA	Supplied in BCA kit from Thermo Scientific
$CaCl_2$	Ajax Chemicals (Univar)
CHAPS	GE Healthcare
Chymotrypsin	Roche Diagnostics
cOMplete™ ULTRA tablets	Roche Diagnostics
Coomassie G-250	Fluka Analytical
Cuvettes (disposable)	BioRad
DNAse I	Thermo Scientific
DTT	Apollo Scientific Ltd.
EtOH	Milton Adams Ltd.
Formic Acid	Fisher BioReagents
GccF	Purified from *Lb. plantarum* KW30
Glacial acetic acid	Thermo Fisher Scientific
Glycerol	Ajax Finechem (Thermo Fisher Scientific)
HCl	Merck or Fisher Scientific
HPLC vials and inserts	Thermo Fisher Scientific
Iodoacetamide	GE Healthcare
LoBind tubes	Eppendorf
MeOH	Fisher Chemical
$MgCl_2$	BDH Ltd.
Microcentrifuge tubes	Eppendorf
MOPS	Fisher Bioreagents (Thermo Fisher Scientific)

MRS (medium/broth)	Acumedia
MS-grade water	Fisher Chemical
HCOONa	Fluka Analytical
NaOH	Fisher Scientific
Precision Plus Standard	Bio-Rad
Protease inhibitor	Roche Diagnostics
RNAse	Sigma Aldrich
SDS	Affymetrix (Thermo Fisher Scientific)
SOLu-Trypsin	Sigma Aldrich
SP-Sephadex resin	Sigma Aldrich
TCA	Prolabo
TCEP	Gold Biotechnology
TEMED	Sigma Aldrich
TFA	Apollo Scientific Ltd.
Tris-HCl	Pure Science
Trypsin	Sigma Aldrich
Urea	GE Healthcare

List of Equipment

Centrifugation/mixing

Bead mill	Fast Prep Ribolyser™	Hybaid, USA
Benchtop centrifuge(s)	Fresco 17 and Pico 17 models	Thermo Fisher Scientific
Floor model centrifuge	Sorvall™ RC-6 Plus	Thermo Fisher Scientific
Sonicator	Elmasonic S 15 H	Elma, Germany
Vacuum concentrator	SPD111V Digital SpeedVac™ System	Thermo Fisher Scientific
Ultracentrifuge	Sorvall™ MTX 50 Micro-Ultra.	Thermo Fisher Scientific

Chromatography

Analytical column	AcclaimPepMap™ C_{18} 2 μm particle 75 μm inner diameter, 50 cm length	Thermo Fisher Scientific, USA
Glass column	5 x 20 cm Econo-Column	BioRad, USA
Mass spectrometer	Q-Exactive™ Plus	Thermo Fisher Scientific, Germany
MS HPLC system	UltiMate 3000 RSLCnano system	Thermo Fisher Scientific
Purification HPLC system	UltiMate 3000 Analytical HPLC system	Thermo Fisher Scientific
Trapping column	AcclaimPepMap™ C_{18} 3 μm particle 75 μm inner diameter, 2 cm length	Thermo Fisher Scientific, USA

Gel electrophoresis

Gel casting frame	Mini-PROTEAN III casting frame	BioRad, USA
Gel electrophoresis unit	Mini-PROTEAN III cell	BioRad, USA
Gel power pack unit	PowerPac™ basic power supply	BioRad, USA

Spectrophotometers

Cary-UV spectrophotometer	Cary 300 Bio Spectrophotometer	Agilent, USA
$OD_{600\ nm}$ spectrophotometer	SmartSpec Plus Spectrophotometer	BioRad, USA

Miscellaneous

Milli-Q water dispenser	Barnstead™ Nanopure™ system	Thermo Fisher Scientific, USA

List of Software & Servers

Chromatography software	Chromeleon	Thermo Fisher Scientific, USA
KEGG database	KEGG	Kanehisa Laboratories
Microsoft Excel	Excel	Microsoft Office, USA
MS system control	Xcalibur	Thermo Fisher Scientific, USA
Proteome Discoverer software	Versions 2.4 and 2.5	Thermo Fisher Scientific, USA
TOPCONS	Version 2	Elofsson Lab
BLAST2GO	Version 6.0.1	Biobam.com, Spain
STRING	Version 11.5	Elixir core data resource, UK

List of Figures

List of Tables

1 Introduction

1.1 Antimicrobial compounds

The survival of a bacterium hinges on its capacity to defend itself from other microbes. To do so, microorganisms produce an array of antimicrobial compounds. While these defence systems are innate in nature, they can be harmful, and even fatal, to higher organisms, such as humans, if the bacteria that survive are pathogenic. The revolutionary discovery of the first antibiotic by Sir Alexander Fleming in the late 1920s paved the way for the discovery and synthesis of today's extensive list of antimicrobial compounds. What could not have been predicted was the capacity of microorganisms to overcome and adapt to the use of antimicrobial agents by humans. It is widely accepted among scientific communities and in the clinical arena that the exposure of both targeted and non-targeted microorganisms to antibiotics, from both prescription and their extensive use in agriculture, has resulted in the development of antibiotic resistance in microbes. Although scientists and health professionals constantly urge consumers to use these substances correctly, this advice is often met by non-compliance as a result of ignorance. Consequentially, there has been a significant increase in antimicrobial resistance, especially in pathogens that present a growing risk to human health (*e.g.* methicillin-resistant *Staphylococcus aureus* [134], vancomycin-resistant Enterococci [56], multidrug-resistant *Neisseria gonorrhoeae* [135]).

1.2 Antimicrobial resistance

Antimicrobial resistance (AMR) is a broad term that is defined by the resistance of microorganisms to specific antibacterial, antifungal, antiviral and antiparasitic compounds [344]. Such microbes can spread through the environment (including the food chain), between people and animals, and from person to person [5]. Their ability to spread depends on the presence of host resistance factors, and the ability to transfer resistance genes between bacteria. Serendipitous genetic mutations that provide resistance can also occur and are preserved through bacterial species as they provide an advantage to the bacterial population. Since the 1960s, the relationship between AMR bacteria and the production of new antimicrobials has become unbalanced, with an increase in the former and a decrease in the

latter. These trends have driven the need for urgent development of new antimicrobials from other sources. In recent years, antimicrobials from bacterial species such as lactic acid bacteria (LAB) have become a focus for AMR research as they present a largely unexplored avenue for a potentially viable source of antimicrobial substances that are generally safe for human consumption. One of these groups comprises the antimicrobial peptides known as bacteriocins.

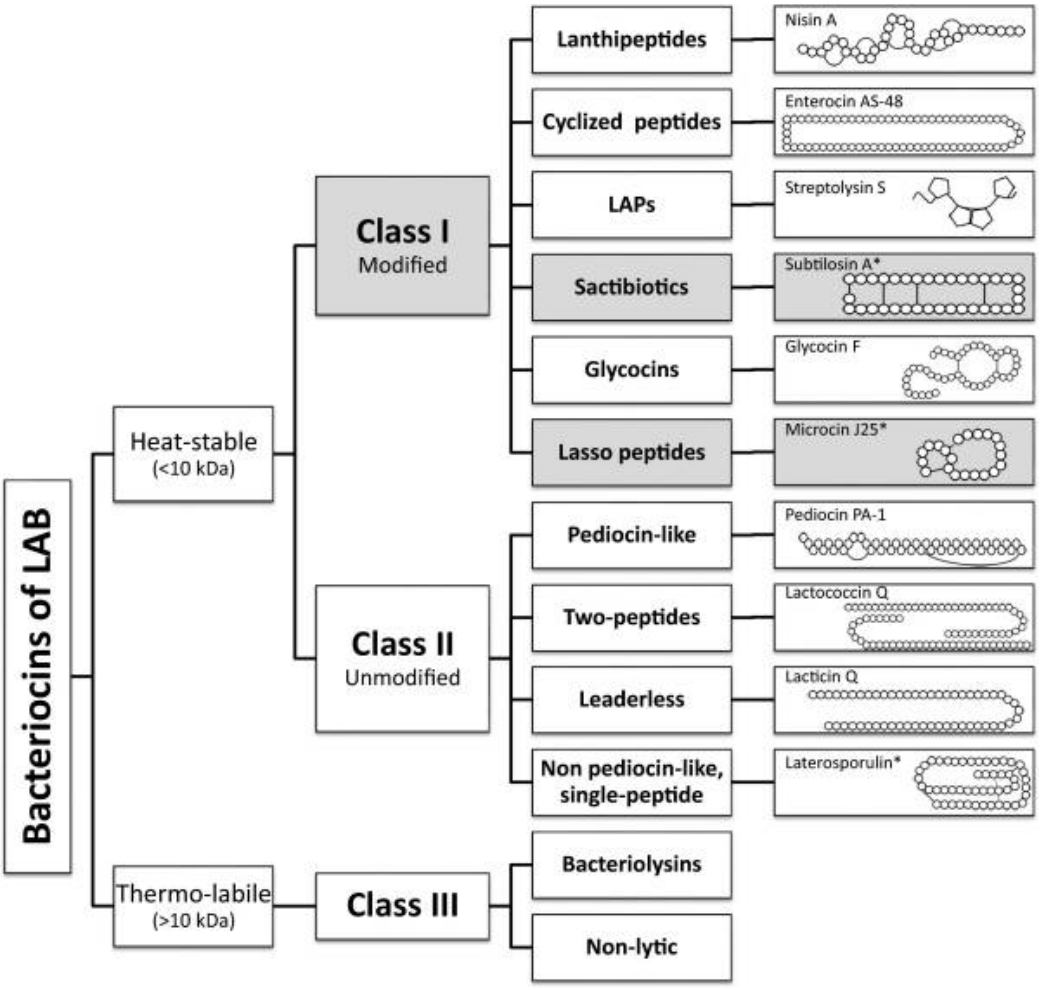

Figure 1: Current classification of bacteriocins from LAB. The current classification scheme for bacteriocins of LAB based on heat stability, modification status and size. Grey boxes indicate classes of bacteriocins identified *in silico*. Non-LAB bacteriocins are specified with an asterisks (*) and included as examples (Figure reproduced from Alvarez-Sieiro, *et al*., 2016 [6], © 2016, with permission from Elsevier).

1.3 Bacteriocins

Bacteriocins are a distinct group of ribosomally synthesised antimicrobial peptides secreted by all bacteria. These peptide toxins target specific bacteria and are used as a defence mechanism by the host organism to protect their ecological niche [258][126]. Both closely and distantly related bacteria can be targeted by the bacteriocin-producing strain in one of two ways, either by a bactericidal (cell killing) or bacteriostatic (cell-growth inhibiting) mode of action. Differences between various bacteriocins, such as their respective modes of action, are governed by their structure which includes any post-translational modifications. These elements have allowed bacteriocins to be grouped into classes, such as those suggested by Alvarez-Sieiro *et al*., 2016 [6] (Fig. 1). Ribosomally synthesised and post-translationally modified peptides (RiPPs) are a category of class I bacteriocins [15]. The most well-known of these is nisin, discovered in 1929, but characterised in Palmerston North, New Zealand at the New Zealand Dairy Research Institute in 1933 [334]. It is widely used as a preservative in the food industry along with bacteriocins of other LAB [61][121] due to being 'generally regarded as safe' (GRAS) [194][313]. LAB commonly occur in the gastrointestinal (GI) tract of humans [24] where they are thought to help maintain normal gut function by inhibiting the growth of pathogens in the gut [318], and through their immunogenic properties [57]. LAB are also frequently utilised by the dairy industry for fermenting milk to make cheese, yoghurt and other products [71]. During such fermentations, LAB convert the carbon source in milk into lactic acid, thus lowering the pH which helps to prevent the growth of other, more harmful, species of bacteria [163]. With such extensive research into LAB since their discovery in 1857 [312], it is not surprising that LAB are now being mined for bacteriocins that, although known about, have, until recently, been largely unexplored as alternatives to antibiotics [244][115].

1.3.1 Glycocins

Glycosylated-bacteriocins, or glycocins, are a sub-class of RiPPs defined by the post-translational addition of one or more monosaccharide groups to the hydroxyl sidechain of a serine (Ser) or a threonine (Thr), or the thiol sidechain of a cysteine (Cys) residue [291][15]. They are secreted by a small number of gram-positive bacteria, namely *Lactiplantibacillus plantarum* (*Lb. plantarum*), *Enterococcus* and *Bacillus* or *Aeribacillus* species; although the number of species that are predicted to secrete them is growing [286].

Currently, there are eleven experimentally verified glycocins; sublancin 168 [240][238], glycocin F (GccF) [291][323][89], ASM1 [132][204], thurandacin [328], pallidocin [167], enterocin 96 [155], enterocin F4-9 [205], listeriocytocin, bacillicin BAG20, bacillicin CER074, and geocillicin [255]. Of these, GccF, ASM1, and enterocin 96 are bacteriostatic [291][204][155], and sublancin 168, enterocin F4-9, thurandacin, and pallidocin are bactericidal [205][328][167]. So far, only three (GccF, ASM1 and enterocin F4-9) have been shown to be unequivocally glycoactive (*i.e.* at least one of the monosaccharides is essential for activity) [235], although it is possible that sublancin may also be glycoactive [29]. ASM1, sublancin 168 and thurandacin, are the only members of this group that have been shown to contain glycosylated cysteine residues [132][240][238], and prior to their discovery, β-S-linked glycosylation had not been known to exist naturally in proteins [235]. More recently it has been shown that cysteine residues modified by a *N*-acetylglucosamine (GlcNAc) is a common post-translational modification in mammalian cells, where it is most likely involved in signalling, similar to phosphorylation [347].

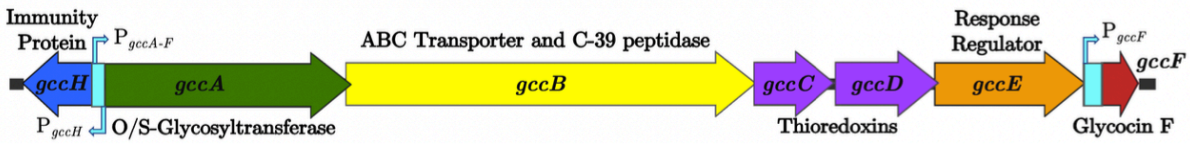

Figure 2: The *gcc* gene cluster. Arrangement of the *gcc* gene cluster with promoter regions in cyan. *gccH* encodes the cytosolic immunity protein. *gccA* encodes a glycosyltransferase. *gccB* encodes an adenosine triphosphate (ATP)-binding cassette (ABC) transporter with a C39 peptidase domain. *gccC* and *gccD* are both predicted to encode thioredoxin-domain proteins. *gccE* encodes a LytTR-family response regulator (RR). *gccF* encodes the pre-bacteriocin GccF (Figure reproduced from Drummond, B. J., 2020 [88], © 2020, with permission from the author).

1.3.2 Identification of glycocins

The most common method that has been used to identify glycocins secreted by bacteria is genome mining. As research aimed at identifying bacteriocins such as glycocins is becoming more widespread, this method is among the most efficient for fast identification of new gene clusters involved in glycocin production, as shown by Ren and colleagues (2018) [255]. This is largely due to the similarities seen between the gene clusters encoding these antimicrobial compounds (Fig. 2) and the recent advances in genome sequencing technologies. All bacteriocin clusters contain genes

encoding dedicated adenonsine triphosphate (ATP)-binding cassette (ABC) transporter proteins and most contain a gene encoding an immunity protein (such as *gccH* in the *gcc* gene cluster; Fig. 2). Those that are modified are present in a cluster containing genes that encode proteins responsible for the modifications (*e.g.* the glycocin clusters that include a glycosyltransferase).

1.3.3 Biochemical and structural characterisation of glycocins

Only two glycocins, GccF and sublancin 168, have had their three-dimensional (3D) structures determined, both using nuclear magnetic resonance (NMR) [323][113]. For GccF, the relationship between structure and function has been further explored using both enzymatic dissection, chemical synthesis and, more recently, site directed mutagenesis to probe the role of specific residues and the two GlcNAc sugars in its activity [291][40][9][28][89]. Similar studies focusing on the type of saccharide modifying the glycocin, the role of the disulfide bonds and the position of the glycosylated residue have been carried out on sublancin 168, and studies to determine whether the sugar is a di- or monosaccharide have been carried out on enterocin 96 and thurandacin [328]. These collective efforts have formed the basis of the understanding of the role of glycocin structure to both activity and maturation, allowing them to be categorised into different types based on their mode of action [235] [286].

1.3.3.1 Glycocin F

Glycocin F, or GccF, is a 43 amino acid polypeptide secreted by the gram-positive, LAB *Lb. plantarum* KW30. It is modified by two GlcNAc moieties, one linked to Ser18 (*β-O*-linked) and one linked to Cys43 (*β-S*-linked), and two nested disulfide bonds; all of which are essential for full activity [291][28]. The solution structure [323] resulted in a model characterised by two, two-turn antiparallel α-helices, joined by an eight-residue loop that is constrained by two nested disulfide bonds ($(C\text{-}X_6\text{-}C)_2$ architecture), and a flexible C-terminal 'tail' (Fig. 3). The *β-O*-linked 'loop' sugar is essential for GccF activity, while the *β-S*-linked tail sugar enhances it significantly [28][291].

The GccF pre-peptide is encoded by *gccF*, one of seven genes in the *gcc* cluster which are all essential for normal GccF synthesis, maturation, export and immunity (Fig. 2). Apart from the structural gene (*gccF*), the cluster includes genes encoding a glycosyltransferase (GccA), an ABC transporter and its associated N-terminal C39-peptidase domain (GccB), two thioredoxin-

like proteins (GccC and GccD), an immunity protein (GccH), and a protein (GccE) with a C-terminal LytTR deoxyribonucleic acid (DNA)-binding domain (PF04397; typically found in two-component RRs), and an N-terminal domain that is not homologous to any known protein except AsmE [4][204][89].

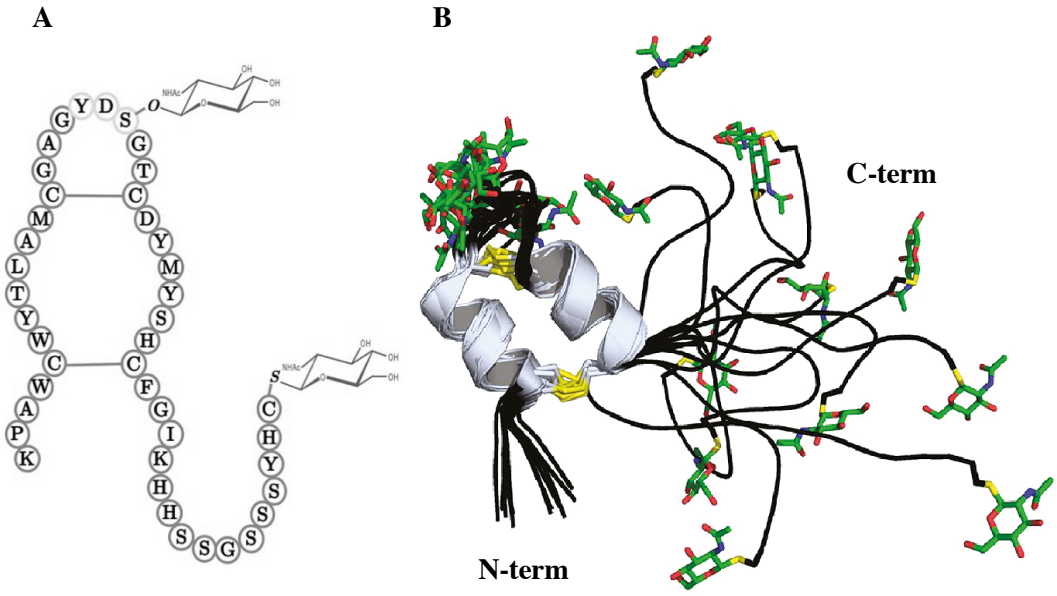

Figure 3: Structural representations of GccF. (A) A schematic diagram of GccF showing the single letter identifier of each amino acid, the two nested disulfide bonds, and the *O*- and *S*-linked GlcNAc moieties (Figure reproduced from Drummond *et. al.,* 2021 [89], © 2021, with permission from the American Society for Microbiology). **(B)** Structural representation of GccF resolved by NMR spectroscopy (Figure reproduced from Venugopal, *et al.,* 2011 [323], © 2011, with permission from the American Chemical Society).

A remarkable feature of GccF is its ability to act fast (affecting growth rates within two minutes), and at extremely low concentrations (2-10 pM) on the most susceptible bacterial strains. The IC_{50} value (the concentration of a given bacteriocin that results in 50 % growth inhibition of the target bacteria) of GccF against *Lb. plantarum* ATCC 8014 cells was reported to be approximately 1.1-2 nM [28]. The minimum inhibitory concentration (MIC), which is more frequently reported for bacteriocins, is the concentration required to elicit complete growth inhibition overnight. The MIC of GccF is reportedly 20 nM against *Lb. plantarum* ATCC 8014 [27], and 50 nM against *Lb. plantarum* NC8 [87]. For comparison, the MIC of the novel bacteriocin produced by *Lb. coryniformis* MXJ 32 (lactocin MXJ 32) is 2.8 mM against both *Staphylococcus aureus* (*S. aureus*) and *Escherichia coli* (*E. coli*) [199], whilst the two-peptide lantibiotic lacticin 3137 displays potent antimicrobial activity against *Listeria*

monocytogenes (*L. monocytogenes*) at nM concentrations [208]. Unusually, growth-inhibition of *Lb. plantarum* by GccF can be reversed by the addition of relatively high concentrations of GlcNAc [291]. Some *Enterococcus faecalis* (*E. faecalis*) strains (*e.g.* JH2-2) are also susceptible to GccF, and when these strains are treated simultaneously with GccF and GlcNAc the protective effect of GlcNAc lasts only as long as there is free GlcNAc in the growth medium, after which, growth is inhibited by GccF. A second addition of GlcNAc again restores normal growth rates, but when this GlcNAc is exhausted the ensuing growth inhibition is much stronger, leading to rapid and complete bacteriostasis [27].

Although recent work has shown how the post-translational modifications and the primary structure of GccF contribute to its activity [9][28][89], the exact mechanism it uses to inhibit the growth of target cells remains a mystery. The fact that the effects can be seen within two minutes suggests that GccF is unlikely to be affecting transcription or translation, although this may be a secondary effect. What has been shown is that GccF localises at the membrane of susceptible cells *via* association with the GlcNAc-specific phosphoenolpyruvate (PEP) phosphotransferase system (PTS) transporter, 'PTS18CBA' [87][20]. The events that succeed this initial interaction, however, remain elusive, despite other PTS systems being a known target of other bacteriocins to kill susceptible bacterial cells [69][54]. As GccF is bacteriostatic rather than bactericidal, it clearly uses a different mechanism, that could very well be novel, to effect growth-inhibition in its target cells.

1.4 Mechanisms of action

The mechanism(s) used by different antimicrobial compounds to act upon susceptible bacterial targets varies considerably. Antibiotics and bacteriocins share a list of five common targets in susceptible bacterial cells. These include, peptidoglycan/cell wall synthesis, DNA replication and transcription, protein synthesis (translation), the physical bacterial cell membrane, and septum formation (Fig. 4) [54]. Nisin is one of the most well-known and extensively studied bacteriocins to date. It has been shown to act in two ways, i.) by binding to lipid II (a precursor necessary for peptidoglycan synthesis), and ii.) by aggregating as pore-forming units in the cell membrane, ultimately resulting in cell death [336]. It is possible that the current low level of resistance to nisin is a likely result of its ability to affect susceptible cells *via* these two distinct events (*i.e.* as opposed to a singular mechanism of action) [263]. In comparison, the broad-spectrum glycopeptide antibiotic vancomycin similarly targets lipid II by binding the precursor D-alanine-D-alanine (D-ala-D-ala), thus inhibiting peptidoglycan synthesis and eventually causing cell death [39]. Vancomycin was most notably used as an effective treatment

against bacterial infection where penicillins and cephalosporins could not be used [118]; including those caused by methicillin-resistant *S. aureus* [193]. However, due to its broad-spectrum specificity, as well as its overuse and misuse, pathogenic bacteria have now developed resistance to vancomycin (*e.g.* vancomycin-resistant *S. aureus*, vancomycin-resistant enterococci).

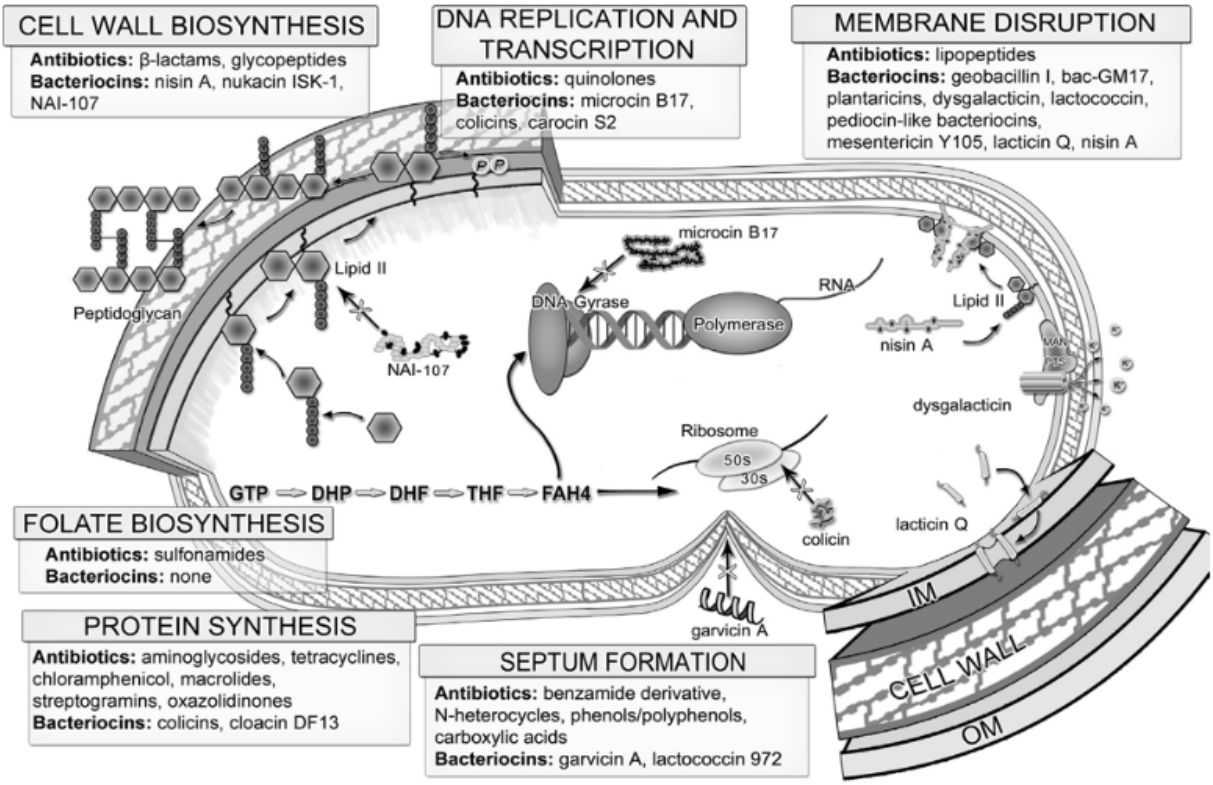

Figure 4: Common mechanisms used by bacteriocins and antibiotics in bacteria. An overview of the mechanisms used by bacteriocins and antibiotics upon the five common targets in bacterial cells (Figure reproduced from Cavera, *et. al.*, 2015 [54], © 2015, with permission from Elsevier B. V. and the International Society of Chemotherapy).

Nisin on the other hand, with its relatively long-standing use in both the industrial and clinical arenas, has displayed comparatively less resistance in susceptible bacteria [263], despite also targeting a broad-spectrum of bacterial species and strains [64]. This comparison highlights the importance of understanding the different mechanisms of action antimicrobials use to prevent the growth of susceptible bacterial cells in order to inform their use as a safe and effective treatment option.

It is worthwhile to note that some bacteriocins have been shown to exhibit mechanisms of action that differ to those of antibiotics, adding further complexity to the characterisation of these antimicrobial peptides. The mechanism of action of the glycocins GccF and ASM1 has proven difficult to characterise [291][323][40][235][20][9][28]. Current research suggests that the mechanism used by

both GccF and ASM1 to rapidly shut down cell growth is likely to be novel, and that due to their sequence and structural similarities, their mechanisms are likely to parallel one another [203]. The following expands on some of the broad definitions of mechanisms known to be used by bacteriocins.

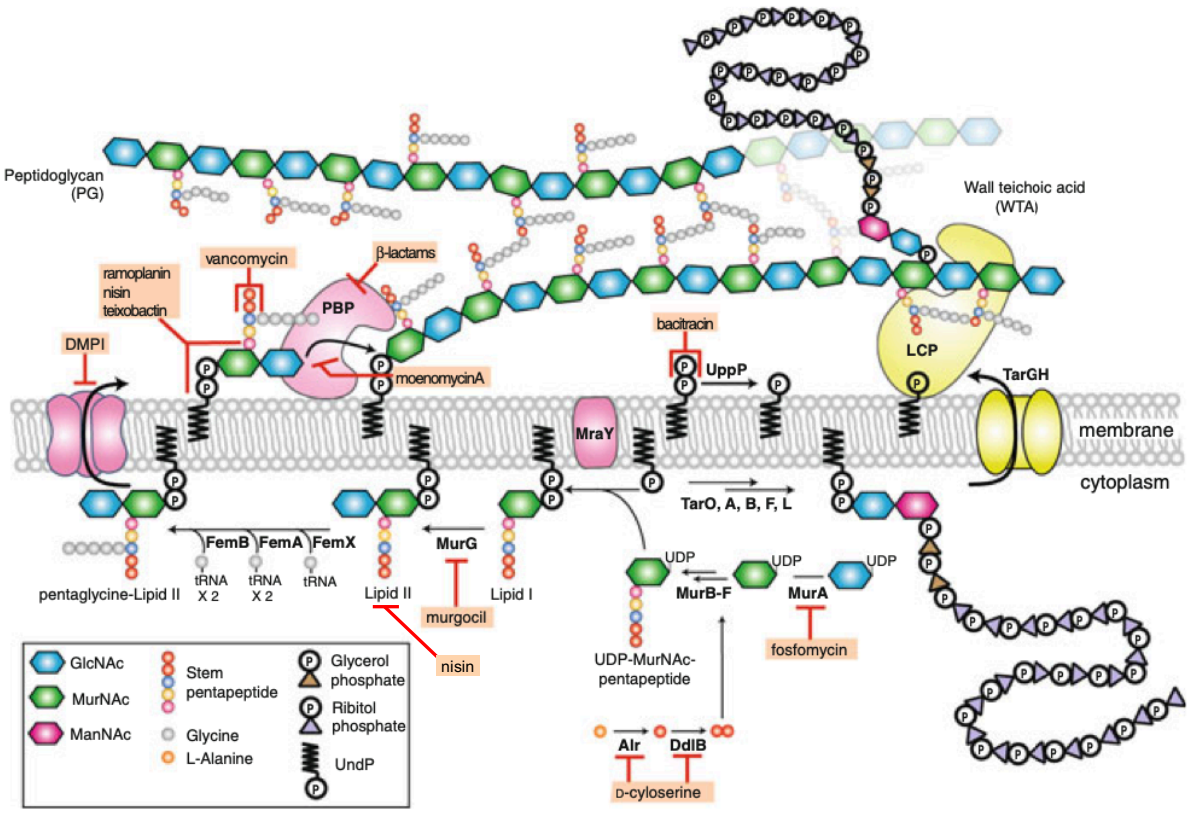

Figure 5: Overview of peptidoglycan synthesis in gram-positive bacteria and antibiotics that target this process. A schematic representation of the major events that occur during cell wall synthesis in gram-positive bacteria including examples of antibiotics known to target enzymes or precursors of this pathway. Peptidoglycan precursor molecules: GlcNAc, *N*-acetylglucosamine; MurNAc, *N*-acetylmuramic acid; ManNAc, *N*-acetylmannosamine; UndP, undecaprenyl phosphate. Major peptidoglycan enzymes common to most gram-positive bacteria: MurA-MurG, synthesise the pentapeptide chains; MraY, attaches pentapeptide chains to the membrane bound lipid I; PBP, penicillin-binding protein, serves to cross-link glycan strands. Other peptidoglycan enzymes: Alr, a racemase that converts L-alanine to D-alanine; DdlB, a ligase that forms the dipeptide D-ala-D-ala; FemX, FemA, and FemB, catalyse the step-wise addition of glycine molecules to the pentapeptide chain. TarO, TarA, TarB, TarF, TarL, and TarGH are involved in wall teichoic acid (WTA) synthesis and export to the outer face of the cell membrane where WTA are incorporated into peptidoglycan by LytR-CpsA-Psr (LCP) enzymes (Figure reproduced from Rajagopal & Walker, 2015 [252], © 2015, with permission from Springer International Publishing Switzerland and Springer Nature).

1.4.1 Inhibition of peptidoglycan synthesis

Most gram-positive and gram-negative bacterial species possess a peptidoglycan layer [17]. Its synthesis is one of the most specific and well-understood processes that occurs in bacteria [147]. The peptidoglycan layer is known to be responsible for the bacterial cell shape [343], cell rigidity, and bacterial tolerance to, and survival in, the variety of environments bacteria frequent [147]. These features not only emphasise the importance of the peptidoglycan layer to bacterial survival in their respective niches, but also explains why inhibition of cell wall metabolism can prove lethal.

Figure 5 shows an overview of peptidoglycan synthesis, including examples of antibiotics that target specific precursors or enzymes of this pathway [252]. Bacteriocins that are known to target specific steps in peptidoglycan synthesis include, nukacin ISK-1 [153], lacticin 3147 [335], and NAI-107 [229], and the previously mentioned nisin. In contrast to bacteriocins and antibiotics that target lipid II, which is an essential intermediate in peptidoglycan synthesis, β-lactam antibiotics such as penicillins and cephalosporins specifically target PBP transpeptidases (Fig. 5), which catalyse the last step in peptidoglycan synthesis [223]. Because peptidoglycan is present in virtually all bacterial species, it is no surprise that its synthesis is a major target for many bacteriocins and antibiotics. It is therefore essential to remain wary of bacteriocin resistance mechanisms that may develop as a result of these compounds using similar mechanisms of action to those used by commonly prescribed antibiotics. This is one reason why bacteriocins which appear to exhibit novel mechanisms of action are attractive options for the treatment of infection and disease caused by pathogenic bacteria.

1.4.2 Inhibition of septum formation

Septum formation is a fundamental aspect of bacterial cell division [295]. In most bacterial species, the formation of the septum is facilitated by the FtsZ protein, which polymerises into the cytokinetic ring structure known as the 'Z-ring' at the midcell, and is then used as a scaffold by proteins involved in cell division [103]. Of the five common mechanisms of action used by bacteriocins and/or antibiotics, inhibition of septum formation is specific to bacteriocins [54]. When it was first discovered, its target had yet to be identified but was later found to be the FtsZ protein [148][256]. Since then, two bacteriocins, garvicin A [206] and lactococcin 972 [209], have been shown to utilise this mechanism of action. Because of the association between septum formation and cell division/remodelling, inhibition of the former can result in excessive cell elongation [206] and deformed cell morphology [209], and ultimately results in cell death. Moreover, inhibition of septum

formation has also been shown to increase the susceptibility of target cells to antimicrobials that act on other proteins involved in cell division/remodelling (*e.g.* penicillin-binding proteins; PBPs), due to their specific association with the Z-ring structure which is absent when FtsZ is inhibited [103]. The latter finding shows how bacteriocins with a novel mechanism of action can be used to overcome resistance to previously effective antimicrobial treatments (*e.g.* methicillin-resistant *S. aureus*), and highlights just one of the reasons why bacteriocins are a viable option as alternatives to traditional antibiotics.

1.4.3 Cell membrane-associated mechanisms

Initial interaction with the target bacterial membrane is essential to the mechanism of action of all antimicrobials as it is the first point of contact [63]. The characteristic structural and physiological features of the bacterial cell envelope are precisely what make it an excellent target for antimicrobials (*i.e.* surface proteins, transporters, lipids, phospholipids, lipopolysaccharides, lipoproteins). It has been reported that most characterised class II (unmodified) bacteriocins form pores in susceptible bacterial cells [133], albeit, by interacting with several different primary targets, while class I (modified) bacteriocins exhibit a much greater range of mechanisms at the cell surface in order to elicit their mode of action. Although cell-membrane associated mechanisms of action may appear to be similar, in that they mostly form pores in the membrane, there are differences in the molecules they target to do this. For example, nisin has two modes of action, i.) where it targets lipid II, within the cell membrane to prevent peptidoglycan synthesis (Fig. 5), and ii.) where it oligomerises to generate pores in the cell membrane that lead to cell death. The class II bacteriocin, lactococcin A from *Lactococcus lactis* subsp. *cremoris*, targets a mannose-specific PTS transporter and is thought to jam it open allowing efflux of ATP and other molecules from the cell [144][82]. It has also been shown that other antimicrobial peptides are able to penetrate the peptidoglycan layer and enact their effect upon the cytoplasmic membrane of susceptible cells *via* interaction with the cell-envelope structures known as lipoteichoic acids (LTAs) [348]. Others have been shown to interact with membrane-bound proteins, without directly affecting membrane integrity, in order to effect their specific mechanism of action [82][179][110]. Such interactions are able to stabilise the interaction of the bacteriocins at the cell membrane which may result in increased conductance of the specific signal(s) transmitted upon the initial contact of the bacteriocin with the target cell membrane [183].

1.4.4 Inhibition of protein synthesis

A number of antimicrobial agents have been shown to specifically target the cellular protein synthesis machinery of susceptible bacterial cells [70][86][174][131][21][314]. In most of these cases the main targets are either the ribosome, or associated molecules such as ribosomal proteins, ribosomal-ribonucleic acid (rRNA), or transfer-RNA (tRNA). Ribosomes are highly conserved in all living cells where they carry out their essential role in accurately converting messenger RNA (mRNA) into translated polypeptides [53]. It is no surprise, then, that ribosomes and the machinery required for their organisation and/or function are common targets of antimicrobials [337]. The 70S microbial ribosome is made up of a small, 30S, and large, 50S, subunit, each of which facilitates its own function in the overall mechanism of protein synthesis [150]. Three substrate binding sites, annotated as the aminoacyl (A), peptidyl (P) and exit (E) sites, reside in the core of the ribosome where decoding of the mRNA into protein occurs [53]. Briefly, the 30S subunit is responsible for the alignment of each mRNA codon with the correct anti-codon of the complementary aminoacyl-transfer RNA (aa-tRNA) at the A-site, while the 50S subunit mediates peptide bond formation at the P-site [337]. In concert, the two ribosomal subunits also facilitate the translocation of the codon-anti-codon pairing through the ribosome complex [53]. Antimicrobials that are known to inhibit protein synthesis have been shown to enact their bacteriostatic or bactericidal mode of action on specific ribosomal targets. For example, the aminoglycoside antibiotic, kanamycin, binds to the 30S subunit which affects the accuracy of codon:anti-codon pairing and ultimately results in the production of non-functional proteins [281], while the antibiotic chloramphenicol targets the peptidyltransferase centre of the 50S subunit, effectively inhibiting its ability to form peptide bonds and, thus, polypeptide chains [346]. These mechanisms of action ultimately result in protein synthesis inhibition which is detrimental to the survival of the target bacteria.

1.4.5 Inhibition of DNA replication/transcription

In all living systems, DNA replication is carried out by DNA polymerase enzymes, which have been shown to vary slightly between different organisms in terms of their structure [269] and activity (*e.g.* polymerase and exonuclease activity) [47]. Similarly, RNA polymerases facilitate the transcription of DNA to produce mRNA, which can then be ribosomally translated to synthesise functional proteins [66]. DNA replication and transcription are both targets of some of the most successful antimicrobial agents used today [269]. Examples of these include the quinolones, a group of antibiotics which specifically target the DNA gyrase/topoisomerase machinery of the replisome, thus, inhibiting

relaxation of the supercoiled DNA strands [322]; and the rifamycins, which are a class of antibiotics that bind and inhibit RNA polymerase [227]. Interestingly, antimicrobials that inhibit DNA replication do not usually directly target the core polymerase enzyme itself, in contrast to antimicrobials that inhibit RNA synthesis [269]. More recently, however, several antimicrobials that act on DNA polymerases have been discovered, expanding the diversity of target specificity in antimicrobial compounds that target DNA replication. Due to the carefully orchestrated events that transpire in order for DNA replication or transcription to proceed, it is no wonder that any disruption to the respective machineries results in their inhibition [269]. This begs the question, then, as to why very few antimicrobial inhibitors of DNA replication have been shown to target enzymes other than the gyrase/topoisomerase machinery, considering that the major enzymes involved in replication differ between organisms (*e.g.* bacteria and humans), and that all DNA replication antimicrobials currently used in the clinical space are only those which specifically inhibit DNA gyrase/topoisomerase activity [322]. The fact that these mechanisms of action appear to use a similar target may simply be due to the complexities of these biological processes, which may have intricate and conserved resistance mechanisms that are, as yet, undiscovered.

1.5 Proteomics

Because the mechanism of action of GccF is likely to be novel, it is of interest that it is identified in order to inform the design of new antibiotics and minimise the potential side effects of their use on eukaryotic cells [21]. Proteins are one of the most vital components of living organisms; essential for regulation, maintaining normal cell function and adaptive response(s). Proteomics is the study of proteins within an organism at a specific time and in a specific environment. The foundation of proteomics is built on protein identification and can produce a comprehensive view of a cell's physiology at the time of sample preparation [21]. It is a powerful method for monitoring the changes in the proteome of a cell under different developmental and environmental conditions [19]. Results obtained from proteomic studies can then lead to further investigation of the functions of the protein(s) in question using biochemical or genetic techniques.

Previous studies have shown how proteomics can be applied in areas of drug discovery [273] and development [45] in studies designed to understand microbial defence systems and pathogenicity [231] by monitoring changes that occur in microbial proteomes during different phases of cell growth [65]. Because exposure of specific cells to nM concentrations of GccF causes them to cease multiplying almost instantaneously, there must be some effect on the proteome of those cells. Among the numerous metabolic effects, it is logical to assume that protein synthesis would be down regulated.

There have been numerous proteomic studies of bacterial cells, including strains of *Lb. plantarum* that have been subjected to a number of stresses including cold [197], acid [138], bile salts [130], and antimicrobial compounds [231][114][257]. Previous studies have used transcriptomics to try to elucidate how GccF might affect the regulation of protein production in *E. faecalis* JM 2-2 cells [27]. Although such a study has not been carried out on *Lb. plantarum* ATCC 8014 cells, a proteomic investigation may show some similarities in protein regulation and/or changes in protein abundances. By comparing changes in the proteomes of target cells at specific times points following their exposure to GccF, relative changes in the protein complement between treated and untreated cells can be estimated (quantitative proteomics). The following expands on some of the current proteomic approaches and technologies used today, how they differ and complement other techniques and/or methods, and an explanation highlighting the reasons the chosen approach was used for this study.

1.5.1 Top-down versus bottom-up proteomics

In traditional proteomics there are two complementary approaches for liquid-based mass spectrometry (MS) analysis, top-down and bottom-up. These distinct analytical methods differ in that top-down proteomics uses MS to characterise intact proteins, whilst bottom-up proteomics uses enzymatic or chemical proteolytic digestion to generate peptide fragments from the intact protein(s) and is sometimes referred to as 'peptide-based proteomics'. Although each method has its advantages and limitations, analysis of peptides in the bottom-up approach allows for better separation by reverse-phase high-pressure liquid chromatography (RP-HPLC), and better ionisation and fragmentation patterns [353][93]; compared to an intact protein analysis technique, like top-down, which requires the use of Fourier Transform Ion Cyclotron Resonance or Orbitrap mass analysers along with different fragmentation strategies to produce, separate and analyse complex mixtures of highly charged ions.

1.5.2 Fractionation and protein separation methods

The overarching objective of the present study was to identify proteins with the most significant changes in their abundance in *Lb. plantarum* ATCC 8014 cells following exposure to GccF. Given that GccF is known to dock at the cytoplasmic membrane of susceptible target cells by association with the PTS GlcNAc transporter, PTS18CBA, *via* one, or both, of its GlcNAc moieties [20][27], the identification of any change in the abundances of proteins in the membrane fraction was of particular interest in this study.

It is well-known that membrane proteins are notoriously difficult to fractionate and characterise due to their generally low abundance, poor solubility, and contamination by the relatively more abundant proteins of the cytosolic fraction [68][288]. Depending on the type of bacterial cell (*i.e.* gram-positive or gram-negative), different fractionation methods must be employed in order to negate, or at least minimise, the potential of impure isolation of each fraction. In gram-negative bacteria, this can be achieved by using specific detergents or lytic reagents/enzymes that are known to either target (*e.g.* Triton X-100) or act on specific fractions of the cell (*e.g.* lysozyme, commercial lysis reagents, French Press lysis) [303]. In gram-positive species, the relatively thicker peptidoglycan layer poses an additional challenge for solubilisation due to its rigid structure, on top of the usual difficulty of membrane fraction isolation and membrane protein solubilisation [68]. Despite the advances in MS-based technologies over the years [267], the difficulty in analysing membrane proteins usually occurs prior to MS analysis, during fractionation and separation, where the intrinsic physiochemical properties of these proteins makes them problematic [289]. This is one of the reasons why multiple separation approaches and techniques are often used in proteomic studies [289], which, in turn, constitutes one of the many sources of complexity in a proteomic workflow. The more techniques that are utilised, the greater the likelihood of losses due to the multiple layers of processing; not to mention the accompanying normalisation steps at each stage of separation. It is due to the collective efforts of those who conduct research in the microbial proteomic space that these intricacies are starting to be overcome. Techniques such as membrane shaving [284], and combined approaches such as multi-omics [165], are only two examples of the more recent methods being used that have established a sound foundation from which further advancement of the intricate cell fractionation and protein separation techniques of proteomics can be developed.

1.5.3 Quantitation methods

In proteomics, quantitation is a fundamental aspect of the methodology as it allows for a better understanding of the level of proteins being expressed under the specific conditions applied to the sample(s) in any given study. Quantitation can be achieved *via* two primary methods, labelled and label-free. The differences between these methods seem obvious, however, both can be divided further into more specific labelled or non-labelled techniques, for relative or absolute quantitation, and each have their advantages and limitations which are described below.

1.5.3.1 Labelled approach

Various labelling approaches have been developed for protein/peptide quantitation in proteomic studies. Examples of these include, metabolic labelling, isobaric chemical labelling [196], and enzymatic labelling [354], each with their own unique application in proteomics. Where the labelled approach differs again from that of the label-free approach is during sample preparation where, following labelling, the samples are pooled together and then subjected to analysis by MS-based techniques (Fig. 6) [354].

The purpose of a labelled approach is to decrease the interference from nonsense data, commonly referred to as 'noise', resulting from general experimentation and sample preparation [49]. This allows easier interpretation of the MS data as it pertains to protein abundances (peak height or volumes) in the sample(s) which, in turn, provides a more accurate representation of the events that occur in the proteome of the given organism when subjected to the specific conditions of the study. Depending on the labelled approach used, quantitation can also be relative or absolute, where unknown (relative), or known (absolute) amounts of a specific label, or multiple labels, are introduced to the samples either to be incorporated into the proteins, which are then subjected to digestion, or to spike a sample prior to being subjected to proteolysis and MS [175]. The abundance (peak) ratio of specific peptides from each protein is then compared to that of the labelled standard. These methods ultimately offer a means for further control of variation between samples [266].

Common downfalls of using the labelled approach are the additional and complex processing required, the possibility of incomplete labelling, the incompatibility between certain labels and cell cultures, and the high cost [242][239][266]. Compared to a label-free approach, however, the use of labelling in proteomics ultimately provides more efficient quantitation, as well as more accurate and reproducible results [196].

1.5.3.2 Label-free approach

Interest surrounding label-free proteomics was fuelled by the need for a simplified, and more time- and cost-efficient method of quantitating proteins in a wider array of biological samples [49]. Unlike the labelled approach, samples are individually subjected to processing and

analysis by MS in the label-free method, and their peptide spectra are then compared to quantify the abundance of the identified proteins in the sample(s) [354].

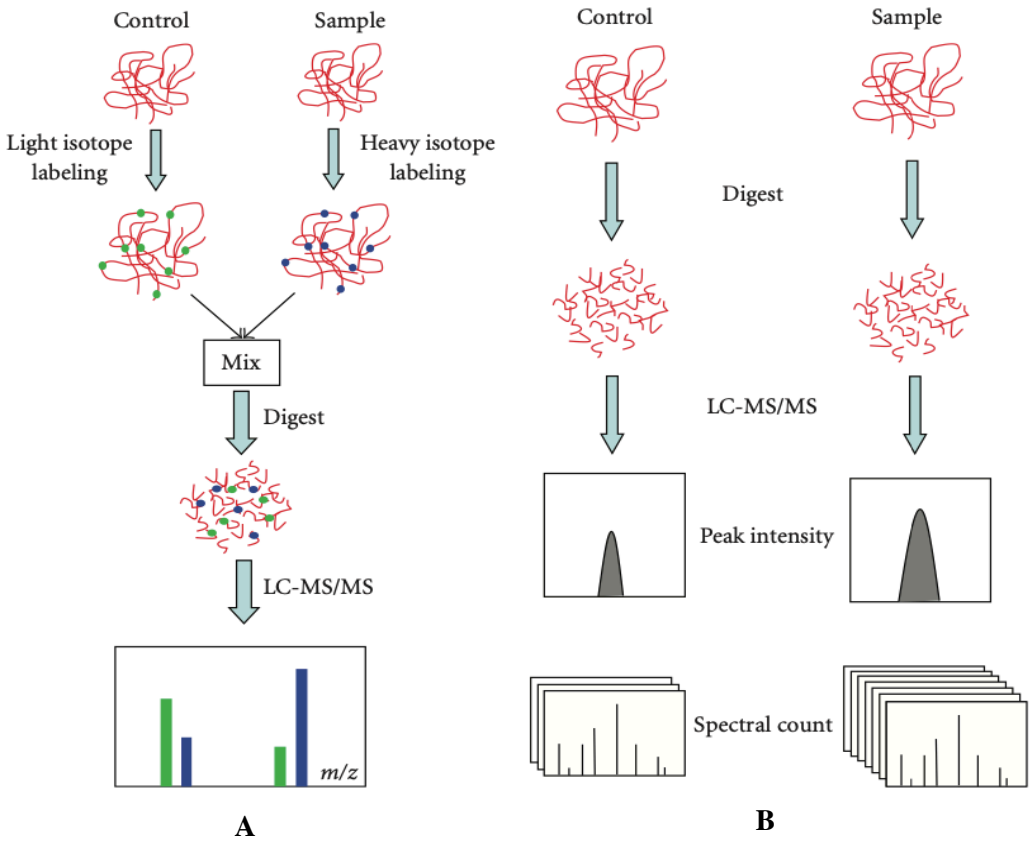

Figure 6: Comparison of labelled and label-free approaches to quantitative proteomics. **(A)** Isotope labelling approach. Sample and control are differentially labelled and then pooled prior to further sample preparation and analysis by MS. Quantitation is achieved by comparing the mass to charge (m/z) ratio of labelled peptide pairs from each preparation. **(B)** Label-free approach. Sample and control are individually subjected to preparation methods and MS analyses. Quantitation is based on two unique measurements, peptide peak intensity and spectral counting (Figure reproduced from Zhu, *et al*., 2010 [354], © 2010, with permission from the authors).

Quantitation using this approach can be achieved *via* two primary methods, the comparison of peptide peak intensities, which exploits the correlation between ionisation signal intensity and ion concentration [326][49], or spectral counting, where the frequency of peptide identification is related to the relative abundance of its parent protein [175]. A notable limitation of the label-free approach is the possibility of sample variation due, in part, to the individual processing of

each sample [14], as well as instrument variations between runs [175]. To overcome these challenges, advances in computational data analysis have enabled the development of specialised normalisation methods and software that account for the intricacies of MS-based sample preparation and analysis [49]. An example of one of these normalisation methods is total ion count (TIC) normalisation, otherwise referred to as total spectral count (TSpC) normalisation, which selects for the sample with the lowest TIC/TSpC in a given replicate and, accordingly, all other samples are adjusted to it by means of dilution or adjustment of the injection volume [119]. Overall, both labelled and label-free approaches to quantitative proteomics each have their place. The complexities associated with either approach, including limitations and advantages, underscores the necessity for diligent investigation into the methods and techniques prior to undertaking such work in an effort to make a more informed choice of the most optimal approach for the specific study.

1.5.4 Gel-based versus gel-free approaches

There are two main methods that can be used to investigate the proteome of cells or tissue, gel-based or gel-free. A study that investigated and compared the use of gel-based and gel-free approaches to investigate the proteome of *Bacillus subtilis* (*B. subtilis*) [341] showed that the two approches were complementary, highlighting the need for different analytical approaches to compile a comprehensive record of, and fully understand the microbial proteome. A similar study published the following year investigated the use of three different proteomic approaches to identify membrane proteins in *S. aureus*. It compared a one-dimensional (1D) gel-LC approach to that of a two-dimentional (2D) gel-LC and a membrane shaving approach to ascertain whether the different techniques generated different results and, if so, how those results varied or agreed. Ultimately the researchers found that the use of a 1D gel-LC and a gel-free membrane shaving approach in combination generated complementary results that allowed for a more comprehensive view of the *S. aureus* membrane proteome [340]. The findings from these studies show that while both the gel-based and gel-free approaches have their place in proteomic studies, in order to generate the most accurate representation of a bacterium's proteome, it is best to employ either method in concert with another technique.

1.5.5 The approach used in this study

The present study utilised both gel-based and gel-free approaches to ascertain the similarities and potential difference between data output, specifically in terms of total protein count and proteins

unique to either method. It was hoped that the use of both approaches would help create a more complete picture of how *Lb. plantarum* ATCC 8014 cells are affected by GccF, whilst also providing evidence to support the findings presented by Wolff and colleagues (2006) [341]. In addition to the overall approach of this work, it was pertinent that the general stress response elicited by the target cells upon treatment with GccF was limited. It was hoped that optimising the dose of GccF given to the target cells, along with the initial cell density used, would help distinguish between the general stress proteins expected to show an increase in abundance as a result of stasis and those involved in a GccF-specific response. To do this, both parameters were varied to obtain an initial slowing of growth that plateaued at the end of one hour, indicating the cells had reached stasis.

1.6 Stress physiology of gram-positive bacteria

The capacity of microbes to monitor and detect changes in their surroundings is essential for their survival in the dynamic environments in which they live [33]. The innate ability of bacteria to sense, adapt to, and overcome environmental challenges depends on their timely response to these changes and varies between different bacteria. A recent review by Bonilla (2020) [33] reported that in gram-positive bacteria various stress responses are linked by what many researchers have coined the bacterial 'general stress response' (GSR) model; a concept which shows how different stresses can be integrated into a singular cascade of signalling events that promote survival. This review combined the results of studies on three representative species of gram-positive bacteria (*B. subtilis, S. aureus and L. monocytogenes*) and assessed their responses to different environmental stresses such as changes in pH, osmotic stress, reactive oxygen species (ROS) and changes in temperature. It was found that upward of 200 proteins are involved in the bacterial general stress response in various gram-positive bacterial species [33]. These findings, together with those presented in a review by Papadimitriou and colleagues (2016) [241], have been collated into a list of general stress proteins that can be found in Appendix 7.2 (Table 14).

1.7 Biochemical pathways

In order to further understand exactly how GccF effects bacteriostasis in its bacterial targets, the Kyoto Encyclopedia of Genes and Genomes (KEGG) [164] was used to identify pathways in *Lb. plantarum* strains potentially affected by treatment with GccF. KEGG is a free, online service that provides a genome map of some *Lb. plantarum* strains, providing additional information about the role of specific

proteins in various biochemical pathways. For these genome analyses, *Lb. plantarum* strains JDM1 and WCFS1 were used in place of *Lb. plantarum* ATCC 8014 as the latter strain is not available on KEGG.

1.7.1 Gene ontology (GO)

The Gene Ontology (GO) project was established in an effort to unify the attributes of genes and gene products into simplified classes that can be easily compared between different organisms on the basis of biology and its processes [16]. To do so, GO uses terms that allow functional descriptions of annotated genes and/or their products. GO covers three major domains that include, cellular component, molecular function, and biological process, which have then been subdivided further into more specific functional annotations. These annotated terms have been given the name 'GO terms' [302], and examples include, 'ribosome' and 'cytosolic membrane' (cellular component), 'transporter' and 'enzyme' (molecular function), and 'cell growth and maintenance' and 'translation' (biological process) [16]. In previous studies which also looked into characterising GccF, GO terms were used to divide the identified genes/proteins into these categories based on the information provided by database and literature searches [27]. In the present study, GO terms have been used to provide a simplified overview of the information obtained from the quantitative proteomic study in order to better understand the effects GccF has on the abundances of proteins in *Lb. plantarum* ATCC 8014.

1.8 Research goals

Previous research has shown that exposure of susceptible cells to GccF results in the rapid, but reversible, onset of bacteriostasis [291][28]. To have this effect, GccF must first interact with the cell envelope by binding to, at least, one receptor molecule. However, as the cells can remain in stasis for up to 7 hours (and hardy recover even after 15 hours), there must be a change in the target cell proteome due to perturbations of cellular processes following the initial interaction. Intuitively, because of the extremely low concentrations of GccF required to effect bacteriostasis, there must be some initial signal that is quickly amplified. Recent research suggests that GccF is localised to the surface of target cells through the interaction of its Cys-*S*-linked GlcNAc moiety with the membrane domain of the GlcNAc-specific PTS transporter PTS18CBA [20]. Although important, this interaction is not essential for activity as without the Cys-*S*-linked GlcNAc, or even the 11 C-terminal residues, GccF remains active. The Ser *O*-linked GlcNAc is, however, essential for activity, and is

thought to interact with a second target [28]. Interestingly, sequence analysis of GccH (the immunity protein) predicts the protein to be cytosolic, even though it appears to associate with the membrane fraction when *Lb. plantarum* cells containing the *gcc* operon are fractionated [27]. It is possible that the abundance of specific cytosolic, membrane and secreted proteins could change when cells are exposed to GccF. With this information the following hypotheses were formulated:

1. GccF interacts first with PTS18CBA as well as a second membrane protein of the target cell proteome, and that this protein is capable of initiating a signalling process controlling cell metabolism in such a way that it induces the rapid onset of bacteriostasis (within two minutes following its addition).
2. Cellular responses to low-to-medium concentrations of GccF should be reflected by a change in the abundance of proteins associated with this signalling pathway.
3. Some proteins associated with cell stress and stasis will be differentially regulated regardless of the bacteriostatic agent used (general stress response).

The overall aim of undertaking this research is to understand how GccF shuts down cell growth. The objectives of this project were to:

- Determine the optimal ratio of GccF:target cells to obtain a steady onset of stasis over 60 minutes
- Treat susceptible cells with an optimised concentration of GccF and analyse the changes that occur in the proteome of these cells at 15, 30 and 60 minutes
- Analyse the results for patterns in protein abundance and attempt to identify any biochemical processes that are being affected

2 Materials and Methods

2.1 General materials

2.1.1 Water

'Millipore' or 'milli-Q' water was obtained from a Barnstead™ Nanopure™ system and used to make up buffers and solutions not used during liquid chromatography mass spectrometry (LCMS). For LCMS, MS-grade water was used for buffers and solutions during gel processing and subsequent LCMS analyses.

2.1.2 De Man, Rogosa & Sharpe (MRS) broth

55 g of *Lactobacilli* MRS broth was made up to 1 L with milli-Q water and sterilised by autoclaving in a pressure cooker for 15-20 minutes. Media was stored at room temperature and inspected for contamination before use.

2.1.3 MRS agar indicator plates

1% (w/v) agar was added to MRS media prior to sterilisation. When required, solidified MRS agar was equilibrated in a 40 °C waterbath. 50 μL of *Lb. plantarum* ATCC 8014 in MRS was added to each 15 mL of MRS agar and then poured into sterile Petri dishes. Indicator plates were stored in a cold room and warmed to room temperature in an incubator prior to use.

2.1.4 Bacterial strains

Table 1: Bacterial strains

Species	Genetic Background
Lb. plantarum KW30 (producer)	Wild-type
Lb. plantarum ATCC 8014 (indicator)	Wild-type

All bacterial cells were supplied by the laboratory cell library and kept as glycerol stocks at -80 °C

2.1.5 Reverse phase high-pressure liquid chromatography (RP-HPLC)

2.1.5.1 Mobile phase

Buffer 'A': 0.1 % trifluoroacetic acid (TFA) in LCMS grade water. Buffer 'B': 98% LCMS grade acetonitrile (MeCN) % 0.08 % TFA. Samples were dissolved in a minimum volume of buffer A, then 0.5 mL aliquots were injected onto the column and eluted using a gradient increasing from 85 % buffer A to 95 % buffer B over 90 minutes at a flow rate of 4 mL/min. The elution was monitored by the absorbance at 280 and 214 nm, peaks were collected manually.

2.1.5.2 Stationary phase

Phenomenex, Jupiter® C_{18} 5 μm (particle size), 300 Å (pore size), 250 x 10 mm (length and diameter) column.

2.2 GccF methods

2.2.1 Purification of GccF

4 L of *Lb. plantarum* KW30 seeded from 400 mL of an overnight culture was incubated at 25 °C for three days without stirring or aeration. Cells were pelleted by centrifugation at 5000 x *g* for 10 minutes. The resulting supernatant was collected and mixed with 100 mL of pre-equilibrated (100 mM sodium formate, pH 4.6) sulfopropyl (SP) Sephadex C-25™ μm resin in a cold room overnight

with constant, gentle, overhead stirring. The resin was then packed into a glass column (5 x 20 cm Econo-Column®) and washed with 1 L 0.1 M 3-morpholinopropapne-1-sulfonic acid (MOPS), pH 7.2, followed by a 1 L solution of 0.1 M ammonium bicarbonate (AMBIC) in 10% MeCN. GccF was eluted from the column in three 100 mL fractions using 0.1 M AMBIC in 60% MeCN. Eluted fractions were tested for GccF activity using an indicator plate. Three active fractions were each transferred into individual round bottom flasks, lyophilised then resuspended in RP-HPLC buffer A (section 2.1.5.1). Resuspended fractions were then individually purified by RP-HPLC (section 2.1.5). Peaks eluting at approximately 35 minutes or 30% buffer B, indicative of GccF (Fig. 7), were manually collected and tested for activity (Fig. 8). Active peaks (labelled '1a', '1b', '2' and '3') were lyophilised then resuspended in a minimum of RP-HPLC buffer A, before being quantified using ultraviolet (UV) absorbance at 205 and 280 nm.

2.2.1.1 Quantitation of GccF

GccF was quantified by measuring its UV absorbance using a Varian multi-wavelength Cary-300 Bio spectrophotometer between 300-200 nm. The concentration of GccF was determined by using the absorbance readings obtained at 205 and 280 nm in the following formula [276]:

$$A_{205\ nm}\,(mg/mL) = 27 + 120(A_{280}/A_{205})$$

Where purification methods did not yield sufficient concentrations or quantities of GccF, additional purified GccF was kindly supplied by Dr Sean Bisset.

2.2.2 Growth curve analysis

A stock of 12 nM GccF was prepared in MRS media. 150 μL aliquots of this was added to the wells of a flat-bottomed 96 well plate along with 150 μL of the indicator *Lb. plantarum* ATCC 8014 cells prepared to six different optical densities ($OD_{600\ nm}$) ranging from 0.1-2. A negative control (300 μL of MRS media without cells or GccF) and a positive control (MRS plus cells without GccF) were allocated to additional wells for comparison. All samples and controls were analysed in triplicate. The plate was analysed using a MultiSkan™ GO plate reader equipped with the SkanIt software. The plate reader was set to measure the $OD_{600\ nm}$ every 15 minutes with a medium-pulse shake setting implemented every hour. The plate chamber was set at 30 °C and growth was measured over 15 hours. Growth curve data was normalised by subtracting the absorbance of the negative control.

2.3 Cell fractionation

2.3.1 Tris-buffered saline (TBS) buffer

6.057 g of Tris-HCl and 8.766 g of sodium chloride (NaCl) were dissolved in 900 mL milli-Q water, adjusted to pH 8.0 with concentrated hydrochloric acid (HCl), and then made up to 1 L with milli-Q water. For buffer containing protease inhibitors, one cOMplete™ ULTRA tablet (either containing ethylenediaminetetraacetic acid (EDTA) or EDTA-free) was dissolved in 50 mL of buffer.

2.3.2 Cell lysis buffer

0.6057 g of Tris-HCl, 0.238 g of magnesium chloride ($MgCl_2$), and 0.0277 g of calcium chloride ($CaCl_2$) were added to 200 mL milli-Q water, adjusted to pH 7.5 with concentrated HCl, and made up to 250 mL with milli-Q water.

2.3.3 Deoxyribonuclease (DNase) I

20 μL of a 10 units/mL stock of grade II DNAse I from bovine pancreas was added to each millilitre of sample. Alternatively, 4 μL of a 50 units/mL stock of DNAse was added to each millilitre of sample in the absence of the 10units/mL stock.

2.3.4 Ribonuclease (RNase)

2.85 μL of a 20 mg/mL stock of RNAse was added to each millilitre of sample.

2.3.5 Fractionation method

Membrane and cytosolic proteins were obtained using a combination of cell fractionation and sodium dodecyl sulfate polyacrylamide gel electrophoresis (SDS-PAGE) methods outlined in the protocol by Sievers (2018) [284]. 15-20 mL of a 50 mL overnight culture of *Lb. plantarum* ATCC 8014 cells was added to 1 L of MRS media pre-equilibrated to 30 °C in an incubator overnight to obtain a starting $OD_{600\ nm}$ of 0.1. Culture absorbance readings were taken every 30-40 minutes until the $OD_{600\ nm}$ was between 0.25-0.30; at which point, a 200 mL sample was taken from the culture and centrifuged at 8000 x *g* for 10 minutes at 4 °C. 12 nm GccF was added to the remaining culture and the time recorded as time zero (T_0). At 15, 30, and 60 minutes following the addition of GccF, 200 mL samples of treated culture were taken and centrifuged. At each time point, the resulting supernatant was carefully decanted and the pellet was washed and resuspended in 2 mL of TBS buffer containing cOMplete™ protease inhibitor with EDTA (prepared according to the manufacturer's instructions; section 2.3.1) The resuspended cells were transferred between two 1.5 mL Eppendorf tubes and centrifuged at 8,000 x *g* for 10 minutes at 4 °C. The resulting pellet was washed with 2 mL TBS buffer containing EDTA-free cOMplete™ protease inhibitor and centrifuged a second time. The resulting supernatant was discarded and the pellets were resuspended in 1.7 mL lysis buffer (per tube) and transferred between two 2 mL bead tubes containing 0.1 mm diameter zirconium beads. The cells were lysed by bead milling in a Hybaid Ribolyser (4 x 30 second cycles at a speed of 6.5s/m) and cooled on ice between each cycle. DNAse and RNAse were added to each bead tube and mixed by inversion. Samples were then incubated at 37 °C for 20 minutes followed by centrifugation at 8000 x *g* for 10 minutes at 4 °C. The supernatant was then transferred to two 1 mL ultracentrifuge tubes for each time point sample and centrifuged at 100,000 x *g* for 1 hour at 4 °C. Same-sample supernatants were pooled in 2 mL Eppendorf tubes and frozen at -80 °C along with the ultracentrifuge tubes containing the pelleted membrane fractions.

2.4 Protein assay

Following ultracentrifugation, membrane and cytosolic fractions were assayed for protein concentration using a bicinchoninic acid (BCA) protein assay kit. BSA standards ranging from 0.125 to 2 mg/mL were used to generate a standard curve (Appendix 7.1; Fig. 22). Reagents, standards and solutions were prepared according to the manufacturer's instructions and MS-grade water was used to dilute samples where appropriate. A 1:2 and 1:5 dilution of both cytosol and membrane fractions was

prepared and analysed. The absorbance of each protein sample was measured in triplicate, while the standards were measure in duplicate at 562 nm. Absorbance data was exported to excel and plotted against the averaged standard curve ($R^2 > 0.97$).

2.4.1 Membrane solubilisation

50 μL of solubilisation buffer (0.0182 g of Tris-HCl, 3.6036 g of urea, and 0.1 g of 3-[(3-cholamidopropyl)dimethylammonio]-1-propanesulfonate (CHAPS) added to 5 mL of milli-Q water, adjusted to pH 7.5 with 0.1 M HCl, and made up to 10 mL with milli-Q water) was added to the pelleted membrane fraction(s) and sonicated in water bath for three, 5 minute cycles. Same-time point samples were pooled and appropriately diluted for the protein assay.

2.5 Sodium dodecyl sulfate polyacrylamide gel electrophoresis (SDS-PAGE)

Proteins extracted from the cytosolic and membrane fractions of *Lb. plantarum* ATCC 8014 cells were separated on the basis of molecular weight (MW) by SDS-PAGE [185]. Membrane and cytosol samples were standardised to the least concentrated sample from their respective fractions based on the protein assay data that showed highly variable concentrations which ranged from ~1.0-5.7 mg/mL across the two fractions (Table 4). Solubilisation buffer or lysis buffer were used to dilute membrane and cytosolic samples, respectively. 5x SDS sample buffer was added to each sample tube, mixed and centrifuged briefly prior to loading 18 μL of sample into each well along with 8 μL of the Precision Plus Protein Unstained Standard #1610363. Voltage was applied across the gel at 200 V until the dye front reached the bottom of the gel. Gels were then fixed and stained overnight as detailed below.

2.5.1 Gel casting

Protein samples were separated and visualised on 7.5% and 12% resolving gels, each with a 4 % stacking gel. The gels were prepared according to Table 2. All resolving gel components were mixed and pipetted between two glass plates held together by a mini-PROTEAN III casting frame. After polymerisation of the resolving gel, the stacking gel was prepared and pipetted on top, followed by the addition of a 10-well, well-forming comb.

Table 2: SDS-PAGE composition

Gel component	Gel %		
	7.5 %	**12 %**	**4 %**
H_20	4.85 mL	4.29 mL	6.29 mL
0.5 M Tris-HCl (pH 6.8)	-	-	2.5 mL
1.5 M Tris-HCl (pH 8.8)	2.5 mL	2.5 mL	-
40 % acrylamide	2.5 mL	3 mL	1 mL
10 % SDS	0.1 mL	0.1 mL	0.1 mL
APS	50 μL	0.1 mL	0.1 mL
TEMED	5 μL	10 μL	10 μL
Total volume	10 mL	10 mL	10 mL

2.5.2 Electrode (running) buffer

A 5X SDS electrode (running) buffer was made up by dissolving 15 g of Tris-HCl, 72 g of glycine and 5 g of SDS in 900 mL of milli-Q water and then made up to 1 L with milli-Q water. When required, an appropriate amount of buffer was poured into the electrophoresis chamber prior to sample loading.

2.5.3 Sample loading buffer

Depending on the number of gels being run and, therefore, the volume of the protein sample required to load the gels, an aliquot of a pre-prepared stock of 5X SDS sample loading buffer was added to each sample tube, prior to loading on a gel, to obtain a final concentration of 1X SDS sample buffer. The pre-made sample buffer contained: 10 % (w/v) SDS, 50 % (v/v) glycerol, 100 mM dithiothreitol (DTT), 0.25 M pH 6.8 Tris-HCl, and 0.05 % (w/v) Bromophenol blue, and was made up to volume with milli-Q water.

2.5.4 Gel fixing solution

A solution of 40% (v/v) MeOH and 10% (v/v) acetic acid was made up to 500 mL with milli-Q water. Gels were soaked in fixing solution with gentle shaking for 15-20 minutes.

2.5.5 Colloidal Coomassie stain

50 g of ammonium sulfate was dissolved in 250 mL of mill-Q water followed by the addition of 10 mL of a 5% Coomassie blue G250 solution and 6 mL of 85% phosphoric acid. This was made up to 500 mL with milli-Q water. Following gel fixing, a working solution of 20 mL of colloidal Coomassie stain and 5 mL 100 % MeOH was used to stain gels overnight with gentle shaking. Milli-Q water was used to de-stain gels the following day.

2.6 Gel slab processing

Gel slabs containing membrane and cytosol fractions were cut into six equal sections per gel lane (across the 7.5 % and 12 % gels; Fig. 9) and diced into smaller gel pieces using a sterile scalpel blade and a glass plate sterilised with 70 % EtOH (*i.e.* four time points per fraction = eight lanes total; cut into six equal sections per lane across two gels = 48 samples per biological replicate; repeated for three biological replicates = 144 samples total). Gel pieces were collected in separate 0.5 mL LoBind Eppendorf tubes and frozen at -80 °C until in-gel digestion processing.

2.6.1 In-gel Tryptic digestion

Proteins contained within the gel pieces were enzymatically digested and the peptides extracted, prior to MS analysis, using the following solutions/reagents and procedures.

2.6.1.1 4X ammonium bicarbonate (AMBIC) stock solution

A 200 mM (4X) AMBIC solution was made by dissolving 1.6 g of AMBIC in 50 mL of MS-grade water, adjusted to pH 8 with NaOH, and made up to 100 mL with MS-grade water.

2.6.1.2 1X AMBIC wash solution

A 1X AMBIC wash solution was made by diluting 10 mL of 4X AMBIC stock solution in 30 mL of MS-grade water.

2.6.1.3 1X AMBIC/50 % MeOH de-staining

25 mL of 4X AMBIC stock solution was diluted in 25 mL of MS-grade water and added to 50 mL of methanol (MeOH). 300 μL of de-staining solution was added to each LoBind Eppendorf tube containing gel pieces and incubated in a heat block at 45 °C for 2-3 hours. The de-staining solution was changed throughout the incubation period as required until the gel pieces were transparent/completely de-stained.

2.6.1.4 Dithiothreitol (DTT) reduction

0.0154 g of DTT was dissolved in 2.5 mL of 4X AMBIC solution and made up to 10 mL with MS-grade water. Following de-staining, 100 μL of reducing solution was added to each lo-bind tube and incubated in a heat block at 40 °C for 1 hour. The reducing solution was decanted and gel pieces were washed with 200 μL 1X AMBIC for 1 minute.

2.6.1.5 80 % MeCN dehydration

200 mL of MS-grade acetonitrile (MeCN) was added to 50 mL of MS-grade water. Gel pieces were dehydrated twice with 200 μL 80 % MeCN following reduction and wash steps. Gel pieces were then dried completely using a SpeedVac concentrator.

2.6.1.6 Iodoacetamide alkylation

0.037 g of iodoacetamide was dissolved in 2.5 mL of 4X AMBIC solution and made up to 10 mL with MS-grade water. 200 μL of alkylating solution was added to each LoBind tube and incubated for 30 minutes in the dark, followed by two washes with 200 μL of 1x AMBIC and one with dehydration solution.

2.6.1.7 Trypsin digestion

57.5 μL of glacial acetic acid was diluted in 20 mL of MS-grade water (50 mM acetic acid). 100 μL of 50 mM acetic acid, 950 μL of 50 mM AMBIC solution and 2 μL of 1M $CaCl_2$ were added to a 20 μg vial of proteomics-grade powdered trypsin (T6567) and incubated on ice for 10 minutes prior to use. 30 μL of activated trypsin was added to each LoBind tube and incubated in a heat block at 37 °C overnight.

2.6.1.8 Peptide extraction

A peptide extraction solution of 5% formic acid (FA)/50% MeCN was made up by adding 5 mL of MeCN and 0.5 mL of FA to 4.5 mL of MS-grade water. A second extraction solution of 0.1% FA/80% MeCN was made up by adding 8 mL MeCN to 1990 μL of MS-grade water and 10 μL of FA. Following centrifugation at 8,000 x *g* for two minutes, and sonication in a water bath for 3 minutes, 60 μL of the 5 % FA/ 50 % MeCN extraction solution was added to each LoBind tube and sonicated again for a further 3 minutes. The tubes were centrifuged for one minute and the extracted peptides (in solution) were carefully collected in a new LoBind tube. The centrifugation and sonication steps were repeated using 60 μL of 0.1 % FA/80 % MeCN extraction solution. The extracted peptides were pooled with those from the first extraction and concentrated using a SpeedVac concentrator set to 45 °C for 30-40 minutes, or until sample volume was reduced to approximately 30 μL. Samples were then centrifuged at 17,000 x *g* for 15 minutes, and stored at -80 °C until analysis by LCMS.

2.6.1.9 Recovery solution

300 μL of MS-grade MeCN and 10 μL of formic acid (FA) were added to 690 μL of MS-grade water. If the extracted peptide samples were reduced to <30 μL during SpeedVac concentration, approximately 30 μL of recovery solution was added to the tubes and sonicated in a water bath twice for 5 minutes; with a one minute centrifugation step in between. Samples were then centrifuged, transferred to HPLC vials and stored at -80 °C until analysis by LCMS.

2.7 Gel-free approach

Following cell fractionation, as well as utilising the aforementioned gel-based methodology, membrane samples were also processed using a gel-free approach.

2.7.1 Trichloroacetic acid(TCA)/acetone solution

200 μL of TCA was mixed with 1600 μL of ice-cold (freezer stored) acetone.

2.7.2 20 mM DTT in TCA/acetone

36 μL of a 1 M stock of DTT was added to 1.764 mL of the TCA/acetone solution.

2.7.3 Re-solubilisation buffer

0.0791 g of AMBIC, 0.1 g of DTT, and 3.60 g of urea were dissolved in 10 mL of MS-grade water and stored at in a refrigerator until required.

2.7.4 Bradford protein assay

Bovine serum albumin (BSA) standards ranging from 0.125-2 mg/mL were made up using MS-grade water. 200 μL of Bradford reagent was added to the wells of a 96-well plate followed by 10 μL of sample (sample/standard). Sample absorbance was measured at 595 nm and compared to the BSA standard curve to determine sample protein concentration.

2.7.5 Trichloroacetic acid (TCA) precipitation

Membrane samples were thawed from -80 °C and sonicated in a water bath for 5 minutes. 10 μL of each sample was pipetted into a 1.5 mL LoBind tube. 90 μL of a 1:9 mixture of TCA and ice-cold acetone was added to each sample tube followed by 90 μL of 20mM DTT in TCA/acetone. Samples were then centrifuged at 17,000 x *g* for 20 minutes at 4 °C. After decanting the supernatant, 100-150 μL of 100 % ice cold acetone was added to each tube, vortexed to resuspend the pellet, and centrifuged at 17,000 x *g* for 15 minutes at 4 °C. The pellets were then washed in acetone twice more before being airdried in a fume hood for 5 minutes. 60 μL of re-solubilisation buffer was added to each sample tube and sonicated for two, three minute rounds. Samples were then stored on ice for 1 hour to allow for complete re-solubilisation of the pellet followed by centrifugation at 17,000 x *g* for 20 minutes at 4 °C. 214.6 μL of 0.1 M AMBIC was added to each sample tube and left to equilibrate at room temperature for five minutes. 1 μL of 1 mg/mL SOLu-Trypsin was added to each tube and incubated at 37 °C overnight. The following day, the samples were made 1 % (v/v) with cold FA and mixed by pipetting. Samples were concentrated using a vacuum concentrator until the sample volume was reduced to less than 50 μL (approximately three hours), then centrifuged at 17,000 x *g* for 20 minutes at 4 °C. The top 2/3 of each sample was transferred to HPLC vials containing an insert and stored at -80 °C until analysis by LCMS.

2.8 Liquid chromatography mass spectrometry (LCMS)

Peptides extracted were separated and analysed by LCMS. The LC system used was a nano-LC system equipped with an in-line RP-HPLC trap for desalting (PepMap100 C_{18}, 3 μm particle size, 75 μm inner diameter, 2 cm length; trap loading buffer: 0.1 % TFA, 2 % MeCN and MS-grade water; flow rate, 15 μL/min) and a 50 cm reverse phase analytical column for separation (PepMap100 C_{18}, 2

μm particle size, 75 μm inner diameter, 50 cm length). LC buffer A (0.1 % FA, 2% MeCN in MS-grade water) and B (0.1 % FA, 98 % MeCN in MS-grade water) were manipulated to generate a gradient which allowed for separation and elution of analytes through the column (flow rate: 300 μL/min). The LC system was coupled to a Q-Exactive Plus mass spectrometer equipped with a higher-energy collision-induced dissociation (HCD) collision cell, an Orbitrap mass analyser and a Nano Flex ion source. A data-dependent tandem MS acquisition method was used, and all samples were analysed in triplicate (biological triplicates). Full MS1 scans were acquired over a mass range of 375-1,600 m/z with a resolution setting of 70,000. Fragment ion spectra produced *via* HCD were acquired with a resolution setting of 17,500. For data-dependent acquisition of HCD spectra, the top ten most intense ions were selected for fragmentation in each scan cycle and full MS, as well as fragment ion spectra were recorded. Exclusion conditions were optimised according to observed chromatographic peak width (typically 15 seconds).

2.9 Data analysis

2.9.1 Proteomic data analysis

2.9.1.1 Program(s)

Raw peptide data was processed and analysed using the Proteome Discoverer 2.4 (PD 2.4) and, later, 2.5 program with Quan. Membrane and cytosol fractions were analysed separately and the relative quantities of proteins in samples taken at each time point were estimated by comparing spectral counts of samples of these samples with those obtained for the respective fractions' untreated control (*i.e.* T_0).

2.9.1.2 Parameters and exclusions

The raw peptide quantitative data was searched using the following parameters: taxonomy database *Lb. plantarum* ATCC 8014*;* ≤2 missed cleavages; carbamidomethyl cysteines as a fixed modification; oxidation of methionine, the addition of *N*-acetyl-hexosamine, hexose or hexosamine on N/S/T/C (residues) and phosphorylation of S/T/H/D (residues) as variable modifications; parent and fragment tolerances of 10 ppm for primary ions and 0.02 Da for fragment ions; a false discovery rate (FDR) of ≤1%; number of unique peptides is ≥2.

2.9.1.3 Normalisation

Membrane and cytosol samples at each timepoint were normalised at three different points throughout this work.

2.9.1.3.1 SDS-PAGE standardisation

First, the protein concentration was normalised across samples according to BCA protein assay data prior to separation and analysis by SDS-PAGE (usually adjusted to ~1 mg/mL depending on the least concentrated sample).

2.9.1.3.2 MS TIC adjustment

MS samples were adjusted according to the TIC; data representing the sum of all ions in each sample. MS samples were either diluted with an appropriate buffer or injection volumes were adjusted to standardise samples prior to MS analyses.

2.9.1.3.3 Manual normalisation

Finally, following MS analyses, sample protein data was manually normalised based on protein abundance and abundance counts using the manual normalisation method (detailed in Appendix 7.3) in Excel.

2.9.1.4 Determination of significant proteins

Manual normalisation using abundances provided statistical data that helped determine the proteins with the most significant change in abundance. Manual analysis of these significant proteins was required to decrease this list to approximately 10-15 proteins per fraction (~20-30 proteins total) for the final discussion. Factors that were taken into consideration include, i.) a P-value of ≤ 0.05; ii.) a statistically significant fold change value in at least 2/3 replicates at each time point; iii.) the correct cellular localisation according to analysis of potential

membrane domains using TOPCONS [315]; and, iv.) a peptide spectrum match (PSM) value ≥ 10.

3 Results and discussion

3.1 GccF purification

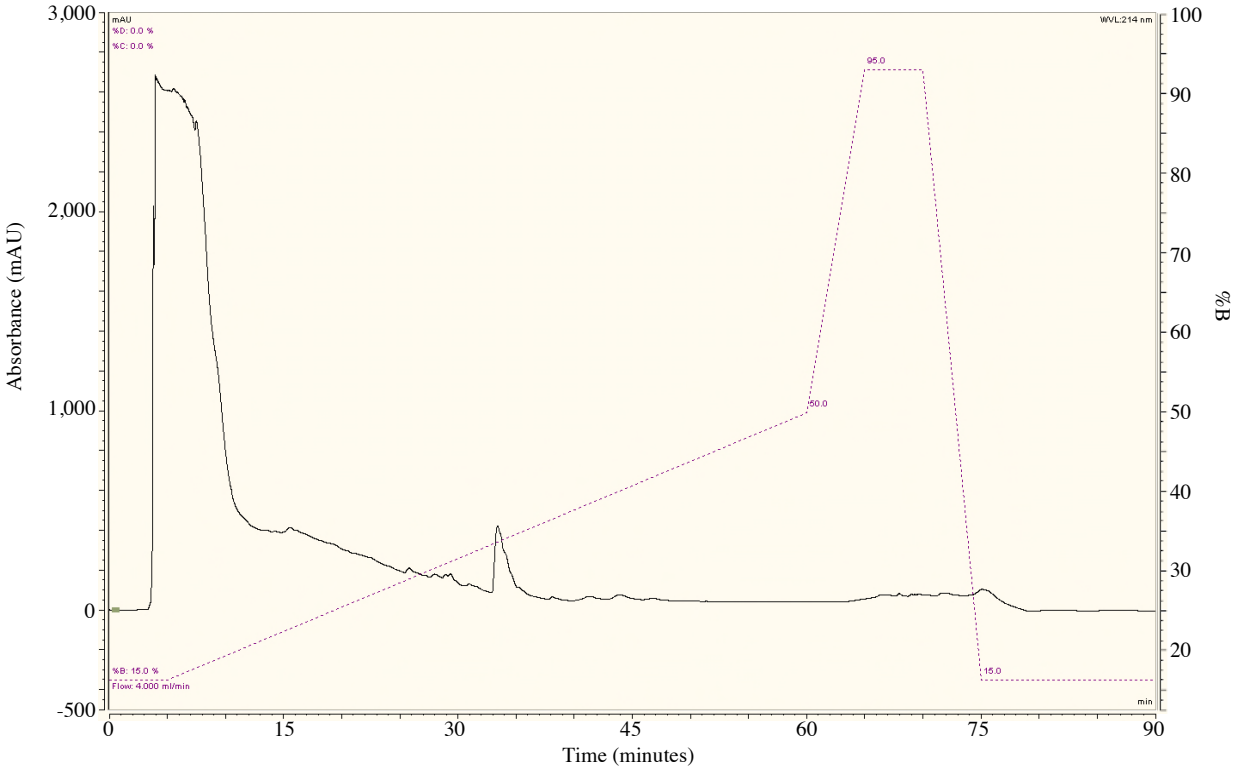

Figure 7: Elution profile of RP-HPLC GccF purification from *Lb. plantarum* KW30. RP-HPLC trace of sample '1b' containing GccF purified by cation-ion exchange (IEX) chromatography using SP-Sephadex C-25™ μm resin. The dotted line represents the percentage of buffer 'B' during the elution. The arrow indicates the time at which GccF eluted from the column and was manually collected for subsequent activity testing and quantitation.

GccF was purified by growing the producer stain, *Lb. plantarum* KW30, in static culture at 25 °C for 72 hours followed by ion-exchange (IEX) chromatography, and RP-HPLC to begin purification. Three successive IEX chromatography fractions were shown to be active using an indicator plate (figure not shown). Each of these fractions was lyophilised separately and then resuspended in RP-HPLC buffer A prior to individual analysis by RP-HPLC. The three samples from IEX were subjected to RP-HPLC purification, with sample one being split in two, hence the labels '1a' and '1b' (Fig. 8).

The active peak fractions (Fig. 7) were manually collected then tested for activity. All but the peak from sample '2' prevented bacterial growth on the indicator plate impregnated with *Lb. plantarum* ATCC 8014 (Fig. 8). It can only be speculated that sample 2 was either not GccF, or was, in some way, denatured, such as missing the *O*-linked GlcNAc, which would still elute at the same position in IEX but would also render GccF inactive. The active fractions labelled 1a, 1b and 3, were quantified using the absorbance at 205 and 280 nm and were shown to have concentrations ranging from 14 to 90 μM. Despite being active, the quantity of GccF purified was insufficient for all the subsequent experiments. The production of small and variable yields of purified glycocins is not an uncommon occurrence, as the same has been reported for the purification of sublancin 168 [158]. As such, purified GccF was kindly gifted by Dr. Sean Bisset for use in this work.

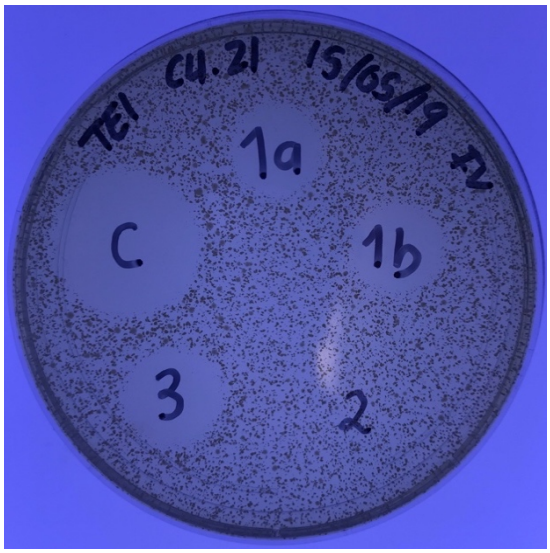

Figure 8: GccF activity assay following RP-HPLC using an adaptation of the spot test [105]**.** Image of an MRS and agar indicator plate impregnated with *Lb. plantarum* ATCC 8014. Sample 'C' is the 10 μM GccF control. Samples '1a', '1b', '2' and '3' are fractions collected during separation by RP-HPLC. 3 μL of the GccF control, and 2 μL of all other samples were applied to the plate. Active fractions prevented bacterial growth in the regions where samples were applied.

3.2 Optimising GccF and target cell concentrations

In order to optimise the likelihood of changes occurring in the proteome of target cells to the primary effect(s) of GccF, rather than changes due to general stress, it was important to look at the changes in the proteome at the early stages of GccF treatment. Initially, different growth conditions, concentrations of GccF, and incubation times were trialled to determine suitable conditions for the

subsequent proteomic experiments. Of prime consideration was the presence of enough cells throughout the time course to allow aliquots of a sufficient volume for fractionation and enough protein in each fraction for visualisation on a gel using colloidal Coomassie stain. Along with these restrictions, it was necessary to see an initial slowing of growth that levelled off at the end of the hour; indicating stasis had been reached. In this way, it was felt that it would be more likely that the changes in the proteome would be less likely due to those of general stress rather than the effect(s) of GccF. It was found that *Lb. plantarum* ATCC 8014 cell cultures with an $OD_{600\ nm}$ between 0.25 and 0.3 when treated with 12 nM GccF grew to a maximum average cell density of 0.35 during the hour and provided sufficient cells for subsequent fractionation and proteomic analysis whilst ensuring a bacteriostatic response without complete growth inhibition. Moreover, to experimentally show that stasis had been reached during cell fractionation, additional $OD_{600\ nm}$ measurements of the treated *Lb. plantarum* ATCC 8014 culture were taken at two, and three hours, post-treatment with GccF. These cell density results are presented in Table 3.

Table 3: Change in optical density ($OD_{600\ nm}$) over time per biological replicate

Time elapsed since addition of GccF (minutes)	$OD_{600\ nm}$ Bio. Rep. 1	Bio. Rep. 2	Bio. Rep. 3
0	0.253	0.259	0.255
15	0.275	0.276	0.269
30	0.291	0.294	0.299
60	0.312	0.311	0.310
120	0.320	0.319	0.335
180	0.335	0.321	0.355

3.3 Expected stress response(s)

Bacteria undergo a variety of biochemical changes in response to various environmental stressors. These changes can occur at the genetic, transcriptional, metabolic or protein level, and depend on the species of bacteria, the specific stressor(s) and their effects on the organism. As this research was predominantly concerned with the changes occurring in the proteome of *Lb. plantarum* (a gram-positive bacteria), an extensive list of proteins involved in the general gram-positive bacterial stress

response was catalogued and is shown in Appendix 7.2 (Table 14). This list was used to help eliminate proteins that showed an increase or decrease in their abundance in response to general stress, allowing focus on proteins that may be specifically involved in the response to GccF. Those highlighted in yellow in Table 14 are stress proteins which have been identified throughout the course of this work (*i.e.* either during analysis of the selected membrane and cytosolic proteins shown to have had the most significant change in their abundance following exposure to GccF, or during other data analysis stages).

3.4 The proteomic response of *Lb. plantarum* ATCC 8014 to GccF

To identify potential protein targets of GccF, protein expression profiling was carried out on both the membrane and cytosolic fractions of *Lb. plantarum* ATCC 8014 cells in response to exposure of the cells to GccF. *Lb. plantarum* ATCC 8014 cells were incubated in 1 L of MRS broth under static conditions to an $OD_{600\ nm}$ between 0.25 and 0.3. At this time, 200 mL of culture was removed (untreated control, T_0) and the remaining 800 mL was then treated with 12 nM GccF and cultured for a further 60 minutes under the same conditions. 200 mL samples were removed at 15, 30 and 60 minutes post-treatment and, along with the control sample, fractionated as described in the method. Following cell fractionation and ultracentrifugation, the concentration of proteins from both membrane and cytosolic fractions, of treated and untreated cells, were normalised to the least concentrated sample using a BCA assay kit (Table 4) prior to running on 7.5% and 12% SDS-PAGE gels (Fig. 9). It should be noted that although the samples were labelled as being taken at 0, 15, 30 and 60 minutes, the initial processing, to the point of cell disruption, took approximately 5 minutes. The cells would have continued to metabolise during this time, albeit more slowly, and GccF would have had more time to exert its effect. Such a delay was however unavoidable and an effort was made to make it as short, and as consistent, as possible.

Unfortunately, the sample dilutions used during the BCA protein assay were not sufficient as extrapolation of the resulting standard curve (Appendix 7.1; Fig. 22) was required to fit the sample protein concentrations on the curve. It should also be noted that following membrane solubilisation, these samples appeared cloudy as a result of the pelleted membrane being resuspended, and did not dissipate prior to being subjected to the BCA assay. It is likely that this cloudiness would have interfered with the absorbance readings of these samples, thus, distorting the data such that the membrane sample concentrations were grossly overestimated (Table 4), as evident by the difference

in band intensities in the 7.5 and 12 % gels (Fig. 9). Despite this discrepancy in the membrane samples, the protein concentrations of the cytosol samples appeared to be similar, which supports the assumption that the cloudiness of the membrane samples indeed skewed these results, as the cytosol samples were in solution and, therefore, did not require solubilisation.

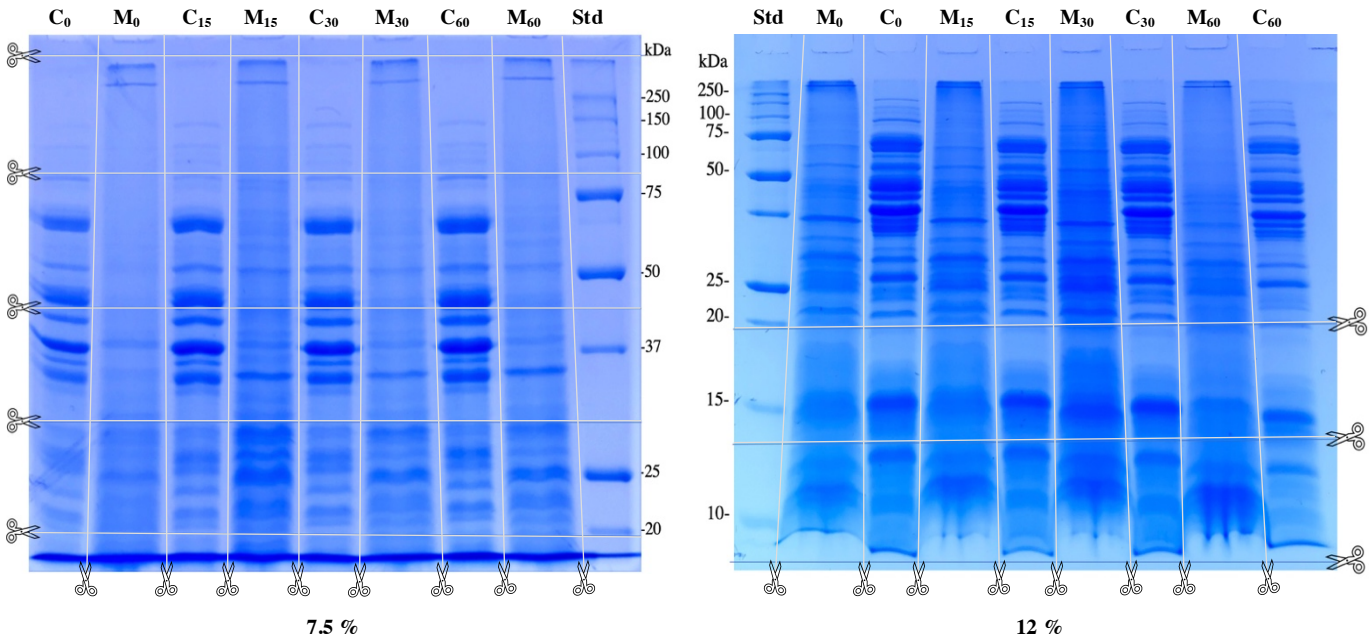

Figure 9: 7.5 % and 12 % SDS-PAGE analysis of membrane and cytosolic fractions of *Lb. plantarum* ATCC 8014 cells. Analysis of membrane (M) and cytosolic (C) fractions on 7.5 % and 12 % SDS polyacrylamide gels following cell fractionation. Time points are denoted by the subscripted text and represent 15, 30 and 60 minutes following the addition of GccF. Marker (Precision Plus unstained protein standard #1610363) lane is labelled 'Std'. The scissors and white lines show how the gel slabs were cut and represent the sections taken from each lane for subsequent processing.

Protein concentrations were calculated using the equation of the standard curve (Appendix 7.1; Fig. 22) ((y = 0.5582x + 0.2429) x dilution factor) generated from the average of the duplicate BSA standards prepared during the BCA assay. Final sample protein concentrations listed in Table 4 were averaged from four representative samples of each time point after taking into account the DFs (1:2 and 1:5).

3.5 Gel slab processing

Each lane of the 7.5 % and 12 % gels was cut by hand for peptide extraction according to the schematic diagram shown in (Fig. 9). Both percentage gels were used to allow for maximum band resolution from both the upper and lower MW ranges (250-10 kDa). Since the 7.5 % gel appeared to resolve the highest molecular weight proteins, the majority of this gel was used and each of its lanes were cut into 4 equal sections from the top of the gel to just below the 20 kDa marker (as shown in Fig. 9). Accordingly, the 12 % gel was then cut into two equal sections starting from just below the 20 kDa marker to the bottom of the dye front. A total of 48 gel samples, per biological replicate, were then processed to produce peptides for mass spectrometry analysis (144 samples total across three biological replicates).

Table 4: Membrane and cytosolic protein concentrations determined by BCA assay

Fraction	Time (min)	Average protein concentration (mg/mL)		
		Bio. Rep. 1	Bio. Rep. 2	Bio. Rep. 3
Membrane	**0**	3.017	5.177	5.713
	15	2.546	3.129	4.409
	30	2.743	3.260	2.975
	60	2.031	1.976	3.521
Cytosol	**0**	1.524	1.505	1.302
	15	1.492	1.423	1.611
	30	1.552	1.519	1.107
	60	1.425	1.032	1.306

3.6 KEGG genome and biochemical pathway analyses

To evaluate the effects of GccF on the target cells (*Lb. plantarum* strain ATCC 8014), the sequenced genomes of closely related *Lb. plantarum* strains JDM1 and WCFS1 were used as reference genomes

as that of *Lb. plantarum* ATCC 8014 was not available on KEGG [164]. The accession numbers of proteins identified by PD were used to extract the JDM1 and/or WCFS1 associated coding sequence (CDS)/gene locus identifier using the National Center for Biotechnology Information (NCBI) database. Referring to the two genome maps proved particularly helpful when trying to elucidate more information about proteins identified in this work. KEGG provided a variety of information pertaining to these proteins including, putative and/or confirmed protein identifiers/names, enzymatic reactions and pathways, and genome maps. These factors helped to determine whether each protein was involved in a general stress mechanism or a possible GccF-specific mechanism, and if it were the latter, how these protein(s) might contribute to the effects of GccF on the cells. When and where the KEGG database did not provide sufficient information regarding the proteins of interest, they were listed in a separate table of proteins that could not be described beyond their PD assigned identity (Appendix 7.9; Table 18).

3.7 Proteins identified by mass spectrometry

3.7.1 Gel-based approach

Using the (SDS-PAGE) gel-based approach, the total number of proteins identified by PD was 1,115 in the membrane fraction and 888 in the cytosolic fraction, to give a combined total of 2,003 proteins. These proteins represent 67.4 % of those encoded in the genome of *Lb. plantarum* ATCC 8014 [232]. Of these, 1,094 membrane and 865 cytosolic proteins were identified with high confidence by PD, totalling 1,959 proteins, and are listed in appendix 7.13 (Hyperlink 1 and 2), which compares very favourably with other studies. To compare, a 2017 study which investigated the effects of tetracyclines on the proteome of *E. coli* cells using a gel-based approach identified a total of 1484 proteins [160], which constitutes approximately 31 % of the median protein count of the *E. coli* genomes that have been sequenced [232]. Additionally, a comparative study which sought to add to the existing list of identified proteins in *B. subtilis* during heat shock used both a gel-based and gel-free approach to identify an additional 473 proteins [341]. Added to the existing 745 proteins identified by Eymann and colleagues (2004) [98], this increased the total proteins identified to 1,218, which, according to the NCBI database, makes up approximately 28 % of expressed proteins in the *B. subtilis* 168 genome. These findings show that proteomic studies conducted in bacteria can produce highly variable results which can be attributed to a multitude of factors including, methods of sample preparation, bacteria species and/or strain used, the specific stressor being investigated, and MS instrumentation.

In the present study, a significant change in abundance of the identified proteins was based on the p-values calculated using protein abundances and abundance counts (Appendix 7.3). Using this method, the change in abundance of 281 membrane and 263 cytosolic proteins was shown to be statistically significant. Of the 281 membrane proteins, 219 showed a significant increase in abundance, while only 62 showed a significant decrease in abundance. 92 of the 263 cytosolic proteins showed a significant increase in abundance, whilst the abundance of the remaining 171 cytosolic proteins was shown to be decreased. Further manual analysis of these proteins helped reduce this list to a select total of 23 proteins combined across both fractions which showed the most significant differential change in their abundance (Tables 5, 8, 9, and 11). These 23 proteins are discussed in sections 3.8 (membrane proteins) and 3.9 (cytosolic proteins). Manual analysis of the 281 significant membrane proteins revealed that many were, in fact, cytosolic proteins, including, ribosomal or ribosome-associated proteins, DNA/RNA polymerase proteins and/or subunits, and proteins involved in major metabolic pathways such as glycolysis. This observation suggests contamination had occurred across the two fractions which resulted in approximately 108 of the 281 significant membrane proteins being cytosolic (38.3 % contamination). Of the remaining 173 proteins, approximately 126 membrane proteins were uniquely identified using the gel-based method. These proteins were identified by manual inspection of the data which, for instance, did not take into account the correct cellular localisation of proteins annotated as 'hypothetical proteins' or 'domain of unknown function (DUF)-domain containing proteins'. As a result, these numbers represent approximations of the true number of proteins assigned to each category.

3.7.2 Gel-free approach

Due to the well documented difficulties associated with membrane protein isolation, solubilisation and separation, it was important to ascertain the effects of a different method for the analysis of the proteins in this fraction. Theoretically, because there were fewer steps, a greater number of protein identifications was expected. However, after desalting and TCA precipitation (Section 2.7), a total of only 650 membrane proteins were identified by PD, with 641 of these being identified with high confidence. Further analysis showed that 248 proteins were uniquely identified using the gel-free approach.

In terms of pure fraction isolation, the membrane proteins identified using the gel-based method showed greater coverage of the *Lb. plantarum* ATCC 8014 genome, making up 37 % of the total proteins encoded (2972 proteins), whilst those identified using the gel-free approach made up only 22

%. These findings suggest that the gel-based method used in this study generated more protein identifications as a result of reduced complexity in the peptide mixture analysed by MS [333][246]. The difficulty in interpreting these findings further, in order to propose improvements to the methodology, especially the gel-free approach, results from the complexities of the stepwise preparation associated with either method. What it does reveal, however, is that these methods can be used to complement one another by increasing the total number of identified proteins. The identification of 126 and 248 unique membrane proteins using the gel-based and gel-free approaches, respectively, suggests that both methods have a place in proteomic studies. If time had allowed, a similar analysis would have been done on the cytosol fraction, and is something to be considered in the future.

3.8 Proteins that lack an assigned function

Sourcing information about some of the proteins identified with the most significant change in their abundance in this work proved difficult at times. Positive identification of these proteins beyond that which was provided by PD posed a challenge in some instances as literature searches, general internet searches, NCBI records and KEGG analyses all failed to provide any additional information about these proteins. As a result of this, further investigation into these specific proteins was not carried out. A list of these proteins from both membrane and cytosol fractions was compiled and can be found in Appendix 7.9 (Table 18).

3.9 Proteins identified in the membrane fraction

A total of 281 membrane proteins were identified with a statistically significant change in their abundance compared to the untreated control. The distribution of these proteins at 15 minutes post-GccF treatment can be seen in Figure 10, and 30 and 60 minutes post-treatment in Appendix 7.4 (Fig. 23). 84 of these with the most significant change in abundance (both increased and decreased) were selected and compiled into a list in Appendix 7.6 (Table 15). However, it was found that 47 of those with the most significant increase in abundance- (ranging from 1.2 to 18.9-fold), and 9 with the most significant decrease in abundance (ranging from 0.7 to 0.08-fold) were actually cytosolic proteins. The remaining 28 proteins, of which 22 showed an increase-, and 6 showed a decreased in abundance, were sorted based on their fold-change values. Further analysis of these proteins revealed that many could not be characterised beyond their PD-assigned identifier (section 3.8) and, as such, are included

in Table 18 (Appendix 7.9). The remaining proteins are discussed in the appropriate subsections that follow.

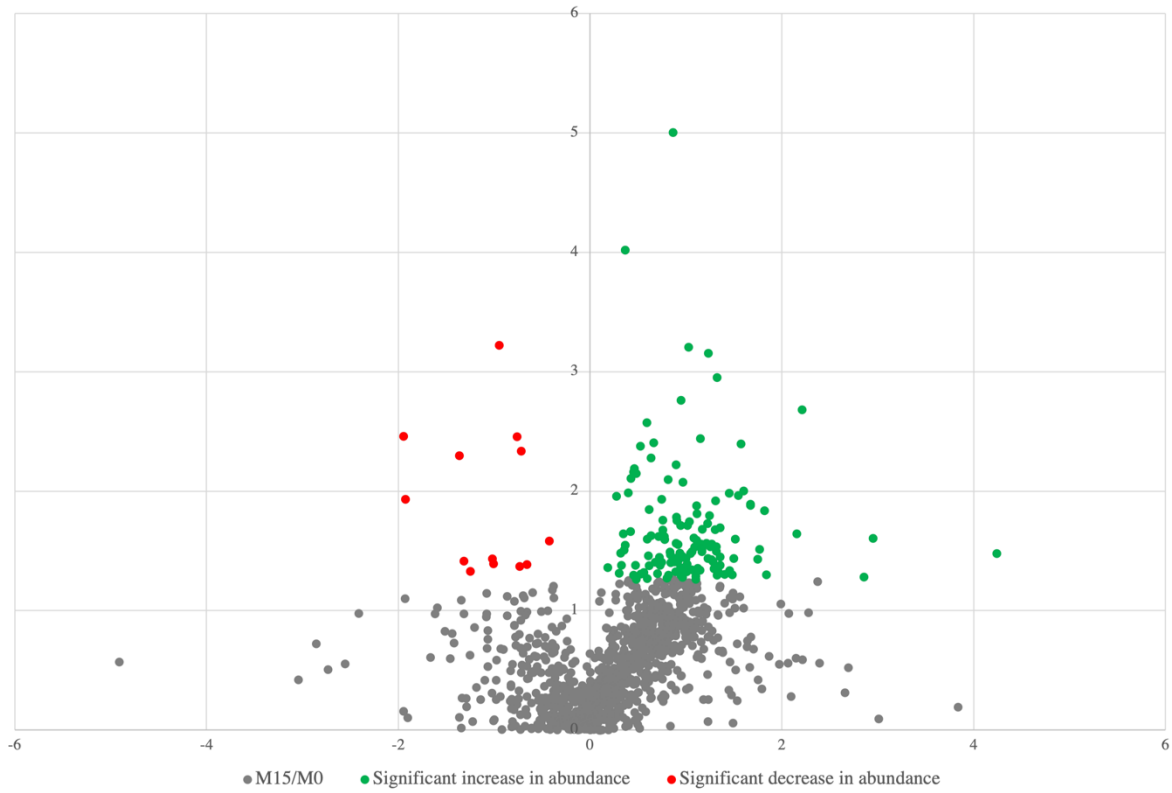

Figure 10: Distribution of proteins identified in the membrane fraction of *Lb. plantarum* ATCC 8014 cells after 15 minutes of exposure to GccF. Volcano plot showing an example of the change in abundance of all proteins identified in the membrane fraction, including those with a significant increase (green) and those with a significant decrease (red) in abundance. Proteins with a p-value ≤ 0.05 were considered significant, as determined by the manual normalisation method outlined in Appendix 7.3.

3.9.1 Membrane proteins with the most significant increase in abundance

The abundances of 219 membrane proteins were shown to have significantly increased following target cell exposure to GccF. Of these, 11 proteins that showed significant changes in abundance (Table 5) that followed a consistent pattern, and were not obviously connected with the general stress response, were selected for in depth analysis are discussed below (in no particular order). To further understand how these proteins might be involved in, or contribute to the effects of GccF on *Lb. plantarum* ATCC 8014 cells, the following subsections provide more information about each protein and the cellular process(es) they are involved in.

Table 5: Membrane proteins with the most statistically significant increase in abundance

Accession #	Protein	Sequence coverage	PSMs	Unique peptides	MW (kDa)	Fold change*		
						T_{15}	T_{30}	T_{60}
ATQ33376.1	Membrane protein insertase, **YidC**	11	118	3	34.2	2.063	**2.166**	**2.014**
ATQ33714.1	PhoH family protein, **PhoH**[+]	54	379	14	35.8	**2.085**	**1.710**	**1.973**
ATQ32187.1	Regulatory protein, **YycI**	24	22	5	31.5	**2.035**	1.397	**1.314**
ATQ33638.1	4-hydroxy-tetrahydrodipicolinate reductase, **DapB**[+]	39	95	5	28.5	**1.756**	**2.420**	2.114
ATQ32925.1	**LCP** family transcriptional regulator	54	777	17	37.7	**1.782**	**1.538**	1.303
ATQ33889.1	Penicillin-binding protein, **PBP2b**	15	48	9	77.2	**1.521**	**1.461**	1.246
ATQ33108.1	Aquaporin family protein, **GlpF4**	9	406	3	25.4	**1.598**	1.303	**1.496**
ATQ34018.1	Rod shape-determining protein, **RodA**	27	114	6	44.5	**1.435**	**1.530**	1.373
ATQ32425.1	ABC transporter permease, **TagG**	18	169	5	31.7	1.379	**2.216**	**1.856**
ATQ33843.1	Cell division protein, **FtsW**	6	56	2	41.9	1.376	**1.721**	**1.650**
ATQ33987.1	Rod shape-determining protein, **MreC**	59	192	11	30.1	1.157	1.179	**1.770**

* Values highlighted in red are not significant. [+] Proteins identified in the wrong fraction.

3.9.1.1 Proteins involved in cell growth and maintenance

3.9.1.1.1 Rod shape-determining protein, 'RodA' (ATQ34018.1)

In both the gram-positive bacterium *B. subtilis* and the gram-negative bacterium *E. coli*, RodA is a membrane protein which functions in the maintenance of the rod shape of these cells [137]. It is part of the peptidoglycan metabolism machinery known as the 'Rod complex' or 'elongasome' [216], where it has been shown to exhibit glycosyltransferase activity upon glycan strands during cell wall synthesis [259]. Although these findings have yet to be confirmed in Lactobacilli, the wealth of evidence that details the involvement of this complex across multiple species of rod-shaped bacteria (*i.e. E. coli*, *B. subtilis* [137]; and *L. monocytogenes* [259]) would suggest it plays a similar role. Table 5 shows that RodA abundance increased at 15 (1.4-fold), 30 (1.5-fold), and 60 minutes (1.4-fold) following treatment with GccF. The fact that this increased abundance is fairly consistent over the time the cells were monitored suggests the cells are trying to overcome the effects of GccF by up-regulating the parts of the peptidoglycan machinery that control the maintenance of cell shape. A STRING diagram showing the interactions (both predicted and verified) of RodA in *Lb. plantarum* WCFS1 showed that it interacts with other proteins that show significant changes in abundance in this study or are discussed in subsequent sections in relation to other identified proteins (Fig. 11). These include 'PBP2b' (Section 3.9.1.1.2) and 'MreC' (Section 3.9.1.1.5) with increased abundance, and 'MurF' (not discussed in-depth), which showed decreased abundance. While it makes sense that RodA, PBP2b and MreC should all have increased abundances, the logic behind the reduced abundance of MurF is not obvious.

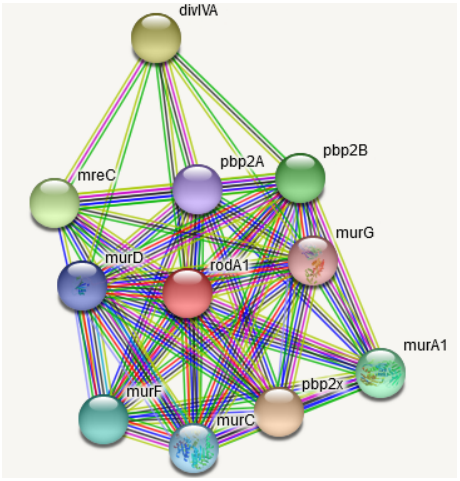

Figure 11: RodA STRING diagram. STRING network showing the first shell of possible interactions of RodA1 from *Lb. plantarum* WCFS1.

Previous unpublished work found that GccF may perturb the cell envelope of its target cells without resulting in cell lysis or a fatal leakage of cellular compounds/metabolites, and resulted

in cells that could not completely divide (Appendix 7.11; Fig. 26). Alternatively, the increased abundance of RodA may be a secondary effect, suggesting that the target cells are attempting to prioritise the translation of proteins involved in the cell regeneration in order to overcome bacteriostasis.

3.9.1.1.2 Penicillin-binding protein, 'PBP2b' (ATQ33889.1)

Named as such due to their affinity for the D-ala-D-ala dipeptide common to their natural substrate (the stem pentapeptide of peptidoglycan) and penicillin, penicillin-binding proteins (PBPs) are a group of proteins that catalyse the final glycosyltransferase and transpeptidase reactions of peptidoglycan synthesis [152][215]. PBPs have been categorised into two main classes based on size (*i.e.* high- and low- molecular weight PBPs; HMW- and LMW-PBPs, respectively) [78]. They can be divided further into subclasses based on amino acid sequence similarities [245], and domains structure, which is related to their specific enzymatic activities. All classes of PBPs contain a penicillin-sensitive C-terminal transpeptidase domain [78], while only the HMW class A PBPs (aPBPs) possess an N-terminal domain with glycosyltransferase activity [84]. The N-terminal domain of class B PBPs is believed to facilitate their involvement in cell morphology by acting as a transpeptidase [271]. According to the *Lb. plantarum* JDM1 genome map in KEGG, the specific PBP identified in this work is the class B 'PBP2b'. In 1996 it was reported that *Streptococcus thermophilus* (*S. thermophilus*) mutants with a gene disruption in *pbp2b* showed altered cell morphology and reduced growth-rate [293], suggesting that PBP2b plays a role in cell morphology by maintaining cell shape and growth. Similar findings were reported in 2002 which supported those of the original study but also found that PBP2b is specifically involved in cell elongation in *S. thermophilus, E. coli* and *B. subtilis* [310]. More recently, a study by David and colleagues (2018) [76] also found that, in *Lactococcus lactis* (*L. lactis*), PBP2b plays an important role in peripheral growth (*i.e.* cell elongation) and septum site positioning during the bacterial cell cycle.

The results of this study show that changes in the abundance of PBP2b in response to GccF (1.5-fold at 15 and 30 minutes, and 1.2-fold at 60 minutes) are similar to those seen for RodA (Table 5). This is not unexpected as the literature contains multiple reports of these proteins interacting with each other [310][76][84][223]. In addition, further analysis of the *Lb. plantarum* JDM1 genome map revealed that *pbp2b* is part of a gene cluster which encodes four other cell division/peptidoglycan synthesis proteins, including, the phospho-*N*-acetylmuramoyl-pentapeptide-transferase 'MraY', the putative cell division protein 'FtsL', the

16S rRNA (cytosine^{1402}-N^{4})-methyltransferase cell division protein 'MraW', and the cell division protein 'MraZ' [164]. Taken together, and in line with the change in abundance of RodA, the increased abundance of PBP2b provides support for the same suggestion, that the target cells are trying to combat the bacteriostatic effects of GccF by up-regulating the expression of proteins involved in the coordinated synthesis and remodelling of the cell wall that are required for cell growth, division and shape maintenance.

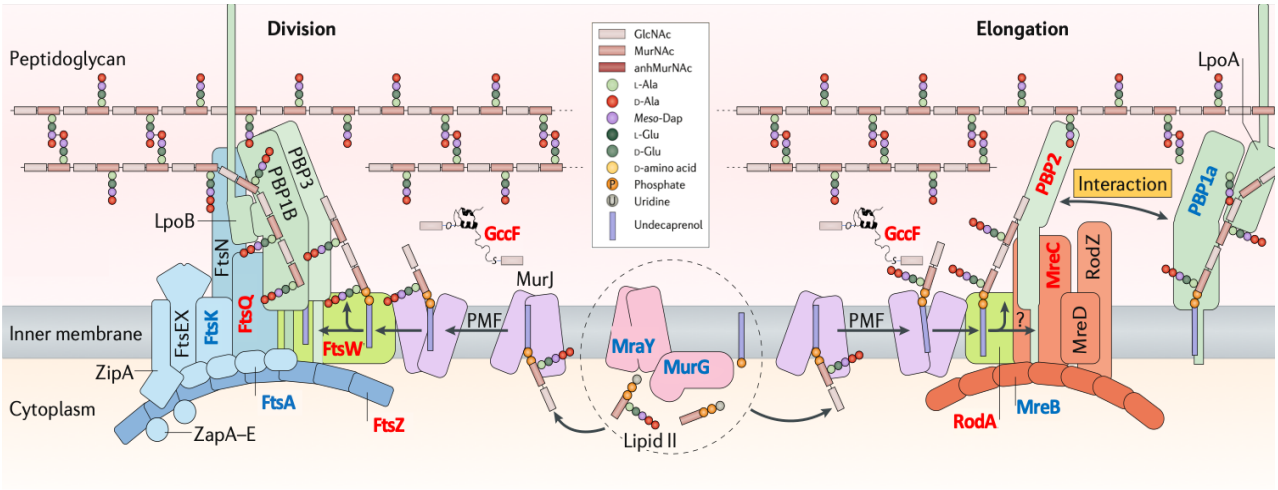

Figure 12: Proteins involved in bacterial cell wall elongation and septum formation. Schematic diagram depicting the roles of the key elongasome (Rod proteins, Mre proteins, and PBPs) and divisome proteins (Fts proteins, PBPs) in cell wall elongation, and septum formation (cell division), respectively. Proteins that were identified in the present study with a decrease in their abundance are highlighted in blue, while those highlighted in red showed an increase in abundance compared to the untreated *Lb. plantarum* ATCC 8014 control (change in abundance was not statistically significant for all highlighted proteins). GccF is also depicted in the extracytoplasmic space showing how its GlcNAc moieties could potentially interact with the cell wall proteins and/or be incorporated into the cell wall (Figure reproduced from Egan *et al.*, 2020 [95], © 2020, with permission from Springer Nature).

3.9.1.1.3 Cell division protein, 'FtsW' (ATQ33843.1)

FtsW is a membrane protein involved in cell division [169]. Its specific involvement in septum formation and cell division is essential in *B. subtilis* [200] and *E. coli* [37], respectively. During cell division, a structure known as the 'Z-ring' is formed by the 'FtsZ' protein at the prospective

cell division site (Fig. 12) [218]. A number of Fts-family proteins, and other cell division proteins, are then recruited to the Z-ring to facilitate cell division. In *E. coli* and *B. subtilis,* FtsW is specifically required for the recruitment of the class B transpeptidase 'FtsI' (PBP2b in *B. subtilis*) to the Z-ring in order for cell division to proceed (Fig. 12) [200][112]. It was previously shown that mutations in *ftsW* and depletion of FtsW reduced Z-ring stability and total Z-ring formation frequency in *E. coli* [37]. These findings, however, have since been refuted by a 2002 study which showed that the same mutation(s) and depletion(s) only inhibit cell division as a result of failure to recruit FtsI/PBP2b to the Z-ring, but have no significant effect on Z-ring stability when compared to mutations/depletions in any of the other cell division proteins [218]. Interestingly, a recent study by Taguchi and colleagues (2019) [300] revealed that FtsW exhibits peptidoglycan polymerase activity that is dependent on the presence of its cognate class B transpeptidase FtsI/PBP2b. The reported interplay between FtsW and FtsI/PBP2b is a curious observation that supports the previous findings of the present study given that the abundance of FtsW is increased at each time point (1.4-fold at 15 minutes, and 1.7-fold at 30 and 60 minutes; Table 5) following exposure to GccF. These results reinforce the idea that the process of cell shape maintenance/elongation in *Lb. plantarum* ATCC 8014 target cells is prioritised by the target cells as stasis is induced by GccF.

3.9.1.1.4 LCP-family transcriptional regulator (ATQ32925.1)

The LytR-CpsA-Psr (LCP) family of transcriptional regulators are involved in peptidoglycan formation [42] and structural maintenance of the cell wall through autolysin regulation [55]. According to KEGG, the specific *Lb. plantarum* LCP family protein identified in this analysis is a cell envelope-related, polyisoprenyl-teichoic acid transferase.

LCP family proteins are widespread in gram-positive bacteria [243], where they have been shown to participate in the biosynthesis of bacterial cell wall teichoic acids (WTAs) and lipoteichoic acids (LTAs), as well as their respective attachment to the cell wall glycan (WTAs) and cell membrane (LTAs) [7] *via* their ligase activity [272]. The increase in production of this protein (1.8-fold at 15 minutes, 1.5-fold at 30 minutes, and 1.3-fold at 60 minutes) indicates that exposure of *Lb. plantarum* ATCC 8014 cells to GccF elicits a response that results in the need for precursors of peptidoglycan, again, suggesting that GccF is interacting with one or more molecules that are signalling the need for an up-regulation of cell wall metabolism; which begs the question, why does the cell think it needs to up-regulate cell wall synthesis when it is, in essence, being forced to slow down cell division and growth, and should be attenuating these

processes? Thus, it is unclear whether this effect is a direct result of GccF exposure, or a secondary effect of induced stasis.

3.9.1.1.5 Rod shape-determining protein, 'MreC' (ATQ33987.1)

It has been shown that in *E. coli*, *B. subtilis* and *L. monocytogenes*, *mre* (murein e) genes encode proteins involved in cell morphology [186]. Much like its previously mention counterpart, the rod shape-determining protein 'RodA', MreC is also required for the maintenance of cell shape in rod shaped bacteria [186]. It has been shown that MreC interacts with PBPs (Fig. 12) [85] in much the same way as RodA, indicating that it has an analogous role in mediating peripheral peptidoglycan synthesis; as opposed to septal formation [186]. A recent study which investigated the regulation of rod shape-determining proteins in an *E. coli* model system found that MreC interacts with the same PBP as RodA [198]. Moreover, the same study also reported that this MreC-PBP interaction elicits a response that results in a conformational change in the PBP such that its transpeptidase activity is effectively 'turned on' [198], suggesting that MreC is a modulator of PBP activity.

KEGG analysis of MreC showed that it is encoded in a cluster of genes that appear to be involved in the determination of cell shape or septum formation, including, the rod shape-determining proteins 'MreD' and 'MreB1', and the septum site-determining proteins 'MinD' and 'MinC'. Mining the proteomic data generated by this study showed that MreC was one of three *mre* encoded rod shape-determining proteins identified, the other two being 'MreB1' and 'MreB2'. Intriguingly, and unlike MreC, the abundances of both MreB proteins had decreased compared to the untreated control (MreC: 1.2-fold at 15 and 30 minutes, and 1.8-fold at 60 minutes; MreB1: 0.3-fold at 15 minutes, 0.1-fold at 30 minutes, and 0.3-fold at 60 minutes; MreB2: 0.2-fold at all time points). This would suggest that their central role in the formation of the actin-like, filamentous cytoskeleton of bacteria was not required, despite the resounding trend of increasing abundance in some of the other proteins related to the regulation of cell shape observed in this study. Whether localisation of MreB proteins at the inside face of the cytoplasmic membrane influences the distinctive way they are affected by GccF treatment compared to their other Mre protein counterparts, cannot be determined from the data collected. However, this decrease in abundance is a curious observation, especially considering the reportedly vital role of MreB in cell shape-determination [316], and the fact that it is usually co-transcribed with *mreC* [321]. It does, however, make sense in cells that had essentially ceased to divide and multiply; the primary effect of exposure to GccF.

3.9.1.1.6 4-hydroxy-tetrahydrodipicolinate reductase, 'DapB' (ATQ33638.1)

DapB is an enzyme which catalyses the nicotinamide adenine dinucleotide phosphate (NAD(P)H)-dependent reduction of 4-hydroxy-tetrahydrodipicolinate (HTPA) to tetrahydrodipicolinate (THDPA), the fourth reaction of the lysine synthesis, or diaminopimelic acid (diaminopimelate/DAP) pathway (Fig. 13) [48].

DapB is classified as being cytosolic, yet it was consistently found in the membrane fraction, albeit with lower PSMs (Table 6). A search of the proteomic results showed that its abundance had decrease in the cytosol fraction, however, only the change at 60 minutes was statistically significant. TOPCONS analysis weakly predicted that DapB contains a transmembrane region between residues 120 and 140, however, considering no evidence was found to support this, it is likely that its localisation in the membrane could be due to contamination, or it may non-covalently, but strongly, associate with the membrane.

Table 6: Comparison of DapB proteomic data values in membrane and cytosol fractions

Fraction	Protein	Sequence coverage %	PSMs	Unique peptides	MW (kDa)	Fold change*		
						T_{15}	T_{30}	T_{60}
Cytosol	DapB	73	496	13	28.5	0.682	0.773	**0.818**
Membrane	DapB	39	95	5	28.5	**1.756**	**2.420**	2.114

*Values in red are not statistically significant.

It has been reported that DapB's catalytic role constitutes one of two committed steps in the biosynthesis of the peptidoglycan precursor DAP [283]. DAP, or more specifically, *meso*-DAP, is a lesser-known amino acid component of the bacterial cell wall [317]. DAP incorporation into the bacterial cell wall is reportedly most common in gram-negative species of bacteria, although studies have shown that DAP is also present in some gram-positive species (*i.e. B. subtilis, Mycobacterium phlei, Streptomyces griseus, Tetrasphaera australis*, and *Rhodococcus rhodochrous*) [214].

KEGG analysis showed that in *Lb. plantarum* JDM1, *dapB* is part of a cluster of three genes which encode a conserved hypothetical protein and the tRNA CCA-pyrophosphorylase 'PapL'. Whether this colocation of genes is significant or not cannot be determined from the proteomic data. However, further analysis of the data showed that the abundances of enzymes involved in the three pathways that branch off from THDPA to synthesise DAP and then peptidoglycan [275], all appeared attenuated in response to GccF (Fig. 13), although the changes were not statistically significant.

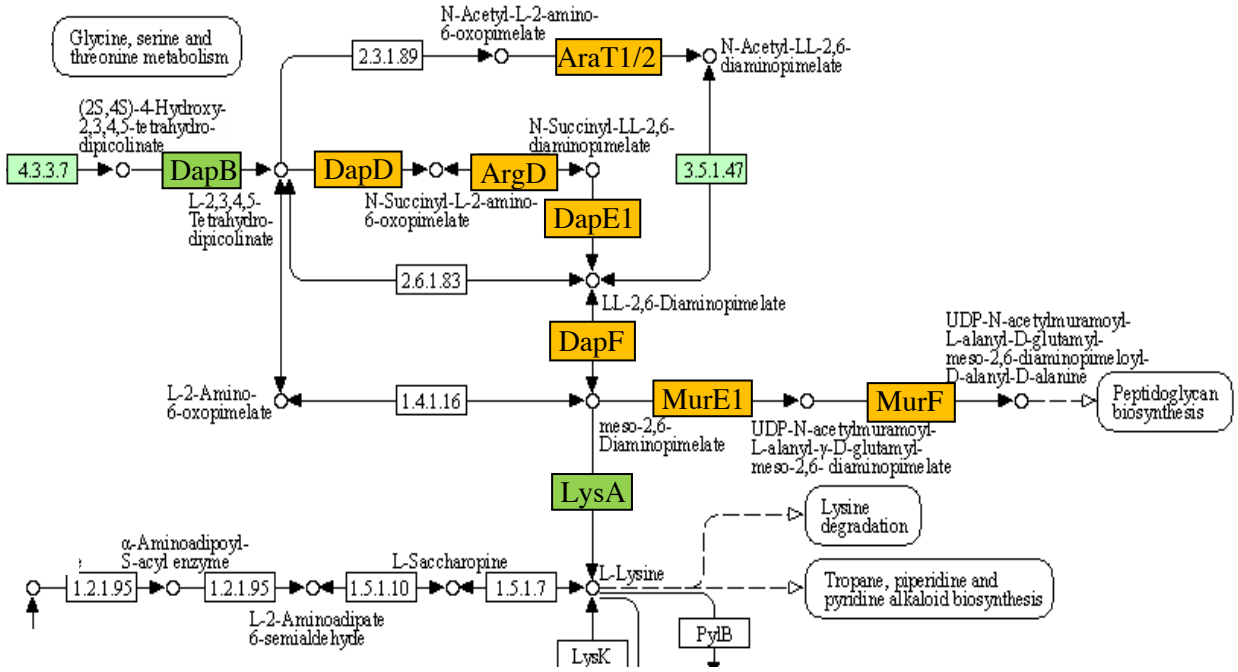

Figure 13: Overview of the DAP-pathway. Part of the KEGG generated DAP pathway for lysine biosynthesis from *Lb. plantarum WCFS1* showing the central position of DapB in this pathway. Proteins encoded by genes coloured orange were less abundant in the present study in GccF-treated cells, while those in olive green had increased abundance (Figure lifted from the *Lb. plantarum* WCFS1 lysine synthesis pathway in KEGG (lpl00300), © 2021, with permission from Kanehisa Laboratories [164]).

This list of enzymes includes those involved in the DAP pathway of peptidoglycan synthesis, namely, 'MurE1' and 'MurF' (uridine diphosphate (UDP)-*N*-acetylmuramoylalanyl-D-glutamate-2,6-diamonpimelate ligase, and UDP-*N*-acetylmuramoyl-tripeptide-D-ala-D-ala ligase, respectively); those involved in the acetyl-branch of DAP synthesis, 'DapD' (a tetrahydropicolinate *N*-acetyl-transferase), 'AraT1/T2' (a bifunctional protein with aminotransferase and dehydrogenase activities), and an *N*-acetyldiaminopimelate deacetylase, as well as those involved in the succinyl branch of DAP synthesis, 'ArgD' (an

acetylornithine/*N*-succinyldiaminopimelate aminotransferase), 'DapE1' (a succinyl-diaminopimelate desuccinylase), and 'DapF' (a diaminopimelate epimerase). Conversely, a protein involved in lysine biosynthesis, 'LysA', showed a four-fold increase in its abundance following GccF treatment. LysA is a decarboxylase which converts *meso*-DAP to L-lysine [35][48]. Taken together, these trends in differential enzyme production suggest that the increase in abundance of DapB in the membrane fraction of this work is not related to peptidoglycan synthesis, but rather to lysine synthesis, which can occur *via* another route (Fig. 13). Conversely, the opposing decrease in DapB shown in the cytosolic fraction of this study suggest that the entire DAP pathway is down-regulated upon GccF-treatment, which begs the question then as to why the abundance of LysA had increased upon exposure to the glycocin. This is especially interesting given the presumed absence of the precursors it requires for lysine biosynthesis as a result of the DAP-pathway being down-regulated. Exactly how either of these potential changes in abundance are involved in the mechanism of GccF requires further investigation. However, at face value, it suggests that GccF elicits a response in *Lb. plantarum* ATCC 8014 cells which prompts the cells to up-regulate lysine production specifically *via* the DAP pathway, despite there being no obvious reason for this to occur.

3.9.1.2 Proteins involved in energy metabolism

3.9.1.2.1 Phosphate starvation-inducible protein 'PhoH' (ATQ33714.1)

PhoH is a member of a family of proteins involved in, and induced under conditions of phosphate starvation in bacteria [11]. Very little is known about PhoH other than its ATP-binding activity shown in *E. coli* [173]. Protein sequence alignment analysis in *E. coli* revealed that PhoH is homologous to the N-terminus of superfamily I helicases [177], a finding that supports its ATP-binding/ATPase activity.

In a similar way to DapB (Section 3.9.1.1.6), TOPCONS analysis showed that PhoH is also a cytosolic protein that is weakly predicted to contain a transmembrane region between residues 142 and 162. This is interesting considering the findings from a preliminary study that investigated the molecular interactions of PhoH and suggested that the protein was cytosolic due to its lack of hydrophobic-hydrophilic domains [173]. However, despite its apparent cytosolic cellular localisation, the much greater PSM counts for PhoH in the membrane fraction suggests it is highly abundant in this fraction, which may, in turn, suggest a strong association between this protein and the membrane (Table 7).

Table 7: Comparison of PhoH proteomic data values in membrane and cytosol fractions

Fraction	Protein	Sequence coverage %	PSMs	Unique peptides	MW (kDa)	Fold change*		
						T_{15}	T_{30}	T_{60}
Cytosol	PhoH	27	9	5	35.8	7.602	0.985	0.788
Membrane	PhoH	54	379	14	35.8	**2.085**	**1.710**	**1.973**

*Values in red are not statistically significant.

Where Pho-family- or homologous phosphate starvation-inducible (psi) proteins have been characterised in bacteria, they are often encoded in 'Pho regulons' [324], however, this does not appear to be the case in *Lb. plantarum* according to KEGG and NCBI data. Analysis of both the *Lb. plantarum* JDM1 and WCFS1 genome maps showed that, in both strains, PhoH is encoded in a cluster with the following proteins: the DNA repair protein, 'RecO', the ribosome biogenesis GTPase, 'Era,' a diacylglycerol kinase, and a metal-binding protein involved in rRNA maturation. At face value this specific clustering of genes does not appear to reveal any additional information about PhoH and/or its activity or function(s) in *Lb. plantarum* cells. A STRING analysis suggests it is involved in homologous recombination (Fig. 14). It has been shown that *phoH* of *B. subtilis* is colocalised in a cluster containing a diacylglycerol kinase gene, *dgkA* [172]. Moreover, a bioinformatics study showed that this specific clustering of genes is conserved in gram-positive organisms [168], suggesting that an evolutionary link exists between these encoded proteins. The same study also showed that *B. subtilis phoH* is not part of a Pho-regulon, but rather that both it, and its orthologs, are involved in phospholipid metabolism and RNA modification.

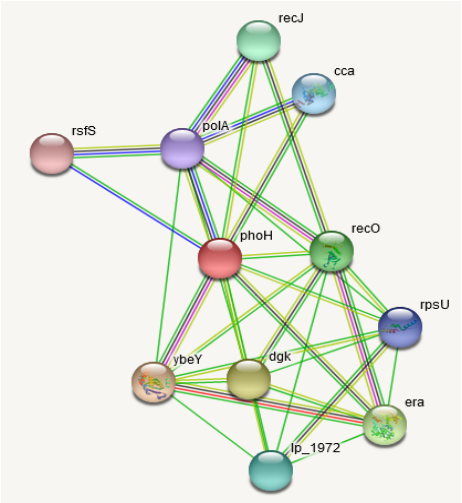

Figure 14: PhoH STRING diagram. STRING network showing the potential protein/gene interactions of PhoH in *Lb. plantarum* WCFS1.

Interestingly, the STRING analysis (Fig. 14) predicts an interaction with a ribosome silencing factor (rsfS), which was the protein showing the largest change (increase) in abundance in this study (Section 3.10.1.1.1). This would suggest there could be some cross talk between these two proteins and may provide a clue as to the signalling pathway used by GccF to bring about rapid stasis, and that this may be a specific GccF response.

3.9.1.3 Proteins involved in cellular transport

3.9.1.3.1 Aquaporin family protein, 'GlpF4' (ATQ33108.1)

Aquaporins belong to a large family of channel proteins that facilitate the transport of water and other small molecules across biological membranes in order to maintain the homeostasis of many physiological processes [182]. These integral membrane proteins are present in almost all living organisms [151]. Although water permeation was the first, and best-characterised function of these channel proteins, some aquaporins are also capable of transporting other molecules including, urea, glycerol, lactic acid, hydrogen peroxide [25], and even gaseous substrates such as carbon dioxide (CO_2), oxygen (O_2) and nitric oxide (NO) [52].

Lb. plantarum JDM1 and WCFS1 genome map analyses in KEGG showed that the specific aquaporin family protein identified in this work is an aquaglyceroporin known as the glycerol uptake facilitator protein 4, or 'GlpF4'. Despite the name, a 2013 study by Bienert and colleagues [25] revealed that while GlpF4 is indeed involved in glycerol transport, it was also shown to facilitate the transport of lactic acid, and is one of the first functionally characterised lactic acid transport systems to be described in *Lb. plantarum* cells. It has been postulated that aquaglyceroporins such as GlpF4 serve a physiological role in osmoregulation by excreting osmolytes in order to maintain a normal cell volume [151], and as a general response to lactic acid stress [25].

In the present study, the abundance of GlpF4 had increased at all three time points compared to the untreated control (1.6-fold at 15 minutes, 1.3-fold at 30 minutes, and 1.5-fold at 60 minutes). It is worth mentioning that only two aquaglyceroporins were identified out of the six that are encoded in *Lb. plantarum* (with only one of the two showing a significant change in abundance in this study). 'GlpF6' was the other aquaglyceroporin identified and, interestingly, its abundance was increased at the 15 minute time point (although the value was not statistically

significant) but decreased at both the 30 and 60 minute time points, although, again, without statistical significance.

Currently, very little is known about the function(s) of GlpF6 in any living system. The study by Bienert and colleagues (2013) [25] is the only one to date, and they reported that GlpF6 does not facilitate the transport of water, glycerol, urea, hydrogen peroxide, lactic acid or dihydroxyacetone. At the low cell density observed during the duration of this experiment, there is little reduction in pH, thus, little likelihood of an increase in lactic acid concentration. It is therefore likely that the increase in GlpF4 abundance in the present study can be attributed to the general stress response of the target *Lb. plantarum* cells, as opposed to a being a GccF-specific response.

3.9.1.3.2 Oxa1 family membrane protein insertase, 'YidC' (ATQ33376.1)

Membrane insertase proteins are capable of facilitating the insertion, correct folding and/or complex formation of integral membrane proteins [171]. Discovered in 2000 [265], YidC possesses insertase, foldase and translocase activity, and also participates in complex formation of integral membrane proteins in bacteria [72]. Although YidC is capable of facilitating insertion on its own, it commonly associates with other proteins involved in similar integration pathways, such as, 'Sec' proteins *via* the Sec-dependent pathway [73] and signal recognition particle (SRP) proteins such as 'FtsY' [171]. It has also been shown that membrane insertion by YidC (or its homologs) can occur both co-translationally [339], and post-translationally [225]. Interestingly, YidC has been shown to exhibit different activities depending on the insertion pathway(s) being utilised by the cell [59]. For example, the mechanosensitive channel protein 'MscL' only requires YidC for its insertion into the membrane [100], whereas the multi-spanning membrane protein 'MtlA' is integrated into the membrane by 'SecE' followed by its correct folding inside the membrane which is facilitated by the foldase activity of YidC [72].

It is difficult to determine the specific role YidC plays in *Lb. plantarum* ATCC 8014 cells during stasis based on the proteomic data collected in this study. Here, the abundance of YidC had increased 2-fold across all three time points (2-fold at 15 and 60 minutes, and 2.2-fold at 30 minutes). KEGG analysis of the *Lb. plantarum* JDM1 genome map, and YidC-related physiological pathways, revealed no obvious clues as to the possible effects of this increase abundance of YidC in the target cells during stasis. However, it does appear to coincide with the findings from a 2016 study which showed that upon bacterial exposure to cell surface

stressors, YidC protein levels were elevated [301]. The same study also revealed that YidC depletion in *E. coli* cells results in the up-regulation of several genes encoding stress proteins such as 'GroEL' and 'DnaK' [301]. Taken together, these findings suggest that YidC plays a more general role in bacterial stress response, and that the increase in abundance of YidC in the present work is most likely a general response, as opposed to a GccF-specific response. Moreover, the finding by Thakur and colleagues (2016) [301] suggest that the foldase activity of YidC, in particular, is prioritised during bacterial cell stress.

It is tempting to speculate that the rationale behind this response is due to ability of YidC to co-translationally interact with proteins prior to their insertion into the membrane and subsequent folding, as the machinery required for targeting (and folding) newly translated integral membrane proteins to the cell membrane may not be available in the state of GccF-induced bacteriostasis. If this is correct then specific YidC-dependent proteins should be prioritised for membrane insertion and proper folding under GccF-induced stasis. The significant increase in the abundance of the YidC-dependent MscL channel protein seen in this study is consistent with this theory.

3.9.1.3.3 ABC transporter permease, 'TagG' (ATQ32425.1)

ABC transporters constitute one of the largest superfamilies of transporter proteins that are universally distributed across various phyla from prokaryotes to humans [139]. They function primarily in the translocation of solutes across biological membranes in an ATP-dependent manner, a function which helps lend these transporters to many cellular processes including, nutrient uptake [274], export of toxic molecules [77], bacterial cell wall synthesis [187], multi-drug resistance and disease pathogenesis [351], and bacterial immunity [159], to name a few.

The specific ABC transporter protein identified in this work belongs to the teichoic acid glycerol (Tag) family which is involved in teichoic acid (TA) translocation across the cytoplasmic membrane [187]. Teichoic acids are anionic polymers of polyglycerol phosphate units that are incorporated into the cell envelope of gram-positive bacteria in two ways, either as wall teichoic acids (WTAs), covalently attached to peptidoglycan, or as lipoteichoic acids (LTAs), anchored to the cytoplasmic membrane *via* a glycolipid [233]. It has been shown that WTAs in the cell envelope of gram-positive bacteria mediate extracellular interactions, and influence membrane integrity (*e.g.* stability and permeability) similar to their functions in the outer membrane of gram-negative bacteria [296]. Additionally, WTAs have also been shown to play a crucial role

in the recruitment of enzymes involved in peptidoglycan biosynthesis by colocalising, and physically interacting with them [109].

The increase in abundance of the TagG ABC transporter permease in the present study (1.4-fold at 15 minutes, 2.2-fold at 30 minutes, and 1.9-fold at 60 minutes) suggests that TA translocation across the cell membrane had increased in the GccF-treated *Lb. plantarum* ATCC 8014 cells in an effort to supply these molecules for incorporation into the cell envelope. Considering that many of the proteins already mentioned in this section are in some way implicated in peptidoglycan synthesis (*e.g.* RodA, PBP2b, FtsW, the LCP transcriptional regulator, MreC, and DapB), the rationale for the increase in TagG in cells approaching stationary phase might be that some of these enzymes require the WTA scaffold in order to arrange themselves prior to carrying out their specific activity.

Further analysis of the proteomic data revealed that the cognate ATP-binding protein of the TagGH transporter complex, 'TagH' showed a statistically significant decrease in abundance following target cell exposure to GccF (Section 3.10.2.1.3). This decrease in TagH abundance alone renders any potential suggestion of TA translocation across the cell membrane redundant as the ATPase activity of TagH is required for the activation of the TagG permease. Regardless, the fact remains that the increase in TagG abundance following target cell exposure to GccF may still be a GccF-specific response, as it has not as yet been implicated in the general stress response in bacteria. With these findings in mind, it is possible that the increase in abundance of the TagG permease observed following GccF treatment occurs in response to the inability of the cell to divide, prompting the cell to up-regulate the machinery required for teichoic acid export.

3.9.1.4 Proteins involved in signal transduction

3.9.1.4.1 Two-component system regulatory protein, 'YycI' (ATQ32187.1)

In bacteria, a two-component system (TCS) involves two proteins, typically a sensor kinase and a response regulator which, together, serve the basic, but fundamental, function of sensing and responding to environmental stimuli [294]. Briefly, the sensor kinase (usually a histidine kinase; HK) is involved in sensing specific, external signals which are then transferred (*via* the process of autophosphorylation inside the kinase protein) to the response regulator (RR; usually a transcriptional regulator) which acts on the appropriate genes in order to alter their expression

for bacterial adaptation and/or survival [329][140]. TCSs themselves are also regulated by dedicated proteins such as 'YycI' and 'YycH' [299]. In *B. subtilis*, YycI regulates the activity of the TCS known as 'YycFG' [299], whilst in *S. aureus* the same complex is referred to as 'WalRK' [111]. To avoid any confusion, this system will from herein be referred to as YycFG.

Part of the 'OmpR' family of TCSs, YycFG is essential for growth in almost all bacteria species that encode it [99] [294] [338], with the exception of some pathogenic species of bacteria, such as *Streptococcus pneumoniae* (*S. pneumoniae*), which only require the RR, YycF, for cell viability [311]. This is likely to be due to the central role of YycFG in maintaining cell wall metabolism by controlling the expression of specific autolytic enzymes [299][111][140]. Where the YycFG regulatory protein YycI is concerned, Szurmant and colleagues (2007) [299] found that deletion of *yycI* in *B. subtilis* results in growth and cell wall 'defects' that render the cells susceptible to SDS-induced lysis. Moreover, electron microscopy analyses from the same study revealed that the cell wall 'defect' did not result in a thinner cell wall, suggesting that it was the result of a change in either the cell wall composition or its rate of synthesis [299]. In *S. aureus*, YycI has been shown to specifically regulate the kinase protein (YycG) of YycFG when in complex with the regulator YycH, ultimately altering its capacity to phosphorylate and, thus, transmit the signal(s) it receives [50][111]. Additional findings by Cameron and colleagues (2016) [50] revealed that depletion of *yycI* and *yycH* in *S. aureus* resulted in the down-regulated transcription of the genes encoding the autolysins 'AtlA', 'IsaA', 'Sle1' and 'SsaA' [50], implicating YycI and YycH in the regulation of autolytic gene expression *via* the regulation of YycFG.

KEGG analysis of both *Lb. plantarum* JDM1 and WCFS1 genome maps showed that YycI is encoded in a cluster of genes including YycG (the HK) and YycF (the RR), proteins it (presumably) regulates, as well as the second regulatory protein, YycH. Further analysis of the proteomic data showed there was a decrease in the abundances of both YycG and YycH in the membrane fraction (YycG: 0.6-fold at 15 and 60 minutes, and 0.2-fold at 30 minutes; YycH: 0.9-fold at 15 and 30 minutes, and 0.7-fold at 60 minutes), while the abundance of YycF had increased (2.5-fold at 15 minutes, 2-fold at 30 minutes, and 2.2-fold at 60 minutes), although all values (apart from the YycF 15 minute sample) were not statistically significant. Considering that YycI and YycH are both required for interaction with, and full activation of YycG [299][50][111], the discrepancy in their respective changes in abundance found in this study is puzzling (YycI: 2-fold at 15 minutes, 1.4-fold at 30 minutes, and 1.3-fold at 60 minutes), although it may help explain the discrepancy observed in the abundance of YycF and YycG. The fact that YycF alone is indispensable in some species of bacteria suggests it is able

to function independently of its cognate HK. The decrease in abundance of YycG may, therefore, be a direct result of the increase in abundance of YycI, a speculation supported by the findings of Szurmant and colleagues (2007) [299] who showed that YycI is capable of forming homodimers that strongly interact with the YycG promoter. This finding, along with those mentioned above, suggest that YycI possesses the ability to regulate both the expression and activity of YycG but only when complexed with YycH.

Given the vital sensing and signalling functions of YycG in bacteria, the decrease in abundance observed here may suggest that these processes are not required following exposure of *Lb. plantarum* ATCC 8014 to GccF as, perhaps, the initial sensing of GccF is sufficient enough to produce the appropriate signal and response. It is possible that the significant increase in abundance of YycI in GccF-treated *Lb. plantarum* ATCC 8014 cells is a response generated to specifically regulate the expression of YycG in order to lessen the sensing of other environmental stimuli and the corresponding signalling and response(s) that would ensue. Whether this increase in abundance is GccF-specific, or a general stress response is difficult to determine from the data. However, Dubrac and colleagues (2008) [91] noted that during cell stasis in *B. subtilis*, activation of the HK, YycG, is reduced, resulting in less autolysin synthesis and decreased expression of the cell division genes *ftsAZ*; which was also observed in the present study. Moreover, it has been shown that various TCSs are implicated in general stress in bacteria [241] [33]. These findings suggest that the differential change in abundance of YycFG, YycH and YycI observed here is likely to be a general stress response to stasis in *Lb. plantarum* ATCC 8014 cells.

3.9.2 Membrane proteins with the most significant decrease in abundance

The abundances of 62 membrane proteins were shown to have decreased upon target cell exposure to GccF. As previously mentioned under section 3.9, following manual analysis of the 84 selected (cytosolic and membrane) proteins which showed the most significant change in there abundance, only 6 of these were found to be true membrane proteins which showed a decrease in their abundances (Appendix 7.6; Table 15). To further understand how these proteins might be involved in, or contribute to the effects of GccF on *Lb. plantarum* ATCC 8014 cells, the following subsections provide more information about each protein and the cellular process(es) they are involved in. In the interested of time and space, only three (Table 8) of the six proteins which showed the largest significant decrease in their abundance are discussed below.

Table 8: Membrane proteins with the most statistically significant decrease in abundance

Accession #	Protein	Sequence coverage %	PSMs	Unique peptides	MW (kDa)	Fold change*		
						T_{15}	T_{30}	T_{60}
ATQ33988.1	Rod shape-determining protein, **MreB1**	66	1325	20	35.1	**0.263**	**0.141**	0.287
ATQ33447.1	Signal recognition particle-docking protein, **FtsY**	31	58	9	53.6	**0.607**	**0.306**	**0.507**
ATQ32657.1	PIN/TRAM domain-containing protein, **PilT**	39	341	12	44.3	0.921	**0.755**	1.098

*Values highlighted in red are not statistically significant.

3.9.2.1 Proteins involved in cell growth and maintenance

3.9.2.1.1 Rod shape-determining protein, 'MreB1' (ATQ33988.1)

As mentioned previously in section 3.9.1.1.5 (MreC section), the rod shape-determining protein MreB1 functions in the formation of the actin-like cytoskeleton in bacteria, which has been shown to be essential for maintaining cell morphology in many rod shape bacteria [108][79]. MreB1 is a membrane-associated, cytosolic protein which interacts with its membrane bound Mre counterparts, 'MreC' and 'MreD', to form short, helical-like structures along the intracellular face of the cytoplasmic membrane [102]. Analysis of the raw proteomic data identified two MreB proteins in *Lb. plantarum* ATCC 8014 cells, namely, 'MreB1' and 'MreB2', both of which were present at lower abundance following GccF treatment. Interestingly, KEGG analysis of the *Lb. plantarum* JDM1 and WCFS1 genome maps showed that these proteins are encoded in separate gene clusters. MreB1 is encoded in the same cluster described in section 3.9.1.1.5 along with genes encoding the septum site-determining proteins 'MinD' and 'MinC', as well as the cell shape-determining proteins 'MreD' and 'MreC'. MreB2 is encoded in a cluster along with genes encoding the glycine cleavage system H protein

'GcsH2', the previously mentioned rod shape-determining protein 'RodA' (Section 3.9.1.1.1), a hypothetical protein, the alpha-hemolysin-like protein 'HlyA', a ribosomal-protein serine acetyltransferase, and the UDP-*N*-acetylglucosamine 1-carboxyvinyltransferase 'MurA2'. It is possible that the separate genomic localisation or, more specifically, the grouping of either MreB protein in their respective gene clusters implies that MreB1 and MreB2 are, i.) involved in two distinct pathways which may or may not converge, and/or ii.) bear specialised functions which complement one another during cell wall elongation and/or division. These speculations are supported by the MreB1 STRING diagram (Fig. 15) which shows a lack of MreB2. Studies that have made the comparison between the individual MreB proteins/homologs/paralogs often found in different bacterial species (*e.g. B. subtilis* encodes: MreB, MreBH (a MreB homolog) and Mbl (MreB-like)) [108], have shown that, in most cases, MreB(1) fulfils the most frequently assigned MreB function; the formation of actin-like, helical filaments at the cell membrane, while MreBH performs the same function within the cytosol (*i.e.* away from the membrane) [79]. Mbl behaves similarly to MreB at the cell membrane, although it has also been shown to interact with, and recruit both integral membrane and cytosolic proteins to the cell membrane [79]. Considering the essential role of MreB proteins in maintaining cell shape, as well as the evidence that has repeatedly shown that a lack of MreB, by depletion [74], inhibition [154], mutation, and/or deletion [108], results in a change in cell morphology and/or growth, the decrease in abundance of MreB1 observed in this study (0.3-fold at 15 and 60 minutes, and 0.1 at 30 minutes) strongly suggests that this is also the case for *Lb. plantarum* ATCC 8014 cells treated with GccF.

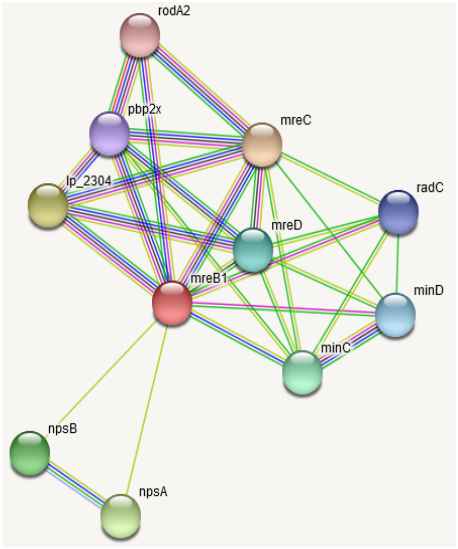

Figure 15: MreB1 STRING diagram. STRING network showing the first shell of interactions of MreB1 in *Lb. plantarum WCFS1*.

Evidence from unpublished microscopy experiments performed in *Lb. plantarum* ATCC 8014 cells showed that cell morphology is indeed altered following treatment with GccF (Appendix 7.11; Fig. 26). However, these morphological differences appear to be constrained in some way as these microscopy images show that, while some treated cells appear as linked chains or

sausage-like due to their inability to divide, others appear normal when compared to the images of the untreated control cells. The linked chain and extremely elongated cell morphology of *Lb. plantarum* ATCC 8014 cells treated with GccF suggests that proteins involved in cell division are specifically affected by GccF in such a way that the cells are able to form (what appears to be) the start of the septum, however, division does not go to completion.

3.9.2.2 Proteins involved in cellular transport

3.9.2.2.1 Signal recognition particle-docking protein, 'FtsY' (ATQ33447.1)

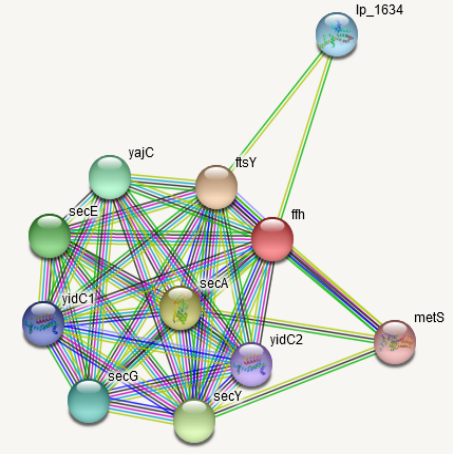

Figure 16: FtsY STRING diagram. STRING network showing the protein interactions of FtsY in *Lb. plantarum* WCFS1.

From curated data bases
Experimentally determined
Gene neighbourhood
Gene co-occurrence
Gene fusions
Text Mining

Signal recognition particle (SRP)-docking (receptor) proteins such as FtsY are involved in targeting and facilitating the insertion of newly synthesised proteins into the bacterial cell membrane [282]. To be more specific, in both gram-positive and gram-negative bacteria, FtsY functions in a similar way to that of the secretory pathway protein 'SecB', which delivers nascent proteins to the Sec channel complex, SecYEG, and are then incorporated into the cytoplasmic membrane or secreted into the periplasm [125]. The function of FtsY differs slightly to that of SecB however, in that FtsY guides the newly translated protein to the SecYEG channel in the membrane while it remains complexed with its cognate SRP and the ribosome. Then, as the protein is translated, it passes through the channel into the membrane where it remains [125].

According to KEGG, *ftsY* in *Lb. plantarum* JDM1 is part of a gene cluster which also encodes the ribonuclease III 'Rnc', the chromosome segregation protein 'Smc', an uncharacterised hypothetical protein, and the SRP protein 'Ffh'. KEGG also shows that FtsY is implicated in quorum sensing, protein export, and the bacterial secretion system in *Lb. plantarum* JDM1, findings which corroborate the connection between FtsY and the Sec pathway in this organism (Fig. 16). Analysis of the proteomic data showed that the abundance of Ffh, the cognate SRP

protein of FtsY, had also decreased in the membrane fraction following exposure to GccF. The decreased abundance of both FtsY and Ffh suggests that the recognition and binding of nascent proteins (by Ffh), and the subsequent delivery of these proteins (by FtsY) to the cell membrane is attenuated upon exposure of the target cells to GccF (0.6-fold at 15 minutes, 0.3-fold at 30 minutes, 0.5-fold at 60 minutes). As a result, the integration of newly synthesised proteins into the cell membrane *via* this specific pathway is also likely to be attenuated. Further analysis of the proteomic data identified three other proteins associated with the Sec pathway, namely, 'SecA', 'SecY' and 'Asp1', which were all present in lower abundance compared to the control cells, although these changes were not significant. Collectively, these results suggest that in *Lb. plantarum* ATCC 8014 cells treated with GccF, both the Sec pathway and the SRP pathway are inhibited.

Findings from a 2010 study which investigated membrane protein biogenesis in FtsY-depleted *E. coli* cells showed that both integral membrane protein expression, the number of membrane-associated ribosomes was decreased [349]. Moreover, a similar study from 2009 found that FtsY-depletion in *E. coli* resulted in the reduced rate of protein synthesis, not as a consequence of ribosome down-regulation, but rather because of the inhibition of translation by a ribosome modulator [18]. Taken together, these findings suggest that the decrease in abundance of FtsY in the present study indirectly affects protein translation as a result of a multifaceted response to GccF. The intricacies of this response (*i.e.* the assumed increase in abundance of a ribosome modulator that inhibits translation as a result of FtsY decrease in abundance) make it difficult to ascertain whether this is a GccF-specific response. However, given that FtsY has not been linked to the general stress physiology of gram-positive bacteria, it may indeed be that this decrease in abundance is the result of the exposure of *Lb. plantarum* ATCC 8014 cells to GccF. Just how the control is exerted, however, remains elusive.

3.9.2.3 Proteins with no associated GO terms

3.9.2.3.1 PIN/TRAM domain-containing protein, 'PilT' (ATQ32657.1)

PilT N-terminus (PIN) domain-containing proteins usually function as ribonucleases (RNases) that cleave RNA in a sequence-specific manner [13] with the TRAM (TRM2 and MiaB) domain facilitating RNA-binding [10]. The specific PIN/TRAM domain-containing protein identified in this work was categorised as an ATPase by KEGG, and designated 'PilT'.

Studies have shown that PilT functions specifically in the retraction of (type IV) pili as a 'retraction ATPase' in bacteria [62]. Not to be confused with flagella or fimbriae, pili are proteinaceous cell surface polymers composed of hundreds (potentially thousands) of small (15-25 kDa) pilin protein subunits [250] that allow bacteria to interact with their surrounding environment [201]. In gram-positive bacteria, pilin subunits are synthesised in the cytosol, secreted *via* the Sec pathway (*i.e. via* the SecYEG channel protein), crosslinked and extended at the outer face of the cytoplasmic membrane, then covalently attached to the cell wall as fully assembled pili [237][181][180]. The function of pili varies depending on the type of pili synthesised (*e.g.* type I, II, IV, S-type, P-type) but can include adhesion, invasion, aggregation, biofilm formation, and immunomodulatory functions [279]. Most pili, however, are involved in bacterial adhesion for pathogenesis, although pili from non-pathogenic bacteria, of which few have been described, are implicated in adhesion for niche-adaptation (such as in the GI tract) [181]. As one might assume, the different types of pili confer different functions and/or activities dependent on the bacteria from which they are produced. In the interests of space, only those pili relevant to *Lactobacillus*, type IV pili, will be discussed here.

Type IV pili play roles in host cell and surface adhesion, cell motility, biofilm formation, DNA and phage uptake, and cellular invasion. A remarkable, and distinguishing, feature of type IV pili is their ability to reversibly extend and retract [201], which has been proposed as the reason for the observed twitching motility of bacteria in which flagella are absent [212]. These cycles of pili extension and retraction are facilitated by the 'PilU' and 'PilT' proteins, respectively [213]. Studies have shown that pili retraction by PilT is the sole driving force for the twitching motility of bacteria, generating motor forces that can exceed 100 pN [202]. As such, studies which investigated PilT depletion in range of different bacterial species (*e.g. Neisseria gonorrhoeae, Acinetobacter baylyi, Pseudomonas stutzeri, and Neisseria meningitidis*) found that pili function was completely lost when PilT was absent, despite pili still being abundant [342][124][41][192]. Additionally, it has also been shown that PilT depleted cells commonly exhibit altered surface adherence and lack the ability to mediate DNA uptake [2].

With these findings in mind, the decrease in PilT abundance seen in the present study suggests that the *Lb. plantarum* ATCC 8014 cells are unable to adhere to surfaces, such as in the GI tract of humans, following exposure to GccF suggesting that these cells would struggle to colonise, form biofilms and, thus, thrive in such environments, greatly reducing their likelihood of survival. The specific decrease in abundance of PilT observed upon exposure of *Lb. plantarum* ATCC 8014 cells to GccF (0.9-fold at 15 minutes, 0.8-fold at 30 minutes, and 1.1-fold at 60

minutes) has not yet been described as a general stress response in gram-positive bacteria and, as such, it is possible that this is indeed a GccF-specific response in these cells.

3.10 Proteins identified in the cytosolic fraction

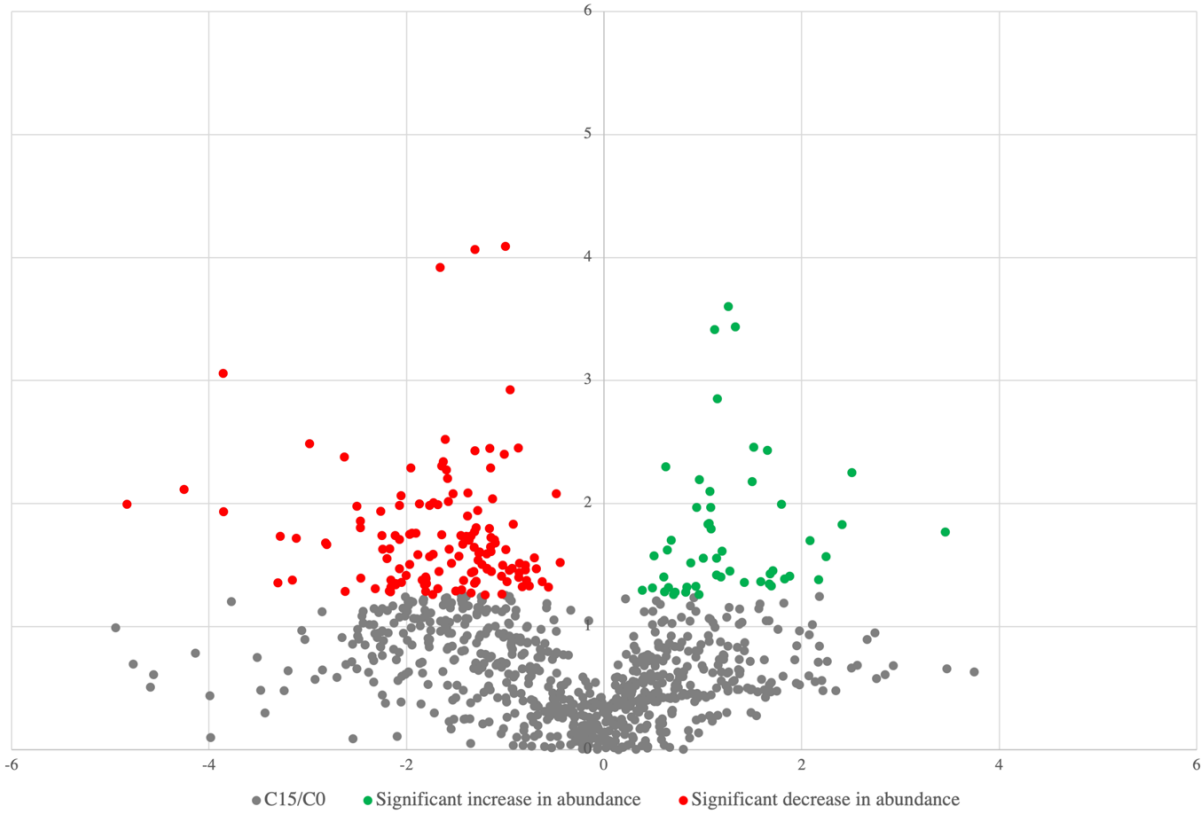

Figure 17: Distribution of proteins identified in the cytosolic fraction of *Lb. plantarum* ATCC 8014 cells after 15 minutes of exposure to GccF. Volcano plot showing an example of the change in abundance of all proteins identified in the cytosolic fraction, including those with a significant increase (green) and those with a significant decrease (red) in abundance. Proteins with a p-value ≤ 0.05 were considered significant, as determined by the manual normalisation method outlined in Appendix 7.3.

A total of 281 cytosolic proteins were identified with a statistically significant change in their abundance compared to the untreated control. Unlike the proteins identified in the membrane fraction, those selectively identified with the largest significant change in their abundance in the cytosolic fraction (62 total) were, for the most part, identified in the correct fraction, with the exception of only

seven membrane proteins contaminating the data (Appendix 7.7; Table 16). Of these 62 proteins, 22 showed a significant increase in their abundance (ranging from 1.5 to 10-fold), whilst 40 showed a significant decrease (ranging from 0.7 to 0.03-fold) (distribution at 15 minutes shown in Fig. 17). Some of these proteins which could not be characterised beyond their PD identifier were excluded and listed in Appendix 7.9 (Table 18). The remaining list of proteins was narrowed down to four with the most statistically significant increase (Table 9), and six with the most significant decrease (Table 11). These are discussed in the appropriate subsections that follow.

Table 9: Cytosolic proteins with the most statistically significant increase in abundance

Accession #	Protein	Sequence coverage	PSMs	Unique peptides	MW (kDa)	Fold change		
						T_{15}	T_{30}	T_{60}
ATQ33363.1	Ribosome silencing factor, **RsfS**	54	58	5	13	**10.952**	**7.809**	**9.408**
ATQ33208.1	Large conductance mechanosensitive channel protein, **MscL**[+]	58	57	5	14	**5.298**	**4.923**	**6.952**
ATQ34034.1	Uracil phosphoribosyl-transferase, **Upp**	54	462	9	23	**3.469**	**3.567**	**4.326**
ATQ32782.1	UDP-*N*-acetylenolpyruvoyl-glucosamine reductase, M**urB**	39	254	8	32.3	**1.783**	**1.990**	**2.352**

[+] Proteins identified in the wrong fraction.

3.10.1 Cytosolic proteins with the most significant increase in abundance

The abundances of a total of 92 proteins were shown to be significantly increased in the cytosolic fraction of *Lb. plantarum* ATCC 8014 cells over time in response to treatment with GccF. To further understand how these proteins might be involved in, or contribute to the effects of GccF on *Lb.*

plantarum ATCC 8014 cells, the following subsections provides more information about each protein and the cellular process(es) they are involved in. Four of the six proteins which showed the most significant increase in abundance are discussed below.

3.10.1.1 Proteins involved in translation

3.10.1.1.1 Ribosome silencing factor, 'RsfS' (ATQ33363.1)

Averaging an 8.5-fold increase in abundance compared to the untreated control, this ribosome silencing factor was identified as having one of the most significant changes in abundance across all proteins identified in this work (Table 9). Ribosome silencing factors (Rsf) are repressor proteins that bind to specific ribosomal components (*e.g.* ribosomal proteins, subunits) and tRNAs to effectively silence ribosome activity and thus, inhibit protein translation [127]. Considering that the target *Lb. plantarum* ATCC 8014 cells in the present study were approaching stationary phase at the time of sampling/fractionation, it is no surprise that the protein translation machinery was down-regulated.

Protein synthesis, in itself, constitutes one of the most energy-demanding processes in bacterial cells [127]. During stasis, non-essential cellular components are generally degraded to yield nutrients and other basic building blocks for bacterial cell survival [350]. However, because ribosomes are essential for growth and represent a major investment of material and energy, the ribosomal machinery is instead stored and its activity is significantly reduced to, i.) preserve energy, and ii.) only synthesise proteins that are absolutely necessary for survival during stasis [350]. The mechanism by which bacterial ribosome silencing factors effect translation inhibition has only recently been experimentally confirmed in the gram-positive bacterium *S. aureus* [170]. It was found that the association between the bacterial ribosomal subunits (50S and 30S) is inhibited when the ribosome silencing factor, RsfS, binds to the L14 ribosomal protein of the 50S subunit [127][170], which is similar to the mechanism used by RsfS in gram-negative bacteria [127][195]. Analysis of the proteomic data revealed that the abundance of L14 increased approximately three-fold following exposure to GccF, although the result was not significant. This increase may explain the greater (8.5-fold) increase in RsfS abundance, as a way to ensure that an excess of RsfS is available to bind L14 proteins during stasis, therefore guaranteeing ribosome silencing. Although not the only mechanism of ribosomal shutdown to be reported in bacteria, this specific mechanism has been shown to be up-regulated as a result of general stress in both gram-positive and gram-negative bacteria [241][320]; findings which

suggest that the significant increase in RsfS abundance in the present study is unlikely to be a GccF-specific response in treated *Lb. plantarum* ATCC 8014 cells. It is, however, consistent with what is observed when cells are treated with GccF. Just how the response is so quickly implemented remains unexplained.

3.10.1.2 Protein involved in cellular transport

3.10.1.2.1 Large mechanosensitive channel protein, 'MscL' (ATQ33208.1)

Mechanosensitive channels (MSCs) such as MscL are proteins involved in translating membrane tension caused by external forces (*e.g.* change in osmotic pressure) into electrophysiological signals [184]. To enact this function, MSC proteins effectively act as a release valve to spontaneously allow efflux of osmolytes or other small molecules from the cytosol in order to alleviate turgor pressure and prevent cell lysis [264][141][241]. Although MscL is a known membrane protein, TOPCONS analysis showed that residues 40-65 are strongly predicted to be cytosolic. Further analysis of the proteomic data showed that while the PSM counts were much greater, and that the abundance of this protein was also increased in the membrane fraction, this change was not statistically significant at any time point (Table 10).

Table 10: Comparison of MscL proteomic data values in membrane and cytosol fractions

Fraction	Protein	Sequence coverage %	PSMs	Unique peptides	MW (kDa)	Fold change*		
						T_{15}	T_{30}	T_{60}
Cytosol	MscL	58	57	5	14	**5.298**	**4.923**	**6.952**
Membrane	MscL	63	172	6	14	1.542	1.756	1.557

*Values in red are not statistically significant.

The lower PSM counts in the cytosol may be a reflection of the small percentage of this protein that appears in this fraction. It may also be true that, due to the impending GccF-induced stasis, these proteins accumulate in the cytosol as a result of potential delays in membrane insertion. The fact that MscL was consistently detected in the cytosolic fraction at all time points, although its abundance was low as indicated by the low PSM counts, suggests that it is possible that the

protein has not been correctly processed, which may be an indirect effect of exposure of the cells to GccF.

Most bacterial species commonly encode the single, large MSC protein, MscL [224], however, two other MSC proteins, 'MscS' (small) and 'MscM' (mini), have also been identified in some species [23]. The main difference between the three MSCs is their respective conductance capacity, hence the assigned large, small, and mini labels [94]. It is worthwhile mentioning that although similar, MSC proteins from different bacteria can show variation in their mechanosensitivity and kinetics [224]. This may explain why the expression of certain encoded MSCs is favoured over others, such as in the case of *L. lactis* which uses MscL as its principal MSC, despite also encoding MscS [107].

Analysis of the proteomic data from the present study revealed a second MSC in *Lb. plantarum* ATCC 8014 cells which was annotated as a 'moderate' MSC in the reference *Lb. plantarum* JDM1 and WCFS1 genome maps in KEGG. The abundance of this MSC had also increased following target cell exposure to GccF. The significant increase in abundance of MscL (and MscS) in the present study suggests that a change in osmolarity had been detected in the *Lb. plantarum* ATCC 8014 cells following exposure to GccF. If this is correct, it would implicate GccF in a osmotic-stress inducing role. It is interesting to note that the mechanism of another glycocin, sublancin 168, has been shown to involve both a glucose PTS [113][345][30] and the MscL channel protein [179][29] in order to kill its target cells.

It has already been established that GccF-induced bacteriostasis uses the GlcNAc PTS, PTS18CBA, to dock the bacteriocin [20]. To find a change in the abundance of the MscL channel protein in *Lb. plantarum* is very interesting and may point to a common mechanism between GccF and sublancin. It is possible that this 'docking' of GccF at the cytoplasmic membrane of susceptible bacterial cells potentially stimulates changes in the tension of the lipid bilayer, resulting in the activation/recruitment of MSCs. Despite MSC proteins being implicated in the general stress response in gram-positive bacteria, the fact that the addition of GccF to the culture of target cells was the only alteration made to this system prior to sampling and fractionation, and that MscL could be involved in the mechanism of sublancin, it is tempting to speculate that the significant increase in MscL abundance in this work is indeed a GccF-specific response.

3.10.1.3 Proteins involved in genetic material precursor biosynthesis

3.10.1.3.1 Uracil phosphoribosyltransferase, 'Upp' (ATQ34034.1)

As the name suggests, uracil phosphoribosyltransferases (UPRTs) catalyse the reaction that converts uracil and phosphoribosylpyrophosphate (PRPP) to the RNA monomer uridine monophosphate (UMP) and pyrophosphate [210]. This reaction is one of six enzymatic reactions that make up the pyrimidine salvage pathway; a nucleotide synthesis pathway used by bacteria to effectively recycle and reuse RNA-specific nucleic acids [330].

'Upp' is the specific uracil phosphoribosyltransferase identified in this work, and in *Lb. plantarum* JDM1 and WCFS1 it is encoded in the *upp* gene cluster along with the uracil permease 'PyrP', a hydroxymethyltransferase, a SUA5-family L-threonylcarbamoyladenylate synthase, the glutamine methyltransferase release factor 'HemK', the peptide chain release factor 'PrfA', and a thymidine kinase 'Tdk'. Analysis of the proteomic data showed an increase in abundance of PyrP (uracil permease), Tdk (thymidine kinase), and PrfA (peptide chain release factor), while the abundance of the uncharacterised hydroxymethyltransferase had decreased. All other proteins encoded in the *upp* gene cluster were not identified by PD. The increased abundance of these Upp-associated proteins along with that of Upp itself (3.5-fold at 15 minutes, 3.6-fold at 30 minutes, and 4.3-fold at 60 minutes), strongly suggests that pyrimidine synthesis *via* the pyrimidine salvage pathway is up-regulated in *Lb. plantarum* ATCC 8014 cells following exposure to GccF. Consistent with this idea, it was no surprise then that the pyrimidine attenuation regulatory protein, PyrR, had also decreased in abundance [123], as this protein is involved in (negatively) regulating the expression of pyrimidine biosynthetic genes such as *upp*. Considering that the activity of the enzymes involved in the pyrimidine salvage pathway are subjected to feedback control by UMP [236], the increased abundance of these proteins suggests that the cells are deficient in cellular UMP following GccF treatment.

With these findings in mind, it appears that upon treatment with GccF, and as its bacteriostatic effects start to take place, *Lb. plantarum* ATCC 8014 cells prioritise RNA-specific pyrimidine synthesis, perhaps, in an effort to increase the pool of bioavailable precursors for RNA synthesis.

3.10.1.4 Proteins involved in cell growth and maintenance

3.10.1.4.1 UDP-*N*-acetylenolpyruvoylglucosamine reductase, 'MurB' (ATQ32782.1)

MurB is a peptidoglycan synthesis enzyme which catalyses the NADPH-dependent reduction of enolbutyryl-UDP-GlcNAc to UDP-*N*-acetylmuramic acid (UDP-MurNAc) [190]. Subsequent addition of the polypeptide chain consisting of, L-alanine, D-glutamate, *meso*-diaminopimelate (*meso*-DAP) or L-lysine, and D-ala-D-ala to UDP-MurNAc constitutes the formation of the central peptidoglycan precursor molecule phospho-*N*-acetylmuramoyl-pentapeptide [8]. MurB plays a crucial role in the formation of the bacterial cell wall (Fig. 18), as it has been shown that inhibition of MurB results in reduced peptidoglycan synthesis as a consequence of a lack of the pentapeptide precursor it is responsible for synthesising [332] [290]. This reduction evidently renders the cells vulnerable to antimicrobials that act on the cell wall and has also been shown to alter cell morphology [254].

Due to its central role in the peptidoglycan synthesis pathway (Fig. 18), at face value the increased abundance of MurB in response to exposure of *Lb. plantarum* ATCC 8014 cells (1.8-fold at 15 minutes, 2-fold at 30 minutes, and 2.4-fold at 60 minutes) would suggest that cell wall synthesis is up-regulated, however, analysis of the proteomic data showed that all other Mur proteins (*e.g.* 'MurA1', 'MurA2', 'MurC', 'MurD', 'MurE', and 'MurF') had decreased in abundance following target cell treatment with GccF. The only other pathway that utilises MurB and/or the product of its reaction (UDP-MurNAc), is that of D-glutamine and D-glutamate metabolism [164], which also requires the enzyme 'MurC'. These findings suggest that, as a result of the significant increase in MurB abundance, *Lb. plantarum* ATCC 8014 cells accumulate UDP-MurNAc following exposure to GccF. If this is true, the exact reason for this is unclear. It is possible that the enzyme machinery that uses UDP-MurNAc is compromised which, however unlikely, could be a specific effect of GccF.

Further analysis of the appropriate KEGG pathways (amino sugar and nucleotide sugar metabolism, and peptidoglycan synthesis) and the proteomic data revealed that all (characterised) enzymes involved in MurNAc synthesis-related pathways showed a decrease in abundance (Fig. 10). The scope of this KEGG pathway analysis encompassed processes from the import of extracellular MurNAc *via* the uncharacterised MurNAc-specific PTS transporter,

to MurNAc synthesis *via* fructose and mannose metabolism, and even the 'peptidoglycan recycling' pathway which salvages MurNAc from the cell wall [34].

Considering MurB has not been implicated in the general stress response in bacteria, these findings make it difficult to ascertain the exact, or even potential, reasoning behind the increased abundance of MurB in *Lb. plantarum* ATCC 8014 cells following exposure to GccF and, as such, needs to be investigated further.

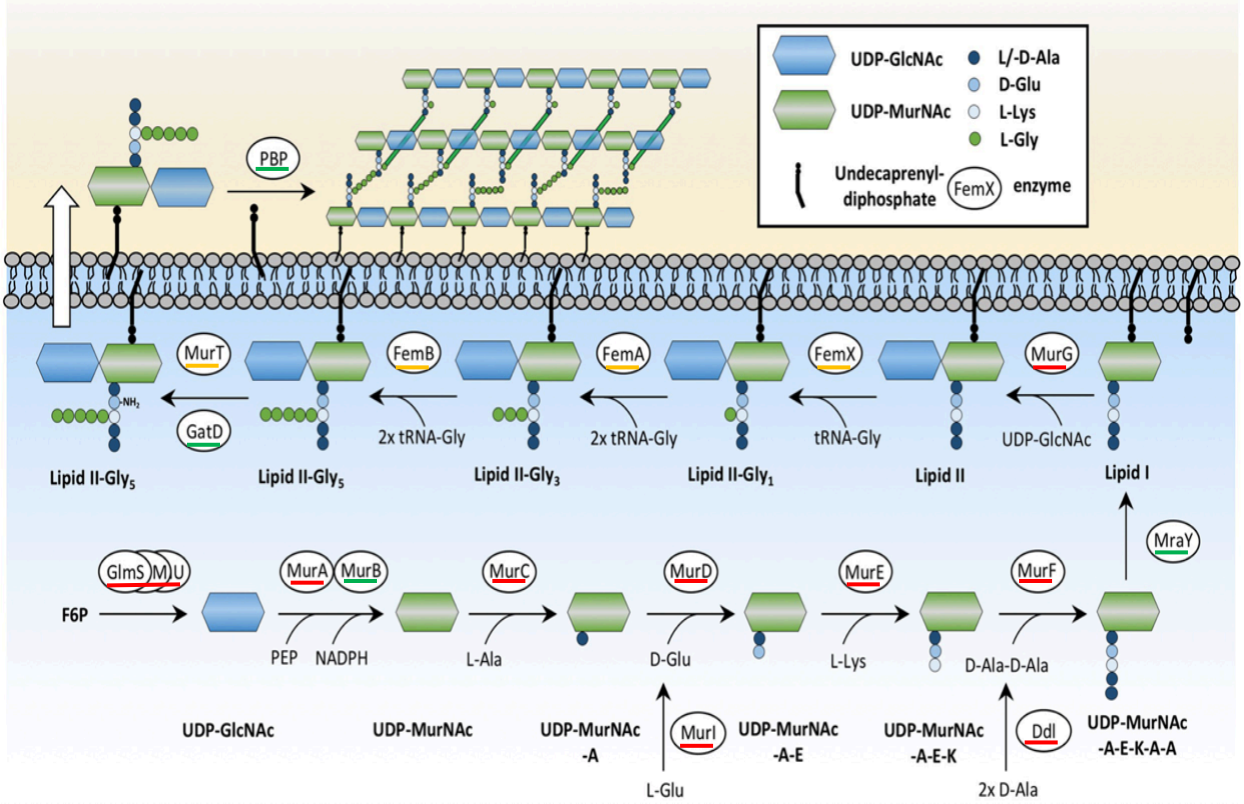

Figure 18: The peptidoglycan synthesis pathway in gram-positive bacteria. Schematic representation highlighting the cytosolic steps of cell wall synthesis in the gram-positive bacterial model *S. aureus*. Proteins that were identified in the present study with a decrease in their abundance are underlined in red, while those underlined in green showed an increase in abundance compared to the untreated *Lb. plantarum* ATCC 8014 control. Proteins underlined in yellow were not identified in this study (Figure reproduced from Jarick, *et al.*, 2018 [156], © 2018, with permission Springer Nature and the authors).

3.10.2 Cytosolic proteins with the most significant decrease in abundance

The abundances of 171 proteins in the cytosolic fraction of *Lb. plantarum* ATCC 8014 cells were shown to be significantly decreased over one hour in response to treatment with GccF. Of those having the most significant change in abundance (62 total; Appendix 7.7, Table 16), 40 proteins showed a decrease in abundance. To further understand how these proteins might be involved in, or contribute to the effects of GccF on *Lb. plantarum* ATCC 8014 cells, the six with the largest fold-change in abundance are discussed in the following subsections (Table 11).

Table 11: Cytosolic proteins with the most statistically significant decrease in abundance

Accession #	Protein	Sequence coverage	PSMs	Unique peptides	MW (kDa)	Fold change*		
						T_{15}	T_{30}	T_{60}
ATQ33988.1	Rod shape-determining protein, **MreB1**	29	59	7	35.1	**0.035**	**0.045**	**0.124**
ATQ34023.1	UDP-*N*-acetylglucosamine 1-carboxyvinyltransferase, **MurA2**	36	63	13	47.1	**0.143**	**0.073**	**0.053**
ATQ34093.1	PTS GlcNAc transporter (IIABC), **PTS18CBA**[+]	24	109	9	70.3	**0.273**	**0.436**	0.590
ATQ33166.1	Glycosyltransferase family 4 protein, **UgtP**	45	112	10	44.2	**0.300**	**0.170**	**0.158**
ATQ32737.1	Thioredoxin disulfide reductase, **TrxB1**	52	200	13	33.4	**0.400**	**0.230**	**0.218**
ATQ32426.1	Teichoic acids export ATP-binding protein **TagH**	36	99	8	40.8	**0.579**	**0.600**	0.612

* Values highlighted in red are not significant. [+] Proteins identified in the wrong fraction.

3.10.2.1 Proteins involved in cell growth and maintenance

3.10.2.1.1 GlcNAc 1-carboxyvinyltransferase, 'MurA2' (ATQ34023.1)

MurA proteins catalyse the first committed step in bacterial peptidoglycan synthesis where they are involved in transferring enolpyruvate from phosphoenolpyruvate (PEP) to UDP-GlcNAc, thus forming UDP-GlcNAc-enolpyruvate and inorganic phosphate [262]. Two structurally and functional similar copies of MurA exist in low-G+C gram-positive bacteria species and are usually annotated as 'MurA1' and 'MurA2' [90], although MurA2 is sometimes referred to as 'MurAB' [176] or 'MurZ' [31]. A previous study which investigated the potential differences between the two MurA proteins in *S. pneumoniae* found that both proteins are active and catalyse the same reaction in the peptidoglycan synthesis pathway [90]. It was also shown that inactivation of either MurA gene had no effect on cell viability, suggesting that MurA1 and MurA2 are able to substitute for one another in *S. pneumoniae* [90]. Conversely, a later study found that in *B. subtilis* MurA1 is essential, while MurA2 is not [176], which suggests that the MurA isozymes function differently in different species of bacteria. These findings were supported by experimentation performed in *S. aureus* which showed that inactivation of *murA* resulted in a 25 % reduction in peptidoglycan, while inactivation of *murZ* had almost no effect on peptidoglycan metabolism [31]. Analysis of the proteomic data generated by the present study showed that the abundance of MurA1 had also decreased to a greater degree (although not statistically significant) compared to that of MurA2 following target cell exposure to GccF. Considering the structural and functional similarities between the two MurA proteins, the fact that MurA2 was significantly affected by the addition of GccF (0.1-fold at 15 minutes, 0.07-fold at 30 minutes, and 0.05-fold at 60 minutes) while MurA1 was not (0.6-fold at 15 minutes, 0.06-fold at 30

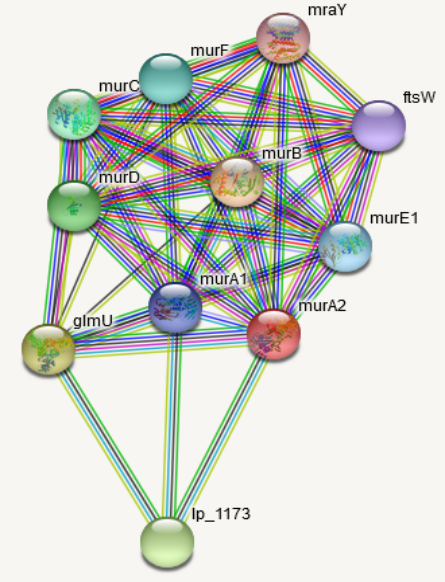

Figure 19: MurA2 STRING diagram. STRING networks showing the first shell of protein interactions made with MurA2 in *Lb. plantarum* WCFS1.

minutes, and 0.5-fold at 60 minutes) and, further, that the abundance of either protein had decreased by such varied amounts, suggests that the two proteins may indeed act differently in *Lb. plantarum* ATCC 8014 cells. Exactly how they differ and for what reason, remains to be elucidated. Regardless of these differences, the fact remains that both MurA proteins catalyse the same reaction in cell wall synthesis and therefore, due to their decrease in abundance following target cell exposure to GccF, as well as the near-global decrease in Mur protein abundances in the present study (*i.e.* 'MurA1', 'MurA2', 'MurC', 'MurD', 'MurE', and 'MurF'; Fig. 19), it appears that the majority of this branch of peptidoglycan synthesis is down-regulated in *Lb. plantarum* ATCC 8014 cells in response to treatment with GccF. This is not surprising in light of the fact that the cells stop multiplying. It is difficult to determine, however, whether the decrease in abundance of MurA2 is due to general stress or exposure to GccF as such a response has not been specifically linked to the general stress response in bacteria despite its central role in the formation of peptidoglycan precursors and, thus, its impact on bacterial cell viability.

Interestingly, in 2003 it was reported that MurA2 is specifically degraded by the ClpP protease in bacterial cultures that are approaching stationary phase, and further suggested that an inverse relationship exists between these two proteins such that, as proteolysis by ClpP increases, the levels of MurA2 decrease [176]. Further analysis of the proteomic data showed a decrease in all Clp and Clp-associated proteins in the cytosolic fraction of *Lb. plantarum* ATCC 8014 cells, suggesting that Clp-mediated degradation of MurA2 probably does not occur in these cells. This is also supported by the lack of Clp proteins shown to be associated with MurA2 in the STRING diagram (Fig. 19). Interestingly, this diagram also shows that an interaction between MurA2 and the previously discussed FtsW (Section 3.9.1.1.3) has been experimentally verified, despite these proteins both being associated with different stages of peptidoglycan synthesis. Exactly how, and why, this interaction occurs, cannot be determined from the data generated by the present study, and is only further complicated by the fact that MurA2 showed a decrease in abundance, whilst the abundance of FtsW increased following exposure to GccF. These findings potentially point towards the decrease in MurA2 abundance being GccF-specific, although this cannot be conclusively determined from the data and evidence presented here. However, the fact that MurA isozymes have been shown to behave differently in different species of bacteria may help explain why neither MurA protein has been implicated in the general stress response in bacteria and thus, may indeed be a GccF-specific response in *Lb. plantarum* ATCC 8014 cells.

3.10.2.1.2 1, 2-diacylglycerol-3-glucosultransferase, 'UgtP' (ATQ33166.1)

Identified by PD as a family 4 glycosyltransferase, this protein was later annotated by KEGG as a 1, 2-diacylglycerol 3-glucosyltranferase involved in glucolipid metabolism [164][211]. This enzyme, referred to as either 'UgtP' or 'YpfP' in the literature [161][234], catalyses the transfer of glucose from UDP-glucose to diacylglycerol (DAG) to form monoglucosyldiacylglycerol (MGlcDAG) and UDP [166]. In *B. subtilis*, this reaction constitutes the first of three in the glucolipid synthesis pathway which serves to produce non-bilayer lipids for incorporation into the cell envelope *via* their association with and tethering of LTAs to the cell membrane [211]. In addition to its role in glucolipid synthesis, UgtP has also been shown to directly interact with the Z-ring-forming protein, 'FtsZ' [331][60]. In this instance, UDP-Glc bioavailability governs the interaction between UgtP and FtsZ such that, in UDP-Glc-rich conditions, UgtP binds FtsZ and inhibits cell division, leading to increased cell size, whereas in UDP-Glc-poor conditions, UgtP is sequestered and cell division proceeds in an uncontrolled manner, resulting in a reduction in cell size [60]. These findings evidently implicate this protein-protein interaction in the coordination of *B. subtills* cell size with nutrient availability [60].

Previous studies have shown that cells lacking UgtP have abnormal morphology [249][188]. These observations were later explained by Weart and colleagues (2007) [331] who showed that UgtP is able to act as a sensor of nutrient bioavailability and then communicate this message so that cell division is effectively delayed until cells reach, what the authors coined "critical mass" (*i.e.* the appropriate mass for a given growth rate). With these findings in mind, the decrease in abundance of UgtP in the present study (0.3-fold at 15 minutes, and 0.2-fold at 30 and 60 minutes) suggest two things, i.) that glucolipids (MGlcDAG, DGlcDAG and TGlcDAG) are not synthesised and, therefore, the attachment of LTA to the cell membrane is likely to be hindered, and ii.) that any cell division that does occur is not controlled by the nutrient composition of the cell due to a lack of association between UgtP and FtsZ.

A recent study by Sassine and colleagues (2020) [270] showed that while *ugtP*-mutant *B. subtilis* cells lack glucolipids, LTA molecules are still synthesised, but are also much longer [270]. Interestingly, it has also been reported on multiple occasions that the absence of glucolipids in *B. subtilis*, due to a lack of UgtP/*ugtP*, activates multiple extracytoplasmic function (ECF) sigma factors [278][211][277], which are small, regulatory components of RNA polymerase that determine the promoter selectivity of the holoenzyme [136].

Analysis of the proteomic data generated from the present study showed that the abundance of a single sigma factor, RpoD, increased at 15 minutes, but then slowly decreased at 30 and 60 minutes, however, the fold-changes were not statistically significant. In both *B. subtilis* [247] and *Lb. plantarum* WCFS1 [36], RpoD reportedly plays a role in vegetative transcription and sporulation. Considering that the target *Lb. plantarum* ATCC 8014 cells were approaching stasis at the time of sampling, the activation of RpoD following the decrease in UgtP and, thus, the presumed lack of glucolipid synthesis in these cells, is fitting and suggests that this mechanism is activated in order for the target cells to survive during stasis. Given that sporulation is an adaptive response that bacteria employ during unfavourable growth conditions, it is possible that the decrease in abundance of UgtP is a general stress response in *Lb. plantarum* ATCC 8014 as a result of a perceived nutrient deficiency following exposure to GccF. It may also be true that the glucolipid pathway, where UgtP is implicated, is down-regulated during cell stasis in an effort to preserve cellular UDP-Glc for other processes; again suggesting that the decrease in UgtP abundance is a likely result of general stress rather than a GccF-specific response in these cells.

3.10.2.1.3 Teichoic acid export ATP-binding protein, 'TagH' (ATQ32426.1)

As previously mentioned in section 3.9.1.3.3, the TagH protein is part of the ABC transporter complex 'TagGH' which functions in the export of TAs from bacterial cells [43]. The specific role of TagH in the function of TagGH is to provide energy (ATP) for the translocation of TA chains from the cytosol to the outer face of the cell membrane [43]. Previous studies have shown that bacteria lacking WTAs grow at slower rates than their wild-type counterparts [43], and often exhibit cell shape abnormalities such as, rod-to-coccoid transition in morphology [187][296], irregular swelling of cells [67][187], and defects in septum formation and count [51]. Thus, WTAs are an intrinsic part of the assembly and localisation of the peptidoglycan machinery involved in cell wall elongation and septum formation.

Given the conflicting changes in abundance of the two proteins involved in the 'TagGH' complex (*i.e.* TagH decrease and TagG increase; Section 3.9.1.3.3), the *Lb. plantarum* JDM1 and WCFS1 genome maps in KEGG were used to cross reference the proteins encoded in the TagGH gene cluster(s) with the proteins identified in this study. Unfortunately, KEGG showed there were only three confirmed protein identities for the five proteins encoded; two of them being TagH and TagG, and the other being a major facilitator superfamily (MFS) multidrug

efflux transporter. Based on this grouping of proteins, there is no obvious reason for the disparity seen between the TagG and TagH changes in abundance observed here. The question of whether these changes are a result of a general stress or GccF-specific response therefore arises.

It has been shown that treatment of *S. aureus* cells with a novel small molecule ("1835F03") that inhibits essential enzymes (such as 'Ta**r**G', the **r**ibitol-incorporating equivalent of the **g**lycerol-incorporating 'Ta**g**G') results in growth arrest [297]. It was thought that this could be due to either the accumulation of toxic bactoprenol-linked WTA (and peptidoglycan) precursors in the cytosol, or the lack of precursors available for cell wall synthesis [297]. This was a curious finding, especially considering that neither Tag protein has been implicated in the general stress response in bacteria. A thorough examination of the proteomic data generated from this study failed to detect changes in the abundances of other Tag proteins (*e.g.* 'TagA', 'TagO', 'TagB', 'TagF') in response to GccF-treatment, and analysis of the appropriate KEGG pathways also failed to produce any definitive results. As such, while it is tempting to speculate that the decrease in TagH abundance is a GccF-specific response in treated *Lb. plantarum* ATCC 8014 cells, more work is required to test this hypothesis. A more general conclusion would be that the abundance of TagH is decreased following exposure to GccF in an effort to conserve what little ATP is available in *Lb. plantarum* ATCC 8014 cells as they approach stasis.

3.10.2.2 Proteins involved in nutrient transport

3.10.2.2.1 PTS GlcNAc transporter (EIICBA), 'PTS18CBA' (ATQ34093.1)

PEP-PTS transporters are a major component of the bacterial cell membrane where they facilitate the transport and phosphorylation of extracellular carbohydrates for their use as energy [38]. These systems consist of three general components: enzyme I (EI), and a histidine phosphocarrier protein (HPr), and one or more sugar-specific enzyme II (EII) components which typically consist of three proteins that may or may not be fused [81]. As bacteria are capable of utilising energy from many different carbon sources, it is not uncommon for different species to encode various PTS transporters [157]. This is where the sugar-specific EII subunit of each PTS transporter complex plays an important role, as their specificity allows bacteria to quickly adapt to, and overcome potential challenges caused by a change in their environment whilst still being able to utilise the available carbon sources [157].

The specific PTS transporter identified in this study was the GlcNAc-specific 'PTS18CBA' (Fig. 20). The EIIC domain of this PTS transporter has previously been identified as the primary receptor of GccF, using gene knockout and mutation experiments [87], transgenic and gene editing techniques [20], and subsequent transcriptional and protein interaction studies [27]. The identification and decrease in abundance of the PTS18CBA in the present study was no surprise given that similar findings were shown in a recent transcriptional study in *Enterococcus faecalis* (*E. faecalis*) cells treated with GccF [27].

Intriguingly, in the present study, the PTS18CBA showed a more significant change in its abundance in the cytosol fraction than in the membrane fraction despite the PSM counts being 10-fold greater in the membrane fraction (Table 12). Given that PTS transporters contain both cytosolic and membrane bound domains, it would seem that, at least for PTS18CBA, both sets of result listed in table 7 are true. Analysis of the raw PD data showed that the portion of the protein/peptide identified here (in the cytosolic fraction) was indeed cytosolic. Moreover, the fact that the results from both fractions show a decrease in abundance, supports the previously mentioned findings from Bisset (2019) [27].

Table 12: Comparison of PTS18CBA proteomic data values in membrane and cytosol fractions

Fraction	Protein	Sequence coverage %	PSMs	Unique peptides	MW (kDa)	Fold change*		
						T_{15}	T_{30}	T_{60}
Cytosol	PTS18CBA	24	109	9	70.3	**0.273**	**0.436**	0.590
Membrane	PTS18CBA	67	1012	19	70.3	0.741	0.404	0.591

*Values in red are not statistically significant.

The decrease in abundance of PTS18CBA in the present study suggests that, upon exposure to GccF, translation of *pts18cba* mRNA in *Lb. plantarum* ATCC 8014 cells is down-regulated. This is likely due to the fact that GccF targets the PTS18CBA and docks at the EIIC domain *via* one of its GlcNAc moieties, which not only blocks the uptake of free GlcNAc (which is not essential for cell survival), but binds to a second, as yet unknown, protein, to elicit its characteristic bacteriostatic effect on these cells. Exactly how the signal of GccF docking at the cell membrane is conveyed beyond the PTS18CBA, however, remains elusive.

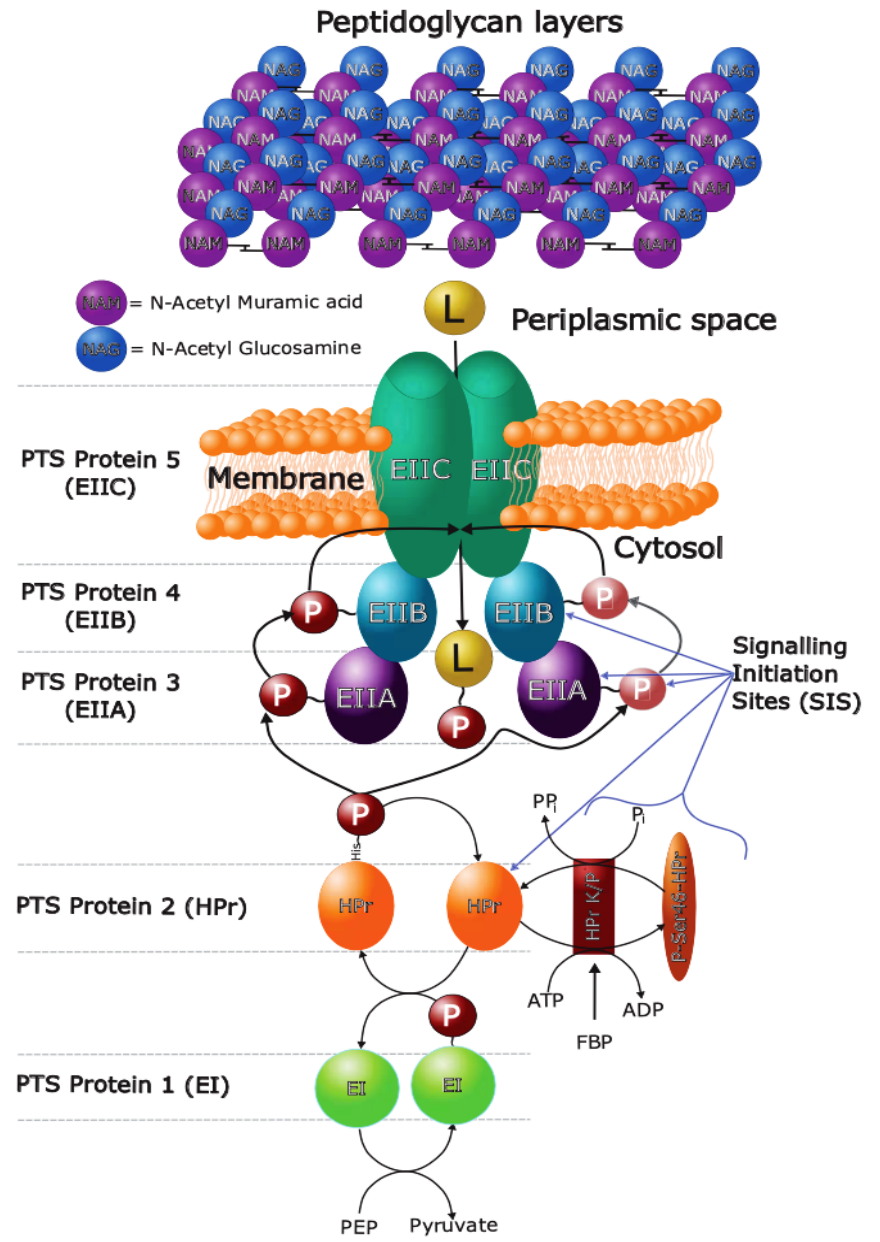

Figure 20: Domain organisation of the PTS18CBA transporter and phosphorelay system in gram-positive bacteria. Schematic diagram of the phosphorylation events that occur to facilitate the uptake of extracellular GlcNAc *via* the PTS18CBA transporter. The PTS18CBA transporter consists of the three domains: enzyme II (EII) A and EIIB, and the core EIIC domain which forms the GlcNAc (ligand)-specific membrane-spanning transporter. Phosphoenolpyruvate (PEP) provides the phosphoryl group that is transferred to the EIIC domain in a step-wise manner *via* the PTS components enzyme I (EI) and the histidine phosphocarrier protein, HPr (both cytosolic), then EIIA, and EIIB. Phosphorylation of HPr can also occur *via* the bifunctional HPr-specific kinase/phosphorylase (HPrK/P) which phosphorylates HPr at Ser46 and implicates HPr in a different biological process (Figure reproduces from Bailey, 2017 [20], © 2017, with permission from the author).

Further analysis of the proteomic data was conducted to investigate any potential signal transduction pathway(s) that might occur following the exposure of *Lb. plantarum* ATCC 8014 cells to GccF. This revealed that the abundance of an unidentified 'HPr' protein had increased in the cytosolic fraction following GccF-treatment (no significant values; 1.5-fold at 15 and 30 minutes, and 2.1-fold at 60 minutes) which would suggest that its phosphorylation activity could be up-regulated. Cross-referencing of this HPr protein with that identified in the transcriptomics study revealed that they were, indeed, the same HPr phosphocarrier [27]. Interestingly, a bifunctional HPr-specific kinase/phosphorylase, 'HPrK/P', was also identified in the present study and, while its abundance initially decreased at the 15 minute time point (0.4-fold), it then slowly increased at the 30 (1-fold) and 60 minute (1.2-fold) time points, although the changes were not statistically significant. Unlike the phosphorylation events that transpire in the PTS:carbohydrate uptake pathway, where HPr is phosphorylated by PEP at histidine 15 (His15) [178], HPrK/P specifically phosphorylates HPr at Ser46 [221], which ultimately results in the activation of what is known as the carbon catabolite repression (CCR) pathway [221], [80]. In *B. subtilis,* it was shown that the overarching consequence of the activation of this pathway was the differential regulation of approximately 10 % of all genes [226].

Given that the abundance of HPrK/P had not increased until after 30 minutes in the present study, the changes observed prior to this time cannot be attributed to the CCR pathway. However, considering that HPr is associated with both the CCR pathway and the PTS18CBA, the eventual increase in the abundance of HPrK/P following the exposure of the target cells to GccF could suggest that this effect is linked to the decrease in abundance of the PTS18CBA and, as such, may be a worthwhile avenue to investigate further. If anything, these findings highlight the complexities of the proteomic response(s) to GccF-treatment in *Lb. plantarum* ATCC 8014 cells and shows how problematic the interpretation of the data can be.

3.10.2.3 Proteins involved in cellular redox homeostasis

3.10.2.3.1 Thioredoxin reductase, 'TrxB1' (ATQ32737.1)

Thioredoxin (Trx) reductases are the only enzymes known to catalyse the NADPH-dependent reduction of thioredoxins [230]. Commonly found in all living systems, thioredoxins function as redox proteins that participate in cysteine thiol-disulfide exchange with their substrates [352]. Together, NADPH, TrxB1, and thioredoxin make up the 'Trx system' which plays a major role in the oxidative stress response in bacteria [352][280].

During oxidative stress, thioredoxins scavenge for reactive oxygen species (ROS) and other pro-oxidant molecules, and also regulate the activity of enzymes using their redox activity [352], with the ultimate aim of preventing and/or repairing damage caused by oxidative stress. When TrxB1 acts on thioredoxin, the protein is converted to its reduced form which is then able to supply electrons to other cellular processes, including, DNA synthesis (ribonuclease reductase activity), protein repair (methionine sulfoxide reductase activity), and sulfur assimilation (phosphoadenosine phosphosulfate reductase activity) [143][191][352]. The diversity of cellular applications where thioredoxins are capable of enacting their activity emphasises the importance of these proteins in the maintenance of cellular redox balance. This is especially important in the cytosol of bacterial cells which, under normal physiological conditions, is a highly reducing environment that is largely, if not solely, maintained by the Trx and/or glutathione reductase-glutaredoxin (GHS-Grx) systems, depending on the species of bacteria [58]. Given that the thioredoxin reductase TrxB1 is responsible for keeping thioredoxin in its reduced state, the decrease in its abundance (0.4-fold at 15 minutes, and 0.2-fold at 30 and 60 minutes) in the present study following exposure of *Lb. plantarum* ATCC 8014 cells to GccF suggests that reduction by thioredoxin is also likely to be decreased, as the redox protein would exist as a thiol oxidase without TrxB1 [260]. These events could ultimately result in a change in the redox balance within the cytosol, thus, rendering the cells more susceptible to oxidative stress.

The proteomic data revealed that only a single thioredoxin protein, 'TrxA2', was identified by PD and its abundance was shown to have increased in the cytosolic fraction of *Lb. plantarum* ATCC 8014 cells following exposure to GccF (1.8-fold at 15 and 30 minutes, and 1.9-fold at 60 minutes). According to KEGG, the genomes of both reference *Lb. plantarum* strains, JDM1 and WCFS1, each encode four thioredoxin proteins, annotated as 'TrxA1', 'TrxA2', 'TrxA3' and 'TrxH', as well as two thioredoxin reductase proteins, 'TrxB1' and 'TrxB2'. It has been reported that these six proteins are highly conserved in *Lb. plantarum* strains [280][207].

The increase in abundance of TrxA2 is an interesting finding especially considering that its cognate reductase, TrxB1, showed a decrease in abundance. This could suggest the possibility of two different occurrences, i) that the second reductase protein, TrxB2, is able to act on TrxA2, thus, restoring its reducing capabilities, or ii.) that the GHS-Grx system becomes the primary reducing mechanism within the cytosol, as TrxA2 exists in its oxidised form. Taking into account that no other major oxidative stress proteins were identified with significant changes in abundance in this study, it begs the question as to why this specific redox system was targeted and, moreover, why TrxA2 and TrxB1 showed such conflicting changes in their respective

abundances following exposure of the target cells to GccF. It is therefore possible, however unlikely, that the significant decrease in abundance of the thioredoxin reductase, TrxB1, is a GccF-specific response in treated *Lb. plantarum* ATCC 8014 cells.

3.11 Proteins omitted due to time and space constraints

The proteins selected for having the most significant change in their abundance are listed in Table 15 (membrane proteins, 84 total; Appendix 7.6) and Table 16 (cytosolic proteins, 62 total; Appendix 7.7, respectively). Due to time and space constraints, however, the majority of these proteins had to be omitted from the in-depth analysis and discussion in the present study. Still, it was thought that a few of these excluded proteins could potentially be grouped into similar GO categories to those which were discussed in detail in the previous sections (Sections 3.9 and 3.10). These specific proteins are highlighted in yellow in Tables 15 and 16 (Appendices 7.6 and 7.7, respectively).

Some of the more notable of these proteins include a universal stress protein, a variety of transcriptional regulators from the following protein families: the 'MarR' family, the 'TetR/AcrR' family, the 'PadR' family, and the 'ArsR' family; the RNA polymerase sigma factor 54 (σ^{54}) , and the UDP-glucose 4-epimerase, 'GalE'. Of these proteins, those that were found to be involved in general stress in bacteria include, the universal stress protein and the TetR transcriptional regulator. The MarR and PadR families of transcriptional regulators have been implicated in antibiotic resistance [253] [104], whilst the ArsR family are involved in metal resistance [46]. σ^{54} and GalE were specifically recognised for their previous mention in other work pertaining to GccF (σ^{54}) [27], and their potential association with other proteins discussed in the present work (GalE). Briefly, σ^{54}, which was identified in a recent transcriptomic study conducted by Bisset (2019) [27], has been shown to regulate the expression of specific PTS transporters, and is also involved in nitrogen metabolism [81][292]. GalE, on the other hand, catalyses the conversion of UDP-galatose to UDP-glucose [142], the latter of which is a precursor required for glucolipid synthesis *via* the activity of the previouly discussed protein, 'UgtP' (Section 3.10.2.1.2).

This brief analysis of just a few of these proteins highlights the wealth of knowledge that remains to be investigated in the proteins that could not be dicussed in the present study. The key to revealing how GccF effects bacteriostasis in *Lb. plantarum* ATCC 8014 may, in fact, reside in these lists of proteins and, as such, it would be worthwhile to continue to investigate them.

3.12 Statistically significant abundance changes associated with the wrong fraction

There was interest in those proteins whose abundances were found to show significant statistical changes but in the wrong cellular location (Table 13). A search for these proteins in the raw data from the correct fraction found them, but showed the changes in abundance were, for the most part, not statistically significant (Table 13). The main difference in the values obtained from PD was the number of PSMs, which was, in most cases, significantly greater for the samples in their correct location. The only exception for this was for 'PhoH', where the changes at all time points are statistically significant. This suggests that it was indeed, for whatever reason, found in the membrane fraction and may either be mis-annotated, or be strongly associated with the membrane. Moreover, given that a TOPCONS analysis did weakly predict PhoH to possess a transmembrane region, these findings may help support this prediction.

Table 13: Values for proteins identified in the wrong cell fraction

Accession #	Protein	Sequence coverage %	PSMs	Unique peptides	MW (kDa)	Fold change		
						T_{15}	T_{30}	T_{60}
Correctly located membrane proteins								
ATQ34093.1	PTS18CBA	67 (24)	1012 (109)	19 (9)	70.3	0.741	0.404	0.591
ATQ33208.1	MscL	63 (58)	172 (57)	6 (5)	14	1.542	1.756	1.557
Correctly located cytosolic proteins								
ATQ33714.1	PhoH	27 (54)	9 (379)	5 (14)	35.8	7.602	0.985	0.788
ATQ33638.1	DapB	73 (39)	496 (95)	13 (5)	28.5	0.682	0.773	**0.818**

*Values in red are not statistically significant. Values in parentheses are those from the same proteins identified in the incorrect location

3.13 Membrane proteins unique to the gel-free method

Two different preparation methods for mass spectrometry analyses were used in this work to ascertain the potential differences in the number of membrane proteins that could be identified by each. As

previously mentioned in section 3.7.1, the gel-based approach identified a total of 1,115 membrane proteins with high confidence. In contrast, a total of only 641 membrane proteins were identified using the gel-free approach (Section 3.7.2). Of these, 248 were shown to be unique to the gel-free approach.

Following manual sorting of this data to discard proteins annotated as 'hypothetical protein' or 'DUF-domain containing protein' by PD, the fact that 38 % of the proteins identified using the gel-free approach were unique to this method reiterates the findings from Wolff and colleagues (2006) [341] who highlighted the need for different analytical approaches to ensure sufficient coverage of a given organism's proteome. Some of the more notable of these uniquely identified proteins include, the cell division protein, 'SepF', protein subunits belonging to the F_0F_1 ATP synthase complex (α, β, ϵ, γ), and the septation ring formation receptor, 'EzrA', two cation-transporting P-type ATPases, and a Leucine-Proline-x-Threonine-Glycine (Leu-Pro-x-Thr-Gly or LPXTG; where x denotes any amino acid residue) cell wall anchor domain-containing protein (Appendix 7.8; Table 17). Briefly, SepF is involved in the late stages of cell division and has been shown to interact with the Z-ring forming protein, 'FtsZ' [129][92]; the F_0F_1 ATP synthase complex generates ATP from adenosine diphosphate (ADP) using power generated from both membrane potential and a proton gradient to drive the movements of the different subunits that make up the complex [75][325]; EzrA has been shown to interact directly with 'FtsZ' where it prevents the assembly of the Z-ring structure, thus, inhibiting septum formation [285][128]; P-type ATPases function as pumps that utilise ATP to drive cellular uptake or export of ions, which effectively helps maintain the electrochemical gradient across the cell membrane [101][44]; and the LPXTG cell wall anchor domain-containing protein represents a class of surface proteins that are characterised by the LPXTG-motif which has been shown to be the target for cleavage and subsequent covalent attachment of these proteins to the cell wall/peptidoglycan [32][116]. If time had permitted, it would have been worthwhile to investigate these proteins, and others listed in Table 17 (Appendix 7.8), further.

Considering that proteomic studies require multiple sample preparation steps prior to MS analysis, it is difficult to pinpoint the exact source or cause of the discrepancy between the number of membrane protein identified using the gel-based and gel-free methods. The major difference in these two approaches is that the gel-based method pre-fractionates the membrane proteins before proteolysis and RP-HPLC separation, making the mixture of peptides from each fraction less complex and, therefore, easier to analyse, despite the relatively high resolution of the orbitrap mass analyser. Thus, despite the known drawbacks of SDS-PAGE in the analysis of membrane proteins, using it as a pre-fractionation method has shown some distinct advantages in this case.

In reference to Table 17 (Appendix 7.8), it should be noted that despite the identification of 248 unique proteins, it was later verified by manual analysis of the data that many of these were in fact cytosolic proteins. This highlights the fact that the hydrophobic properties of membrane proteins could play a role in the efficiency of proteolysis of the membrane proteins in solution, resulting in a smaller number of proteins of 10-12 amino acids, and a large number of long peptides of high charge that could not be identified.

In terms of the uniquely identified proteins, it is difficult to ascertain the exact reason they were not identified using the gel-based approach. It is most likely the result of the naturally low abundance of these proteins in the cell, as it is well established that the limit of detection of a protein or peptide is orders of magnitude lower than by SDS-PAGE.

4 Conclusions

In this study a proteomic approach was used to identify changes in the abundance of specific proteins in both the membrane and cytosolic fractions of *Lb. plantarum* ATCC 8014 cells that may not be part of a general stress response (listed in Table 14; Appendix 7.2), but that could be specific to GccF treatment. To do this, a culture of target cells was innoculated with GccF and a time course was carried out to identify changes in the proteome of the target cells over 60 minutes. These changes were initially identified by eye, following SDS-PAGE analysis (Fig. 9), and again, during MS analysis of the gel pieces.

The findings from sections 3.7.1 and 3.7.2 show that, despite efforts to conduct cell fractionation with the utmost care, cross-contamination of the fractions still occurred. Although not ideal, this is not an uncommon occurrence in proteomic studies, regardless of the organism being investigated [149][228][145], and arises because of the physical association between the different fractions of the cell and the properties of the proteins from those fractions [303]. While efforts to formulate protocols for improved cell fractionation efficiencies have been made, studies have shown that although reduced, contamination still occurs, albeit, in some cases, to a much lesser degree [106][83]. Unfortunately, fraction contamination presents an additional layer of complexity in proteomic studies, requiring manual organisation of the results to ascertain the location of each protein in the cell. In this study several proteins that showed no transmembrane helices or signal peptides were found only in the membrane fraction, and several proteins that should have been located in the membrane were found in the cytosol.

One weakness in the present study was the comparison of treated cells with those T_0. In retrospect it would have been better to take a single culture, divide it in half, and treat one with GccF then incubate both cultures under the same conditions for the same time and use a similar sampling regime to that used in this study. Although the number of samples would be doubled, the analyses of the differences in the proteomes of the two cell populations would be more robust, removing natural variations due to normal cell growth.

In spite of these discrepancies, the analysis from the present study produced some interesting results. Two algorithms were used to analyse the proteins showing the greatest fold changes that are discussed in sections 3.9 and 3.10. BLAST2GO [122] and STRING [298] use different information to assign

GO terms to proteins. The most general GO terms are 'biochemical process' (P), 'molecular function' (F), and 'cellular component' (C). BLAST2GO analyses sequence data for which no GO annotation is yet available and is based on similarity searches with statistical analysis. STRING, on the other hand, uses a protein name or accession number to obtain a network of predicted associations for that protein. Part of the analysis provides GO terms if they are known.

Grouping the proteins identified using the gel-based approach that showed the most significant changes in abundance on the basis of their GO terms showed that those involved in cell wall metabolism made up 65 % of the total proteins (Fig. 21). A second grouping of proteins, found in the cytosol, were involved in protein synthesis. A large percentage had no associated GO terms. The results from the BLAST2GO analysis can be found in Table 19 (Appendix 7.12). It would be interesting to conduct a similar analysis on the proteins identified using the gel-free approach to ascertain how the proportions might differ.

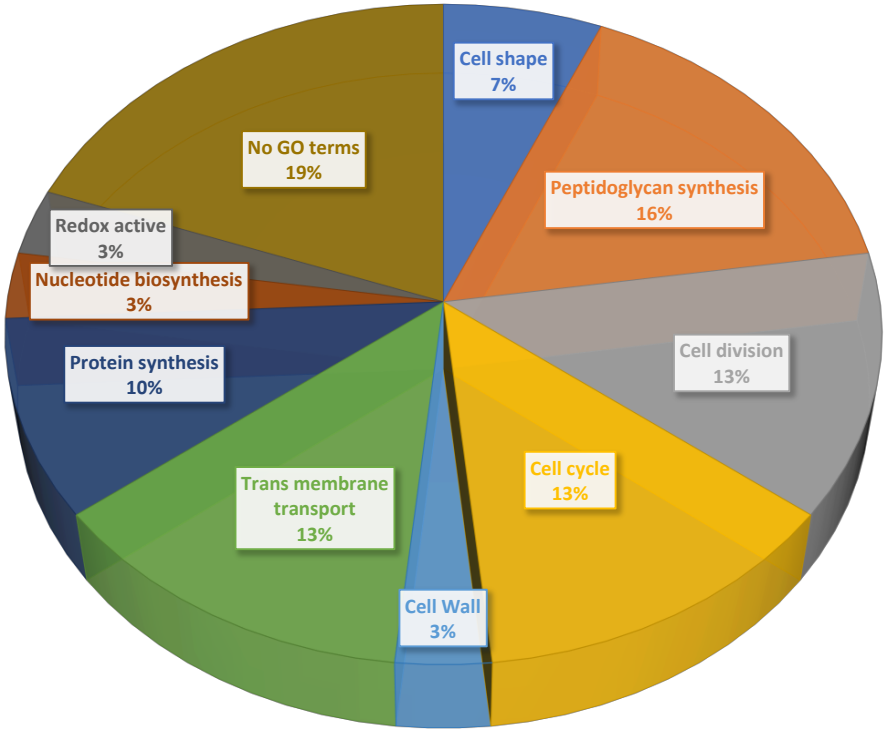

Figure 21: Distribution of the proteins showing the largest fold changes according to their GO catergories. A pi-chart showing the distribution of GO terms for the 23 proteins showing the most statistically significant changes in abundance in *Lb. plantarum* ATCC 8014 cells exposed to GccF.

The stress reponses of bacteria to a number of different environmental stresses are well known (Appendix 7.2, Table 14). Those that were identified throughout the course of this study are

highlighted in yellow in Table 14 (Appendix 7.2). It is possible that the proteins listend in Appendix 7.13 (Hyperlink 1 and 2) which are not associated with the general stress response in bacteria, may, therefore, be part of a GccF-specific response.

The most significant change was the increased abundance of the ribosome silencing factor, a protein associated with ribosome function and hence protein synthesis. This makes perfect sense given that the main effect of GccF is the very rapid cessation of cell growth as measured by $OD_{600\ nm}$.

The use of both a gel-based and gel-free approach in the present study also supports the findings by Wolff and colleagues (2006) [341] who showed that the use of two different approaches for sample preparation is imperative to maximise the representation of the bacterial proteome in proteomic studies. This was made evident by the percentage of unique proteins identified using either method in the present study (*i.e.* gel-based approach, 72.4 %; gel-free approach, 84.4 %) (Sections 3.7.1. and 3.7.2).

Although this study provided no definitive answer as to how GccF works, it did show that one, possibly specific, response is to dramatically increase the abundance of the ribosome silencing factor protein, 'RsfS', which would decrease protein synthesis and limit the degradation of silenced ribosomes during bacteriostasis. What it did not show was an obvious connection between RsfS and the GlcNAc-specific PTS transporter, 'PTS18CBA' (NagE), which is intimately involved in GccF-induced bacteriostasis in *Lb. plantarum*. The study also showed that GccF treatment changes the abundance of some proteins and enzymes that occur in the bacterial elongasome and divisome complexes that mediate peptidoglycan synthesis and remodelling. This is perhaps unsurprising given that the main effect of GccF is to send its target cells into some sort of hibernation from which they can be revived by the presence of a simple sugar (GlcNAc). Cell wall metabolism was the first bacterial process shown to be targeted by an antibiotic (penicillin), and many more recently discovered antibiotics, and indeed some bacteriocins (*e.g.* nisin, lactococcin G), also inhibit susceptible bacteria by interfering with cell wall metabolism.

Whatever the molecular mechanism by which GccF causes bacteriostasis in susceptible cells, it is clearly different to that of the many bacteriocins that form lethal pores or otherwise induce leakiness in target cell membranes. Thus, the way in which it manipulates target cells to hibernate still remains a mystery and will require further work.

5 Future directions

Comparison of the results obtained in this study with those obtained using a second bacteriostatic agent may enable the differentiation between GccF-specific and general stress effects. Future research on the mechanism(s) of GccF-induced bacteriostasis could include investigations into, i.) the effect of GccF treatment on cell membrane permeability and electric potential, ii.) the effect of GccF on the activities of various peptidoglycan synthases in *in vitro* assays, iii.) the effect of GccF on the distribution of green fluorescent protein (GFP)-tagged GlcNAc-specific PTS18CBA (NagE) transporters by fluorescence microscopy, and iv.) non-*pts18CBA* (non-*nagE*) mutations that confer resistance to GccF.

In addition, the recent discovery that some strains of *Enterococcus faecium*, an ESKAPE pathogen [268], are even more susceptible to GccF than the most susceptible *Lb. plantarum* strains, might facilitate the expansion of these investigations to include clinically-relevant bacteria, which would be an exciting biomedical research development.

It would be also be beneficial to investigate the growth-inhibiting mechanism of GccF using the second approach outlined by Sievers (2018) [284] known as membrane shaving. In theory, the results obtained from the use of both proteomic approaches (1D gel-LC and membrane shaving) should provide complementary outcomes, thus providing a more comprehensive view of the proteins involved in GccF's growth inhibiting mechanism. In line with this, it would also be beneficial to perform a more comprehensive investigation into the proteins identified in this study using the gel-free approach, especially those that were uniquely identified.

A metabolomic study (the study of chemical processes involving metabolites) could also supplement the proteomic results and provide a better understanding of the biological pathways that are affected by treatment of *Lb. plantarum* ATCC 8014 cells with GccF.

Lastly, gene knockout technologies could also be used to validate the involvement of proteins potentially involved in the response of the cells exposed to GccF.

6 References

[1] Acumedia Corp. (2021, July 11). *Acumedia*. Retrieved from Acumedia: https://www.acumedia.com

[2] Adams, D. W., Pereira, J. M., Stoudmann, C., Stutzmann, S., & Blokesch, M. (2019). The type IV pilus protein PilU functions as a PilT-dependent retraction ATPase. *PloS Genetics, 15*(9), 1-22.

[3] Agilent Technologies Inc. (2019, May). *Cary 300 UV-Vis*. Retrieved from Agilent: https://www.agilent.com/en/products/uv-vis-uv-vis-nir/uv-vis-uv-vis-nir-systems/cary-300-uv-vis

[4] Ahn, S., Stepper, J., Loo, T. S., Bisset, S. W., Patchett, M. L., & Norris, G. E. (2018). Expression of *Lactobacillus plantarum* KW30 *gcc* genes correlated with the production of glycocin F in late log phase. *FEMS Microbiology Letters, 365*(23), 1-8.

[5] Allock, S., Young, E. H., Holmes, M., Gurdasani, D., Dougan, G., Sandhu, M. S., . . . Torok, M. E. (2017). Antimicrobial resistance in human populations: Challenges and opportunities. *Globacl Health, Epidemiology and Genomics, 2*, e4.

[6] Alvarez-Sieiro, P., Montalbán-López, M., Mu, D., & Kuipers, O. P. (2016). Bacteriocins of lactic acid bacteria: Extending the family. *Applied Microbiology and Biotechnology, 100*(7), 2939-2951.

[7] Amer, B. R., & Clubb, R. T. (2014). A sweet new role for LCP enzymes in protein glycosylation. *Molecular Microbiology, 94*(6), 1197-1200.

[8] Amera, G. M., Khan, R. J., Jha, R. K., Pathak, A., Muthukumaran, J., & Singu, A. K. (2020). Prioritization of Mur family drug targets against *A. baumannii* and identification of their homologous proteins through molecular phylogeny, primary sequence, and structural analysis. *Journal of Genetic Engineering and Biotechnology, 18*(33), 1-22.

[9] Amso, Z., Bisset, S. W., Yang, S.-H., Harris, P. W., Wright, T. H., Navo, C. D., . . . Brimble, M. A. (2018). Total chemical synthesis of glycocin F and analogues: *S*-glycosylation confers improved antimicrobial activity. *Chemical Science, 9*, 1686-1691.

[10] Anantharaman, V., Koonin, E. V., & Aravind, L. (2001). TRAM, a predicted RNA-binding domain, common to tRNA uracil methylation and adenine thiolation enzymes. *FEMS Microbiology Letters, 197*(2), 215-221.

[11] Andrews, E. S., & Arcus, V. L. (2015). The mycobacterial PhoH2 proteins are type II toxin antitoxins couple to RNA helicase domains. *Tuberculosis, 95*(4), 385-394.

[12] Apollo Scientific Ltd. (2021, July 11). *Apollo Scientific*. Retrieved from Apollo Scientific: https://www.apolloscientific.co.uk

[13] Arcus, V. L., McKenzie, J. L., Robson, J., & Cook, G. M. (2011). The PIN-domain ribonucleases and the prokaryotic VapBC toxin-antitoxin array. *Protein Engineering, Design and Selection, 24*(1-2), 33-40.

[14] Arike, L., & Peil, L. (2014). Spectral counting label-free proteomics. In D. Martins-de-Souza, *Shotgun Proteomics: Methods and Protocols - Methods in Molecular Biology* (Vol. 1156, pp. 213-222). Clifton: Springer.

[15] Arnison, P. G., Bibb, M. J., Bierbaum, G., Bowers, A. A., Bugni, T. S., Bulaj, G., . . . Entian, K.-D. (2013). Ribosomally synthesized and post-translationally modified peptide natural products: Overview and recommendations for a universal nomenclature. *Natural Products Reports, 30*(1), 108-160.

[16] Ashburner, M., Ball, C. A., Blake, J. A., Botstein, D., Butler, H., Cherry, J. M., . . . Matese, J. (2000). Gene Ontology: Tool for the unification of biology. *Nature Genetics, 25*(1), 25-29.

[17] Auer, G. K., & Weibel, D. B. (2017). Bacterial cell mechanics. *Biochemistry, 56*(29), 3710-3724.

[18] Bürk, J., Weiche, B., Wenk, M., Boy, D., Nestel, S., Heimrich, B., & Koch, H.-G. (2009). Depletion of the signal recognition particle receptor inactivates ribosomes in *Escherichia coli*. *Journal of Bacteriology, 191*(22), 7017-7026.

[19] Baggerman, G., Vierstraete, E., De Loof, A., & Schoofs, L. (2005). Gel-based versus gel-free proteomics: A review. *Combinatorial Chemistry & High Throughput Screening, 8*(8), 669-677.

[20] Bailie, M. A. (2017). The role of the *N*-acetylglucosamine phosphoenolpyruvate phosphotransferase system from *Lactobacillus plantarum* 8014 in the mechanism of action of glycocin F. 1-178. New Zealand: Massey Univeristy, Palmerston North.

[21] Bandow, J. E., Brötz, H., Leichert, L. I., Labischinski, H., & Hecker, M. (2003). Proteomic approach to undertanding antibiotic action. *Antimicrobial Agents and Chemotherapy, 47*(3), 948-955.

[22] BDH Ltd. (2021, July 11). *BDH: The one stop solution for all your laboratory needs*. Retrieved from Adhme: http://www.adhme.net/about.html

[23] Berrier, C., Besnard, M., Ajouz, B., Coulombe, A., & Ghazi, A. (1996). Multiple mechanosensitive ion channels from *Escherichia coli*, activated at different thresholds of applied pressure. *The Journal of Membrane Biology, 151*, 175-187.

[24] Bested, A. C., Logan, A. C., & Selhub, E. M. (2013). Interstinal microbiota, probiotcis and mental health: from Metchnikoff to modern advances: Part II - contemporary centextual research. *Gut Pathology, 5*(3), 1-14.

[25] Bienert, G. P., Desguin, B., Chaumont, F., & Hols, P. (2013). Channel-mediated lactic acid transport: a novel function for aquaglyceroporins in bacteria. *Biochemical Journal, 454*(3), 559-570.

[26] Bio-Rad. (2021, July 10). *Bio-Rad*. Retrieved from Bio-Rad: https://www.bio-rad.com

[27] Bisset, S. W. (2019). Understanding the mechanism of action of the glycosylated bacteriocin glycocin F. New Zealand: Massey Univeristy, Palmerston North.

[28] Bisset, S. W., Yang, S.-H., Amso, Z., Harris, P. W., Patchett, M. L., Brimble, M. A., & Norris, G. E. (2018). Using chemical synthesis to probe structure-activity relationships of the glycoactive bacteriocin glycocin F. *ACS Chemical Biology, 13*(5), 1270-1278.

[29] Biswas, S., Garcia De Gonzalo, C. V., Repka, L. M., & van der Donk, W. A. (2017). Structure-activity relationship of the *S*-linked glycocin sublancin. *ACS Chemical Biology, 12*(12), 2965-2969.

[30] Biswas, S., Wu, C., & van der Donk, W. A. (2021). The antimicrobial activity of the glycocin sublancin is dependent on an active phosphoenolpyruvate-sugar phosphotransferase system. *ACS Infectious Diseases, 7*(8), 2402-2412.

[31] Blake, K. L., O'Neill, A. J., Mengin-Lecreulx, D., Henderson, P. J., Bostock, J. M., Dunsmore, C. J., . . . Chopra, I. (2009). The nature of *Staphylococcus aureus* MurA and MurZ and approaches for detection of peptidoglycan biosynthesis inhibitors. *Molecular Microbiology, 72*(2), 335-343.

[32] Boekhorst, J., de Been, M. W., Kleerebezem, M., & Siezen, R. J. (2005). Genome-wide detection and analysis of cell wall-bound proteins with LPxTG-like sorting motifs. *Journal of Bacteriology, 187*(14), 4928-4934.

[33] Bonilla, C. Y. (2020). Generally stressed out bacteria: Environmental stress response mechanisms in gram-positive bacteria. *Integrative and Comparative Biology, 66*(1), 126-133.

[34] Borisova, M., Gaupp, R., Duckworth, A., Schneider, A., Dalügge, D., Mühleck, M., . . . Mayer, C. (2016). Peptidoglycan recycling in gram-positive bacteria is crucial for survival in stationary phase. *mBio, 7*(5).

[35] Bouvier, J., Stragier, P., Morales, V., Rémy, E., & Gutierrez, C. (2008). Lysine represses transcription of the *Escherichia coli* DapB gene by preventing its activation by the ArgP activator. *Journal of Bacteriology, 190*(15), 5224-5229.

[36] Bove, P., Capozzi, V., Fiocco, D., & Spano, G. (2011). Involvement of the sigma factor sigma H in the regulation of a small heat shock protein gene in *Lactobacillus plantarum* WCFS1. *Annals of Microbiology, 61*, 973-977.

[37] Boyle, D. S., Khattar, M. M., Addinall, S. G., Lutkenhaus, J., & Donachie, W. D. (1997). *ftsW* is an essential cell-division gene in *Escherichia coli*. *Molecular Microbiology, 24*(6), 1263-1273.

[38] Bramley, H. F., & Kornberg, H. L. (1987). Sequence homologies between proteins of bacterial phosphoenolpyruvate-dependent sugar phosphotransferase systems: Identification of possible phosphate-carrying histidine residues. *PNAS, 84*(14), 4777-4780.

[39] Breukink, E., Wiedemann, I., van Kraaij, C., Kuipers, O. P., Sahl, H.-G., & de Kruijff, B. (1999). Use of the cell wall precursor lipid II by a pore-forming peptide antibiotic. *Science, 286*(5448), 2361-2364.

[40] Brimble, M. A., Edwards, P. J., Harris, P. W., Norris, G. E., Patchett, M. L., Wright, T. H., . . . Carley, S. E. (2015). Synthesis of the antimicrobial *S*-linked glycopeptide, glycocin F. *Chemistry A European Journal, 21*, 3556-3561.

[41] Brown, D. R., Helaine, S., Carbonnelle, E., & Pelicic, V. (2010). Systematic functional analysis reveals that a set of seven genes is involved in fine-tuning of the multiple functions mediated by type IV pili in *Neisseria meningitidis*. *Infection and Immunity, 78*(7), 3053-3063.

[42] Brown, L., Wolf, J. M., Prados-Rosales, R., & Casadevall, A. (2015). Through the wall: Extracellular vesicles in gram-positive bacteria, mycobacteria and fungi. *Nature Reviews Micrbiology, 13*, 620-630.

[43] Brown, S., Santa Maria, J. P., & Walker, S. (2014). Wall techoic acids of gram-positive bacteria. *Annual Review of Microbiology, 67*, 313-336.

[44] Bublitz, M., Morth, J. P., & Nissen, P. (2011). P-type ATPases at a glance. *Journal of Cell Science, 124*(15), 2515-2519.

[45] Burbaum, J., & Tobal, G. M. (2002). Proteomics in drug discovery. *Current Opinion in Chemical Biology, 6*(4), 427-433.

[46] Busenlehner, L. S., Pennella, M. A., & Giedroc, D. P. (2003). The SmtB/ArsR family of metalloregulatory transcriptional repressors: Structural insights into prokaryotic metal resistance. *FEMS Microbiology Reviews, 27*, 131-143.

[47] Butler, M. M., & Wright, G. E. (2008). A method to assay the inhibitors of DNA polymerase IIIC activity. In W. S. Champney, *New Antibiotic Targets*. *Methods in Molecular Medicine* (Vol. 142, pp. 25-36). Humana Press.

[48] Cahyanto, M. N., Kawasaki, H., Fujiyama, K., & Seki, T. (2006). Cloning of *Lactobacillus plantarum* IAM 12477 lysine biosynthesis genes encoding functional aspartate

semialdehyde dehydrogenase, dihydrodipicolinate synthase, and dihydropicolinate reductase. *World Journal of Microbiology & Biotechnology, 22*, 409-416.

[49] Callister, S. J., Barry, R. C., Adkins, J. N., Johnson, E. T., Qian, W.-J., Webb-Robertson, B.-J. M., . . . Lipton, M. S. (2006). Normalization approaches for removing systematic biases assciated with mass spectrometry and label-free proteomics. *Journal of Proteome Research, 5*, 277-286.

[50] Cameron, D. R., Jiang, J.-H., Kostoulias, X., Foxwell, D. J., & Peleg, A. Y. (2016). Vancomycin susceptibility in methicillin-resistant *Staphylococcus aureus* is mediated by YycHI activation of the WalRK essential two-component regulatory system. *Scientific Reports, 6*, 1-11.

[51] Campbell, J., Singh, A. K., Santa MAria, J. P., Kim, Y., Brown, S., Swoboda, J. G., . . . Walker, S. (2011). Synthetic lethal compound combinations reveal a fundamental connection between wall teichoic acid and peptidoglycan biosynthesis in *Staphylococcus aureus*. *ACS Chemical Biology, 6*(1), 106-116.

[52] Carbrey, J. M., & Agre, P. (2009). Discovery of the aquaporins and development of the field. In E. Beitz, *Aquaporins* (pp. 3-28). Berlin: Springer.

[53] Carter, A. P., Clemons, W. M., Brodersen, D. E., Morgan-Warren, R. J., Wimberly, B. T., & Ramakrishnan, V. (2000). Functional insights from the structure of the 30S ribosomal subunit and its interactions with antibiotics. *Nature, 407*, 340-348.

[54] Cavera, V. L., Arthur, T. D., Kashtanov, D., & Chikindas, M. L. (2015). Bacteriocins and their position in the next wave of conventional antibiotics. *International Journal of Antimicrobial Agents, 46*(5), 494-501.

[55] Chatfield, C. H., Koo, H., & Quivey Jr., R. G. (2005). The putative autolysin regulator LytR in *Streptococcus mutans* plays a role in cell division and is growth-phase regulated. *Microbiology, 151*(2), 625-631.

[56] Chavers, L. S., Moser, S. A., Benjamin, W. H., Banks, S. E., Steinhauer, J. R., Smith, A. M., . . . Waites, K. B. (2003). Vancomycin-resistant enterococci: 15 years and counting. *Journal of Hospital Infection, 53*(3), 159-171.

[57] Chen, H., Chen, C., Ai, C., Ren, C., & Gao, H. (2019). Genetic operation system of lactic acid bacteria and its applications. In W. Chen, *Lactic Acid Bacteria: Omics and Functional Evaluation* (pp. 35-76). Singapore: Springer Nature Singapore Pte Ltd. and Science Press.

[58] Cheng, C., Dong, Z., Han, X., Wang, H., Jiang, L., Sun, J., . . . Song, H. (2017). Thioredoxin A is essential for motility and contributes to host infection of *Listeria monocytogenes via* redox interactions. *Frontiers in Cellular and Infection Micrbiology, 7*, 1-19.

[59] Chiba, S., & Ito, K. (2015). MifM monitors total YidC activities of *Bacillus subtilis*, including that of YidC2, the target of regulation. *Journal of Bacteriology, 197*(1), 99-107.

[60] Chien, A.-C., Zareh, S. K., Wang, Y. M., & Levin, P. A. (2012). Changes in the oligomerization potential of the division inhibitor UgtP co-ordinate *Bacillus subtilis* cell size with nutrient availability. *Molecular Microbiology, 86*(3), 594-610.

[61] Chikindas, M. L., Weeks, R., Drider, D., Christyakov, V. A., & Dicks, L. M. (2018). Functions and emerging applications of bacteriocins. *Current Opinion in Biotechnology, 49*, 23-28.

[62] Chlebek, J. L., Hughes, H. Q., Ratkiewicz, A. S., Rayyan, R., Wang, J. C.-Y., Herrin, B. E., . . . Dalia, A. B. (2019). PilT and PilU are homohexameric ATPases that coordinate to retract type IVa pili. *PLoS Genetics, 15*(10), 1-24.

[63] Chongsiriwatana, N. P., & Barron, A. E. (2010). Comparing bacterial membrane interactions of antimicrobial peptides and their mimics. In A. Giuliani, & A. C. Rinaldi, *Antimicrobial peptides: Methods and protocols* (pp. 171-182). Totowa, New Jersey: Humana Press.

[64] Chu, X., Lin, Y., Sun, Z., Huan, L., & Zhong, J. (2010). Advances in the study of nisin resistance - a review. *Wei Sheng Wu Xue Bao, 50*, 1129-1134.

[65] Cohen, D. P., Renes, J., Bouwman, F. G., Zoetendal, E. G., Mariman, E., de Vos, W. M., & Vaughan, E. E. (2006). Proteomic analysis of log to stationary growth phase *Lactobacillus plantarum* cells and a 2-DE database. *Proteomics, 6*(24), 6485-6493.

[66] Cohen, G. N. (2004). Transcription. RNA polymerase. In G. N. Cohen, *Microbial Biochemistry* (pp. 97-101). Dordrecht: Springer.

[67] Cole, R. M., Popkin, T. J., Boylan, R. J., & Mendelson, N. H. (1970). Ultrastructure of a temperature-sensitive rod-mutant of *Bacillus subtilis*. *Journal of Bacteriology, 103*(3), 793-810.

[68] Cordwell, S. J. (2006). Technologies for bacterial surface proteomics. *Current Opinion in Microbiology, 9*, 320-329.

[69] Cotter, P. D., Ross, R. P., & Hill, C. (2013). Bacteriocins - a viable alternative to antibiotics? *Nature Reviews Microbiology, 11*, 95-105.

[70] Cundliffe, E., & Thompson, J. (1979). Ribose methylation and resistance to thiostrepton. *Nature, 278*, 859-861.

[71] da Silva Sabo, S., Vitolo, M., D., G. J., & Olivera, R. P. (2014). Overview of *Lactobacillus plantarum* as a promising bacteriocin producer among lactic acid bacteria. *Food Research International, 64*, 527-536.

[72] Dalbey, R. E., & Kuhn, A. (2004). YidC family members are involved in the membrane insertion, lateral integration, folding, and assembly of membrane proteins. *Journal of Cell Biology, 166*(6), 769-774.

[73] Dalbey, R. E., Kuhn, A., Zhu, L., & Kiefer, D. (2014). The membrane insertase YidC. *Biochimica et Biophysica Acta (BBA) - Molecular Cell Research, 1843*(8), 1489-1496.

[74] Daniel, R. A., & Errington, J. (2003). Control of cell morphogenesis in bacteria: Two distinct ways to make a rod-shaped cell. *Cell, 113*(6), 767-776.

[75] Das, A., & Ljungdahl, L. G. (1997). Composition and primary structure of the F_1F_0 ATP synthase from the obligately anaerobic bacterium *Clostridium thermoaceticum*. *Journal of Bacteriology, 179*(11), 3746-3755.

[76] David, B., Duchene, M.-C., Haustenne, G. L., Perez-Nunez, D., Chapot-Chartier, M.-P., De Bolle, X., . . . Hallet, B. (2018). PBP2b plays a key role in both peripheral growth and septum positioning in Lactococcus. *PLoS ONE, 13*(5), 1-25.

[77] Davidson, A. L., Dassa, E., Orelle, C., & Chen, J. (2008). Structure, function, and evolution of bacterial ATP-binding cassette systems. *Microbiology and Molecular Biology Reviews, 72*(2), 317-364.

[78] Delcour, J., Ferain, T., Deghorain, M., Palumbo, E., & Hols, P. (1999). The biosynthesis and functionality of the cell-wall of lactic acid bacteria. *Antonie van Leeuwenhoek, 76*, 159-184.

[79] Dempwolff, F., Reimold, C., Reth, M., & Graumann, P. L. (2011). *Bacillus subtilis* MreB orthologs self-organize into filamentous structures underneath the cell membrane in a heterologous cell system. *PLoS ONE, 6*(11), 1-9.

[80] Deutscher, J., Aké, F. M., Derkaoui, M., Zébré, A. C., Cao, T. N., Bouraoui, H., . . . Joyet, P. (2014). The bacterial phosphoenolpyruvate:carbohydrate phosphotransferase system: Regulation by protein phosphorylation and phosphorylation-dependent protein-protein interactions. *Microbiology and Molecular Biology Reviews, 78*(2), 231-256.

[81] Deutscher, J., Francke, C., & Postma, P. W. (2006). How phosphotransferase system-related protein phosphorylation regulates carbohydrate metabolism in bacteria. *Microbiology and Molecular Biology Reviews, 70*(4), 939-1031.

[82] Diep, D. B., Skaugen, M., Salehian, Z., Holo, H., & Nes, I. F. (2007). Common mechanisms of target cell recognition and immunity for class II bacteriocins. *PNAS, 104*(7), 2384-2389.

[83] Dimauro, I., Pearson, T., Caporossi, D., & Jackson, M. J. (2012). A simple protocol for the subcellular fractionation of skeletal muscle cells and tissue. *BMC Research Notes, 5*, 1-5.

[84] Dion, M. F., Kapoor, M., Sun, Y., Wilson, S., Ryan, J., Vgouroux, A., . . . Garner, E. C. (2019). *Bacillus subtilis* cell diameter is determined by the opposing actions of two distinct cell wall synthetic systems. *Nature Microbiology, 4*(8), 1294-1305.

[85] Divakaruni, A. V., Ogorzalek-Loo, R. R., Xie, Y., Loo, J. A., & Gober, J. W. (2005). The cell-shape protein MreC interacts with extracytoplasmic proteins including cell wall assembly complexes in *Caulobacter crescentus*. *PNAS, 102*(51), 18602-18607.

[86] Douthwaite, S. (1992). Interaction of the antibiotics clindamycin and lincomycin with *Escherichia coli* 23S ribosomal RNA. *Nucleic Acids Research, 20*(18), 4717-4720.

[87] Drower, K. R. (2014). The bacteriostatic diglycosylated bacteriocin glycocin F targets a sugar-specific transporter. 1-206. New Zealand: Massey University, Palmerston North.

[88] Drummond, B. J. (2020). Heterologous expression of the *gcc* gene cluster and subsequent characterisation of the glycocin F biosynthetic pathway. New Zealand: Massey University, Palmerston North.

[89] Drummond, B. J., Loo, T. S., Patchett, M. L., & Norris, G. E. (2021). Optimizes genetic toold allow the biosynthesis of glycocin F and analogues designed to test the roles of *gcc* cluster genes in bacteriocin production. *Journal of Bacteriology, 203*(7), 1-12.

[90] Du, W., Brown, J. R., Sylvester, D. R., Huang, J., Chalker, A. F., So, C. Y., . . . Wallis, N. G. (2000). Two active forms of UDP-N-acetylglucosamine enolpyruvyl transferase in gram-positive bacteria. *Journal of Bacteriology, 182*(15), 4146-4152.

[91] Dubrac, S., Bisicchia, P., Devine, K. M., & Msadek, T. (2008). A matter of life and death: Cell wall homeostasis and the WalKR (YycGF) essential signal transduction pathway. *Molecular Microbiology, 70*(6), 1307-1322.

[92] Duman, R., Ishikawa, S., Celik, I., Strahl, H., Ogasawara, N., Troc, P., . . . Hamoen, L. W. (2013). Structural and genetic analyses reveal the protein SepF as a new membrane anchor for the Z-ring. *PNAS, 110*(48), E4601-E4610.

[93] Dupree, E. J., Jayathirtha, M., Yorkey, H., Mihasan, M., Petre, B. A., & Darie, C. C. (2020). A critical review of bottom-up proteomics: The good, the bad, and the future of this field. *Proteomes, 8*(14), 1-26.

[94] Edwards, M. D., Black, S., Rasmussen, T., Rasmussen, A., Stokes, N. R., Stephen, T.-L., . . . Booth, I. R. (2012). Characterization of three novel mechanosensitive channel activities in *Escherichia coli*. *Channels, 6*(4), 272-281.

[95] Egan, A. J., Errington, J., & Vollmer, W. (2020). Regulation of peptidoglycan synthesis and remodelling. *Nature Reviews Microbiology, 18*, 446-460.

[96] Elma Schmidbauer GmbH. (2021, July 11). *Elma-Ultrasonic*. Retrieved from Elma-Ultrasonic: https://www.elma-ultrasonic.com

[97] Eppendorf. (2021, July 11). *Eppendorf*. Retrieved from Eppendorf: https://www.eppendorf.com/AU-en/

[98] Eymann, C., Dreisbach, A., Albrecht, D., Bernhardt, J., Becher, D., Gentner, S., . . . Hecker, M. (2004). A comprehensive proteome map of growing *Bacillus subtilis* cells. *Proteomics, 4*(10), 2849-2876.

[99] Fabret, C., & Hoch, J. A. (1998). A two-component signal transduction system essential for growth of *Bacillus subtilis*: Implications for anti-infective therapy. *Journal of Bacteriology, 180*(23), 6375-6383.

[100] Facey, S. J., Neugebauer, S. A., Krauss, S., & Kuhn, A. (2007). The mechanosensitive channel protein MscL is targeted by the SRP to the novel YidC membrane insertion pathway of *Escherichia coli*. *Journal of Molecular Biology, 365*(4), 995-1004.

[101] Fagan, M. J., & Saler, M. H. (1994). P-type ATPases of eukaryotes and bacteria: Sequence analyses and construction of phylogenetic trees. *Journal of Molecular Evolution, 38*, 57-99.

[102] Fenton, A. K., Lambert, C., Wagstaff, P. C., & Sockett, R. E. (2009). Manipulating each MreB of *Bdellovibrio bacteriovorus* gives diverse morphological and predatory phenotypes. *Journal of Bacteriology, 192*(5), 1299-1311.

[103] Ferrer-González, E., Huh, H., Al-Tameemi, H. M., Boyd, J. M., Lee, S.-H., & Pilch, D. S. (2021). Impact of FtsZ inhibition on the localization of the penicillin binding proteins in methicillin-resistant *Staphylococcus aureus*. *Journal of Bacteriology, 203*(16), e00204-21.

[104] Fibriansah, G., Kovács, Á. T., Pool, T. J., Boonstra, M., Kuipers, O. P., & Thunnissen, A.-M. W. (2012). Crystal structures of two transcriptional regulators from *Bacillus cereus* defin the conserved strctural features of a PadR subfamily. *PLoS ONE, 7*(11), 1-11.

[105] Fleming, H. P., Etchells, J. L., & Costilow, R. N. (1975). Microbial inhibition by an isolate of Pediococcus from cucumber brines. *Applied Microbiology, 30*(6), 1040-1042.

[106] Florens, L., Korfali, N., & Schirmer, E. C. (2008). Subcellular fractionation and proteomics of nuclear envelopes. In D. Pflieger, & J. Rossier, *Organelle Proteomics. Methods in Molecular Biology* (Vol. 432, pp. 117-137). Humana Press.

[107] Folgering, J. H., Moe, P. C., Schuurman, -W. G., Blout, P., & Poolman, B. (2005). *Lactococcus lactis* uses MscL as its principal mechanosensitive channel. *The Journal of Biological Chemistry, 280*(10), 8784-8792.

[108] Formstone, A., & Errington, J. (2005). A magnesium-dependent mreB null mutant: Implications for the role of mreB in *Bacillus subtilis*. *Molecular Microbiology, 55*(6), 1646-1657.

[109] Formstone, A., Carballido-López, R., Noirot, P., Errington, J., & Scheffers, D. J. (2008). Localization and interactions of teichoic acid synthetic enzymes in *Bacillus subtilis*. *Journal of Bacteriology, 190*(5), 1812-1821.

[110] Gabrielsen, C., Brede, D. A., Hernández, P. E., & Diep, D. B. (2012). The maltose ABC transporter in *Lactococcus lactis* facilitates high-level sensitivity to the circular bacteriocin garvicin ML. *Antimicrobial Agents and Chemotherapy, 56*(6), 2908-2915.

[111] Gajdiss, M., Monk, I. R., Bertsche, U., Kienemund, J., Funk, T., Dietrich, A., . . . Bierbaum, G. (2020). YycH and YycI regulate expression of *Staphylococcus aureus* autolysins by activation of WalRK phosphorylation. *Microorganisms, 8*(6), 1-16.

[112] Gamba, P., Hamoen, L. W., & Daniel, R. A. (2016). Cooperative recruitment of FtsW to the division site of *Bacillus subtilis*. *Frontiers in Microbiology, 7*(1808), 1-9.

[113] Garcia De Gonzalo, C. V., Denham, E. L., Mars, R. A., Stülke, J., van der Donk, W. A., & van Dijl, J. M. (2015). The phosphoenolpyruvate:sugar phosphotransferase system is involved in sensitivity to the glucosylated bacteriocin sublancin. *Antimicrobial Agents and Chemotherapy, 59*(11), 6844–6854.

[114] García-del Portillo, F., Calvo, E., D'Orazio, V., & Pucciarelli, M. G. (2011). Association of ActA to peptidoglycan revealed by cell wall porteomics of intracellular *Listeria monocytogenes*. *The Journal of Biological Chemistry, 286*(40), 34675-34689.

[115] Garcia-Gutierrez, E., Mayer, M. J., Cotter, P. D., & Narbad, A. (2019). Gut microbiota as a source of novel antimicrobials. *Gut Microbes, 10*(1), 1-21.

[116] Gaspar, A. H., Marraffini, L. A., Glass, E. M., DeBond, K. L., Ton-That, H., & Schneewind, O. (2005). *Bacillus anthracis* sortase A (SrtA) anchors LPXTG motif-containing surface proteins to the cell wall envelope. *Journal of Bacteriology, 187*(13), 4646-4655.

[117] GE Healthcare. (2021, July 11). *GE Healthcare*. Retrieved from GE Healthcare: https://www.ge.com

[118] Geraci, J. E. (1977). Vancomycin. *Mayo Clinic Proceedings, 52*(10), 631-634.

[119] Gokce, E., Shuford, C. M., Franck, W. L., Dean, R. A., & Muddiman, D. C. (2011). Evaluation of normalization methods on geLC-MS/MS label-free spectral counting data to correct for variation during proteomic workflows. *Journal of The American Society for Mass Spectrometry, 22*(12), 2199-2208.

[120] Gold Biotechnology. (2021, July 10). *Gold Bio*. Retrieved from Gold Bio: https://www.goldbio.com

[121] Gomes, J., Barbosa, J., & Teixeira, P. (2019). Natural antimicrobial agents as an alternative to chemical antimicrobials in the safety and preservation of food products. *Current Chemical Biology, 13*(1), 25-37.

[122] Gotz, S., Garcia-Gomez, J. M., Terol, J., Williams, T. D., Nagaraj, S. H., Nueda, M. J., . . . Conesa, A. (2008). High-throughput functional annotation and data mining with the BLAST2GO suite. *Nucleic Acids Research, 36*(10), 3420-35.

[123] Grabner, G. K., & Switzer, R. L. (2003). Kinetic studies of the uracil phosphoribosyltransferase reaction catalyzed by the *Bacillus subtilis* pyrimidine attenuation regulaory protein PyrR. *Journal of Biological Chemistry, 278*(9), 6921-6927.

[124] Graupner, S., Weger, N., Sohni, M., & Wackernagel, W. (2001). Requirement of novel competence genes *pilT* and *pilU* of *Pseudomonas stutzeri* for natural transformation and suppression of *pilT* deficiency by a hexahistidine tag on the type IV pilus protein PilAI. *Journal of Bacteriology, 183*(16), 4694-4701.

[125] Green, E. R., & Mecsas, J. (2016). Bacterial secretion systems: An overview. *Microbiology Spectrum, 4*(1), 1-32.

[126] Gurumayum, S., Senapati, S. S., Rasane, P., Dhawan, K., Kaur, S., Singh, J., & Kaur, D. (2021). Bacteriocins: Biosynthesis, production, purification, and its potential applications in food and human health. In D. K. Verma, A. R. Patel, K. S. Sandhu, A. Baldi, & S. Garcia, *Biotechnical Processing in the Food Industry: New Methods, Techniques, and Applications* (pp. 237-268). New York: Apple Academic Press.

[127] Häuser, R., Pech, M., Kijek, J., Yamamoto, H., Titz, B., Naeve, F., . . . Uetz, P. (2012). RsfA (YbeB) proteins are conserved ribosomal silencing factors. *PLoS Genetics, 8*(7), 1-12.

[128] Haeusser, D. P., Garza, A. C., Buscher, A. Z., & Levin, P. A. (2007). The division inhibitor EzrA contains a seven-residue patch required for maintaining the dynamic nature of the medial FtsZ ring. *Journal of Bacteriology, 189*(24), 9001-9010.

[129] Hamoen, L. W., Meile, J.-C., De Jong, W., Noirot, P., & Errington, J. (2005). SepF, a novel FtsZ-interacting protein required for a late step in cell division. *Molecular Microbiology, 59*(3), 989-999.

[130] Hamon, E., Horvatovich, P., Izquierdo, E., Bringel, F., Marchioni, E., Aoude-Werner, D., & Ennahar, S. (2011). Comparative proteomic analysis of *Lactobacillus plantarum* for the identification of key proteins in bile tolerance. *BMC Microbiology, 11*(63), 1-11.

[131] Hansen, J. L., Ippolito, J. A., Ban, N., Nissen, P., Moore, P. B., & Steitz, T. A. (2002). The structures of four macrolide antibiotics bound to the large ribosomal subunit. *Molecular Cell, 10*(1), 117-128.

[132] Hata, T., Tanaka, R., & Ohmomo, S. (2010). Isolation and characterization of plantaricin ASM1: A new bacteriocin produced by *Lactobacillus plantarum* A-1. *International Journal of Food and Microbiology, 137*(1), 94-99.

[133] Hechard, Y., & Sahl, H.-G. (2002). Mode of action of modified and unmodified bacteriocins from gram-positive bacteria. *Biochimie, 84*(5-6), 545-557.

[134] Heffernan, H., & Bakker, S. (2015). *Annual survey of methicillin-resistant Staphylococcus aureus (MRSA)*. Kenepuru, Porirua: Institute of Environmental Science and Research Limited.

[135] Heffernan, H., Woodhouse, R., & Williamson, D. (2015). *Antimicrobial resistance and molecular epidemiology of Neisseria gonorrhoeae in New Zealand*. Kenepuru, Porirua: Institute of Environmental Science and Research Limited.

[136] Helmann, J. D. (2002). The extracytoplasmic function (ECF) sigma factors. *Advances in Microbial Physiology, 46*, 47-110.

[137] Henriques, A. O., Glaser, P., Piggot, P. J., & Moran, C. P. (2002). Control of cell shape and elongation by the *rodA* gene in *Bacillus subtilis*. *Molecular Microbiology, 28*(2), 235-247.

[138] Heunis, T., Deane, S., Smit, S., & Dicks, L. M. (2014). Proteomic profiling of the acid stress response in *Lactobacillus plantarum* 4232. *Journal of Proteome Research, 13*(9), 4028-4039.

[139] Higgins, C. F. (1992). ABC transporters: From microorganisms to man. *Annual Review of Cell Biology, 8*, 67-113.

[140] Hirakawa, H., Kurushima, J., Hashimoto, Y., & Tomita, H. (2020). Progress overview of bacterial two-component regulatory systems as potential targets for antimicrobial chemotherapy. *Antibiotics, 9*(635), 1-15.

[141] Hoffmann, T., Boiangiu, C., Moses, S., & Bremer, E. (2008). Responses of *Bacillus subtilis* to hypotonic challenges: Physiological contributions of mechanosensitive channels to cellular survival. *Applied and Environmental Microbiology, 74*(8), 2454-2460.

[142] Holden, H. M., Rayment, I., & Thoden, J. B. (2003). Structure and function of enzymes of the Leloir pathway for galactose metabolism. *Journal of Biological Chemistry, 278*(45), 43885-43888.

[143] Holmgren, A. (1989). Thioredoxin and glutaredoxin systems. *The Journal of Biological Chemistry, 264*(24), 13963-13966.

[144] Holo, H., Nilssen, O., & Nes, I. F. (1991). Lactococcin A, a new bacteriocin from *Lactococcus lactis* subsp. *cremoris*: Isolation and characterization of the protein and its gene. *Journal of Bacteriology, 173*(12), 3879-3887.

[145] Holzer, M., Kern, S., Birner-Grünberger, R., Curcic, S., Heinemann, A., & Marsche, G. (2016). Refined purification strategy for reliable proteomic profiling of HDL2/3: Impact on proteomic complexity. *Scientific Reports, 6*, 1-10.

[146] Honeywell International Inc. (2021, July 11). *Fluka Analytical*. Retrieved from Fluka Analytical: https://lab.honeywell.com/en/fluka

[147] Hrast, M., Sosič, I., Šink, R., & Gobec, S. (2014). Inhibitors of the peptidoglycan biosynthesis enzymes MurA-F. *Bioorganic Chemistry, 55*, 2-15.

[148] Huang, Q., Tonge, P. J., Slayden, R. A., Kirikae, T., & Ojima, I. (2007). FtsZ: A novel target for tuberculosis drug discovery. *Current Topics in Medicinal Chemistry, 7*(5), 527-543.

[149] Huber, L. A., Pfaller, K., & Vietor, I. (2003). Implications for subcellular fractionation in proteomics. *Circulation Research, 92*, 962-968.

[150] Innis, C. A., Blaha, G., Bulkley, D., & Steitz, T. A. (2011). Structural studies of complexes of the 70S ribosome. In M. V. Rodnina, W. Wintermeyer, & R. Green, *Ribosomes* (pp. 31-43). Vienna: Springer.

[151] Ishibashi, K., Morishita, Y., & Tanaka, Y. (2017). The evolutuionary aspects of aquaporin family. In B. Yang, *Aquaporins* (pp. 35-50). Dordrecht: Springer.

[152] Ishino, F., Park, W., Tomioka, S., Tamaki, S., Takase, I., Kunugita, K., . . . Matsuhashi, M. (1986). Peptidoglycan synthetic activities in membranes of *Escherichia coli* caused by overproduction of penicillin-binding protein and RodA protein. *The Journal of Biological Chemistry, 261*(15), 7024-7031.

[153] Islam, M. R., Nagao, J.-I., Zendo, T., & Sonomoto, K. (2012). Antimicrobial mechanism of lantibiotics. *Biochemical Society Transactions, 40*(6), 1528-1533.

[154] Iwai, N., Nagai, K., & Wachi, M. (2002). Novel *S*-benzylisothiourea compound that induces spherical cells in *Escherichia coli* probably by acting on a rod shape-determining protein(s) other than penicillin-binding protein 2. *Bioscience, Biotechnology, and Biochemistry, 66*(12), 2658-2662.

[155] Izquierdo, E., Wagner, C., Marchioni, E., Aoude-Werner, D., & Ennahar, S. (2009). Enterocin 96, a novel class II bacteriocin produced by *Enterococcus faecalis* WHE 96, isolated from munster cheese. *Applied and Environmental Microbiology*, 4273-4276.

[156] Jarick, M., Bertsche, U., Stahl, M., Schultz, D., Methling, K., Lalk, M., . . . Ohlsen, K. (2018). The serine/threonine kinase Stk and the phosphatase Stp regulate cell wall synthesis in *Staphylococcus aureus*. *Scientific Reports, 8*, 1-13.

[157] Jeckelman, J.-M., & Erni, B. (2020). Transporters of glucose and other carbohydrates in bacteria. *European Journal fo Physiology, 472*, 1129-1153.

[158] Ji, S., Li, W., Xin, H., Wang, S., & Cao, B. (2015). Improved production of sublancin 168 biosynthesized by *Bacillus subtilis* 168 using chemometric methodology and statistical experimental designs. *BioMed Research International, 2015*, 1-9.

[159] Jones, P. M., & George, A. M. (2004). The ABC transporter structure and mechanism: perspectives on recent research. *Cellular and Molecular Life Sciences, 61*, 682-699.

[160] Jones-Dias, D., Carvalho, A. S., Moura, I. B., Manageiro, V., Igrejas, G., Caniça, M., & Matthiesen, R. (2017). Quantitative proteome analysis of an antibiotic resistant *Escherichia*

coli exposed to tetracycline reveals multiple affected metabolic and peptidoglycan processes. *Journal of Proteomics, 156*, 20-28.

[161] Jorasch, P., Wolter, F. P., Zähringer, U., & Heinz, E. (1998). A UDP glucosyltransferase from *Bacillus subtilis* successively transfers up to four glucose residues to 1,2-diacylglycerol: Expression of *ypfP* in *Escherichia coli* and structural analysis of its reaction products. *Molecular Microbiology, 29*(2), 419-430.

[162] Jordan, S., Hutchings, M. I., & Mascher, T. (2008). Cell envelope stress response in gram-positive bacteria. *FEMS Microbiology Reviews, 32*(1), 107-146.

[163] Kandler, O. (1983). Carbohydrate metabolism in lactic acid bacteria. *Antonie van Leeuwenhoek: Journal of Microbiology, 49*(3), 209-224.

[164] Kanehisa, M., & Goto, S. (2000). KEGG: Kyoto encyclopedia of genes and genomes. *Nucleid Acids Research, 28*(1), 27-30.

[165] Kang, J., David, L., Li, Y., Cang, J., & Chen, S. (2021). Three-in-one simultaneous extraction of proteins, metabolites and lipids for multi-omics. *Frontiers in Genetics, 12*, 1-11.

[166] Karlsson, O. P., Dahlqvist, A., Vikström, S., & Wieslander, A. (1997). Lipid dependence and basic kinetics of the purified 1,2-diacylglycerol 3-glucosyltransferase from membranes of *Acholeplasma laidlawii*. *Journal of Biological Chemistry, 272*(2), 929-936.

[167] Kaunietis, A., Buivydas, A., Čitavičius, D. J., & Kuipers, O. P. (2019). Heterologous biosynthesis and characterization of a glycocin from a thermophilic bacterium. *Nat Commun., 10*, 1115.

[168] Kazakov, A. E., Vassieva, O., Gelfand, M. S., Osterman, A., & Overbeek, R. (2003). Bioinformatics classification and functional analysis of PhoH homologs. *In Silico Biology, 3*(1-2), 3-15.

[169] Khattar, M. M., Begg, K. J., & Donachie, W. D. (1994). Identification of FtsW and characterization of a new *ftsW* division mutant of *Escherichia coli*. *Journal of Bacteriology, 176*(23), 7140-7147.

[170] Khusainov, I., Fatkhullin, B., Pellegrino, S., Bikmullin, A., Liu, W.-T., Gabdulkhakov, A., . . . Yusupov, M. (2020). Mechanism of ribosome shutdown by RsfS in *Staphylococcus aureus* revealed by integrative structural biology approach. *Nature Communications, 11*, 1-10.

[171] Kiefer, D., & Kuhn, A. (2007). YidC as an essential and multifunctional component in membrane protein assembly. *International Review of Cytology, 259*, 113-138.

[172] Kim, S.-A., Woo, J.-H., Hong, S.-D., & Song, B.-H. (1997). Isolation of the *Bacillus subtilis cdd* downstrean region and analysis of genetic structure around the *cdd* vicinity. *Molecules and Cells, 7*(5), 648-654.

[173] Kim, S.-K., Makino, K., Amemura, M., Shinagawa, H., & Nakata, A. (1993). Molecular analysis of the *phoH* gene, belonging to the phosphate regulon in *Escherichia coli*. *Journal of Bacteriology, 175*(5), 1316-1324.

[174] Kirillov, S., Porse, B. T., Vester, B., Woolley, P., & Garrett, R. A. (1997). Movement of the 3'-end of tRNA through the peptidyl transferase centre and its inhibition by antibiotics. *FEBS Letters, 406*(3), 223-233.

[175] Kito, K., & Ito, T. (2008). Mass spectrometry-based approaches toward absolute quantitative proteomics. *Current Genomics, 9*, 263-274.

[176] Kock, H., Gerth, U., & Hecker, M. (2003). MurA, catalysing the first committed step in peptidoglycan biosynthesis, is a target of Clp-dependent proteolysis in *Bacillus subtilis*. *Molecular Microbiology, 51*(4), 1087-1102.

[177] Koonin, E. V., & Rudd, K. E. (1996). Two domains of superfamily I helicases may exist as separate proteins. *Protein Science, 5*(1), 178-180.

[178] Kotrba, P., Inui, M., & Yukawa, H. (2001). Bacterial phosphotransferase system (PTS) in carbohydrate uptake and control of carbon metabolism. *Journal of Bioscience and Bioengineering, 92*(6), 502-517.

[179] Kouwen, T. R., Trip, E. N., Denham, E. L., Sibbald, M. J., Dubois, J.-Y. F., & van Dijl, J. M. (2009). The large mechanosensitive channel MscL determines bacterial susceptibility to the bacteriocin sublancin 168. *Antimicrobial Agents and Chemotherapy, 53*(11), 4702-4711.

[180] Krishnan, V., Chaurasia, P., & Kant, A. (2016). Pili in probiotic bacteria. In V. Rao, & L. G. Rao, *Probiotics and Prebiotics in Human Nutrition and Health* (pp. 115-134). Rijeka: Intech.

[181] Krishnan, V. (2015). Pilins in gram-positive bacteria: A structural perspective. *IUBMB Life, 67*(7), 533-543.

[182] Kruse, E., Uehlein, N., & Kaldenhoff, R. (2006). The aquaporins. *Genome Biology, 7*(2), 1-6.

[183] Kumariya, R., Garsa, A. K., Rajput, Y. S., Sood, S. K., Akhtar, N., & Patel, S. (2019). Bacteriocins: Classification, synthesis, mechanism of action and resistance development in food spoilage causing bacteria. *Microbial Pathogenesis, 128*, 171-177.

[184] Kung, C., Martinac, B., & Sukharev, S. (2010). Mechanosentsitive channels in microbes. *Annual Review of Microbiology, 64*, 313-329.

[185] Laemmli, U. K. (1970). Cleavage of structural proteins during the assembly of the head of bacteriophage T4. *Nature, 227*(5259), 680-685.

[186] Land, A. D., & Winkler, M. E. (2011). The requirement for pneumococcal MreC and MreD is relieved by inactivation of the gene encoding PBP1a. *Journal of Bacteriology, 193*(16), 4166-4179.

[187] Lazarevic, V., & Karamata, D. (1995). The *tagGH* operon of *Bacillus subtilis* 168 encodes a two-component ABC transporter involved in the metabolism of two wall teichoic acids. *Molecular Microbiology, 16*(2), 345-355.

[188] Lazarevic, V., Soldo, B., Médico, N., Pooley, H., Bron, S., & Karamata, D. (2005). *Bacillus subtilis* α-phosphoglucomutase is required for normal cell morphologyand biofilm formation. *Applied and Environmental Microbiology, 71*(1), 39-45.

[189] Lee, K. R.-S., Pi, K., Kim, H.-J., & Choi, Y.-J. (2011). Proteomic analysis of protein expression in *Lactobacillus plantarum* in response to alkaline stress. *Journal of Biotechnology, 153*, 1-7.

[190] Lees, W. J., Benson, T. E., Hogle, J. M., & Walsh, C. T. (1996). (E)-enolbutyryl-UDP-*N*-acetylglucosamine as a mechanistic probe of UDP-*N*-acetylenolpyruvylglucosamine reductase (MurB). *Biochemistry, 35*(5), 1342-1351.

[191] Lennon, B. W., Williams Jr., C. H., & Ludwig, M. L. (1999). Crystal structure of reduced thioredoxin reductase from *Escherichia coli*: Structural flexibility in the isoalloxazine ring of the flavin adenine dinucleotide cofactor. *Protein Science, 8*(11), 2366-2379.

[192] Leong, C. G., Bloomfield, R. A., Boyd, C. A., Dornbusch, A. J., Lieber, L., Liu, F., . . . Lostroh, C. P. (2017). The role of core and accessory type IV pilus genes in natural transformation and twitching motility in the bacterium *Acinetobacter baylyi*. *PloS One, 12*(8), 1-25.

[193] Levine, D. P. (2006). Vancomycin: A history. *Clinical Infectious Diseases, 42*(S1), S5-S12.

[194] Li, H., & Cao, Y. (2010). Lactic acid bacterial cell factories for gamma-aminobutyric acid. *Amino Acids, 39*(5), 1107-1116.

[195] Li, X., Sun, Q., Jiang, C., Yang, K., Hung, L.-H., Zhang, J., & Sacchettini, J. C. (2015). Structure of the ribosomal silencing factor bound to *Mycobacterium tuberculosis* ribosome. *Structure, 23*, 1858-1865.

[196] Li, Z., Adams, R. M., Chourey, K., Hurst, G. B., Hettich, R. L., & Pan, C. (2012). Systematic comparison of label-free, metabolic labeling, and isobaric chemical labeling for quantitative proteomics on LTQ oribitrap velos. *Journal of Proteome Research, 11*, 1582-1590.

[197] Liu, S., Ma, Y., Zheng, Y., Zhao, W., Zhao, X., Luo, T., . . . Yang, Z. (2020). Cold-stress response of probiotic *Lactobacillus plantarum* K25 by iTRAQ proteomic analysis. *Journal of Microbiology and Biotechnology, 30*(2), 187-195.

[198] Liu, X., Biboy, J., Consoli, E., Vollmer, W., & den Blaauwen, T. (2020). MreC and MreD balance the interaction between the elongasome proteins PBP2 and RodA. *PLoS Genetics, 16*(12), 1-23.

[199] Lu, X., Yi, L., Dang, J., Dang, Y., & Liu, B. (2014). Purification of novel bacteriocin produced by *Lactobacillus coryniformis* MXJ 32 for inhibiting bacterial foodborne pathogens including antibiotic-resistant microorganisms. *Food Control, 46*, 264-271.

[200] Lu, Z., Takeuchi, M., & Sato, T. (2007). The LysR-Type transcriptional regulator YofA controls cell division through the regulation of expression of *ftsW* in *Bacillus subtilis*. *Journal of Bacteriology, 189*(15), 5642-5651.

[201] Lukaszczyk, M., Pradhan, B., & Remaut, H. (2019). The biosynthesis and structures of bacterial Pili. In A. Kuhn, *Bacterial Cell Walls and Membranes*. *Subcellular Biochemistry* (Vol. 92, pp. 369-413). Cham: Springer.

[202] Maier, B., Potter, L., So, M., Seifert, H. S., & Sheetz, M. P. (2002). Single pilus motor forces exceed 100 pN. *PNAS, 99*(25), 16012-16017.

[203] Main, P. J. (2014). Investigating the bacteriocin library of *Lactobacillus plantarum* A-1. New Zealand: Massey University, Palmerston North.

[204] Main, P., Hata, T., Loo, T. S., Man, P., Novak, P., Havlíček, V., . . . Patchett, M. L. (2019). Bacteriocin ASM1 is an *O*/*S*-diglycosylated, plasmid-encoded homologue of glycocin F. *FEBS Letters, 594*(7), 1196-1206.

[205] Maky, M. A., Ishibashi, N., Zendo, T., Perez, R. H., Doud, J. R., Karmi, M., & Sonomoto, K. (2015). Enterocin F4-9, a novel *O*-linked glycosylated bacteriocin. *Applied and Environmental Microbiology, 81*(14), 4819-4826.

[206] Maldonado-Barragán, A., Cárdenas, N., Martínez, B., Ruiz-Barba, J. L., Fernández-Garayzábal, J. F., Rodriguez, J. M., & Gibello, A. (2013). Garvicin A, a novel class IId bacteriocin from *Lactococcus garvieae* that inhibits septum formation in L. garvieae strains. *Applied and Environmental Microbiology, 79*(14), 4336-4346.

[207] Margalef-Català, M., Stefanelli, E., Araque, I., Wagner, K., Felis, G. E., Bordons, A., . . . Reguant, C. (2017). Variability in gene content and expression of the thioredoxin system in *Oenococcus oeni*. *Food Microbiology, 61*, 23-32.

[208] Martin, N. I., Sprules, T., Carpenter, M. R., Cotter, P. D., Hill, C., Ross, P., & Vederas, J. C. (2004). Structural charaterization of lacticin 3147, a two-peptide lantibiotic with synergistic activity. *Biochemistry, 43*(11), 3049-3056.

[209] Martínez, B., Rodríguez, A., & Suárez, J. E. (2000). Lactococcin 972, a bacteriocin that inhibits septum formation in lactococci. *Microbiology, 146*(4), 949-955.

[210] Martinussen, J., & Hammer, K. (1994). Cloning and characterisation of *upp*, a gene encoding uracil phosphoribosyltransferase from *Lactococcus lactis*. *Journal of Bacteriology, 176*(21), 6457-6463.

[211] Matsuoka, S. (2017). Biological functions of glucoipids in *Bacillus subtilis*. *Genes & Genetic Systems, 92*(5), 217-221.

[212] Mattick, J. S. (2002). Type IV pili and twitching motility. *Annual Review of Microbiology, 56*, 289-314.

[213] McCallum, M., Tammam, S., Khan, A., Burrows, L. L., & Howell, P. L. (2017). The molecular mechanism of the type IVa pilus motors. *Nature Communications, 8*, 1-10.

[214] McKerrow, J., Vagg, S., McKinney, T., Seviour, E. M., Maszenan, A. M., Brooks, P., & Seviour, R. J. (2001). A simple HPLC method for analysing diaminopimelic acid diastereomers in cell walls of gram-positive bacteria. *Letters in Applied Microbiology, 30*(3), 178-182.

[215] McPherson, D. C., & Popham, D. L. (2003). Peptidoglycan synthesis in the absence of class a penicillin-binding proteins in *Bacillus subtilis*. *Journal of Bacteriology, 185*(4), 1423-1431.

[216] Meeske, A. J., Riley, E. P., Robins, W. P., Uehara, T., Mekelanos, J. J., Kahne, D., . . . Rudner, D. Z. (2016). SEDS proteins are a widespread family of bacterial cell wall polymerases. *Nature, 537*(7622), 634-638.

[217] Meli, R., Pirozzi, C., & Pelagalli, A. (2018). New perspectives on the potential role of aquaporins (AQPs) in the physiology of inflammation. *Frontiers in Physiology, 9*, 1-11.

[218] Mercer, K. L., & Weiss, D. S. (2002). The *Escherichia coli* cell division protein FtsW is required to recruit its cognate transpeptidase, FtsI (PBP3), to the division site. *Journal of Bacteriology, 184*(4), 904-912.

[219] Merck. (2021, July 11). *Merck*. Retrieved from Merck: https://www.sigmaaldrich.com/NZ/en

[220] Microsoft. (2021, July 11). *Microsoft*. Retrieved from Microsoft: https://www.microsoft.com/en-nz/

[221] Mijakovic, I., Poncet, S., Galinier, A., Monedero, V., Fieulaine, S., Janin, J., . . . Deutscher, J. (2002). Pyrophosphate-producing protein dephosphorylation by HPr kinase/phosphorylase: A relic of early life? *PNAS, 99*(21), 13442-13447.

[222] Milton Adams Ltd. (2021, July 10). *Milton Adams*. Retrieved from Milton Adams: https://www.ma-v.co.nz

[223] Miyachiro, M. M., Contreras-Martel, C., & Dessen, A. (2019). Penicillin-binding preoteins (PBPs) and bacterial cell wall elongation complexes. In J. Harris, & J. Marles-

Wright, *Macromolecular Protein Complexes II: Structure and Function. Subcellular Biochemistry* (Vol. 93, pp. 273-289). Cham: Springer.

[224] Moe, P. C., Blount, P., & Kung, C. (1998). Functional and structural conservation in the mechanosensitive channel MscL implicates elements crucial for mechanosensation. *Molecular Microbiology, 28*(3), 583-592.

[225] Moore, M., Harrison, M. S., Peterson, E. C., & Henry, R. (2000). Chloroplast Oxa1p homolog albino3 is required for post-translational integration of the light harvesting chlorophyll-binding protein into thylakoid membranes. *Journal of Biological Chemistry, 275*(3), 1529-1532.

[226] Moreno, M. S., Schneider, B. L., Maile, R. R., Weyler, W., & Saier Jr, M. H. (2004). Catabolite repression mediated by the CcpA protein in *Bacillus subtilis*: Novel modes of regulation revealed by whole-genome analyses. *Molecular Microbiology, 39*(5), 1366-1381.

[227] Mosaei, H., & Zenkin, N. (2020). Inhibition of RNA polymerase by rifampicin and rifamycin-like molecules. *EcoSal Plus, 9*(1).

[228] Moumène, A., Marcelino, I., Ventosa, M., Gros, O., Lefrançois, T., Vachiéry, N., . . . Coelho, A. V. (2015). Protemic profiling of the outer membrane fraction of the obligate intracellular bactrial pathogen *Ehrlichia ruminantium*. *PLoS ONE, 10*(2), 1-20.

[229] Munch, D., Muller, A., Schneider, T., Kohl, B., Wenzel, M., Bandow, J. E., . . . Sahl, H.-G. (2014). The Lantibiotic NAI-107 binds to bactoprenol-bound cell wall precursors and impairs membrane functions. *Journal of Biological Chemistry, 289*(17), 12063-12076.

[230] Mustacich, D., & Powis, G. (2000). Thioredoxin reductse. *Biochemical Journal, 346*(1), 1-8.

[231] Muthaiyan, A., Silverman, J. A., Jayaswal, R. K., & Wilkinson, B. J. (2008). Transcriptional profiling revelas that daptomycin induces the *Staphylococcus aureus* cell wall stress stimulon and gene responsive to membrane depolarization. *Antimicrobial Agents and Chemotherapy, 52*(3), 980-990.

[232] NCBI Resource Coordinators. (2018). Database resources of the National Center for Biotechnology Information. *Nucleic Acids Research, 46*, D8-D13.

[233] Neuhaus, F. C., & Baddiley, J. (2003). A continuum of anionic charge: Structures and functions of D-alanyl-teichoic acids in gram-positive bacteria. *Microbiology and Molecular Biology Reviews, 67*(4), 686-723.

[234] Nishibori, A., Kusaka, J., Hara, H., Umeda, M., & Matsumoto, K. (2005). Phosphatidylethanolamine domains and localization of the phospholipid synthases in *Bacillus subtilis* membranes. *Journal of Bacteriology, 187*(6), 2163-2174.

[235] Norris, G. E., & Patchett, M. L. (2016). The glycocins: in a class of their own. *Current Opinion in Structural Biology, 40*, 112-119.

[236] Nygaard, P., & Saxild, H. H. (2009). Nucleotide metabolism. In M. Schaechter, *Encyclopedia of Microbiology* (pp. 296-307). Academic Press.

[237] Okamoto, S., & Ohmori, M. (2002). The cyanobacterial PilT proteins responsible for cell motility and transformation hydrolyzes ATP. *Plant and Cell Physiology, 43*(10), 1127-1136.

[238] Oman, T. J., Boettcher, J. M., Wang, H., Okalibe, X. N., & van der Donk, W. A. (2011). Sublancin is not a lantibiotic but an *S*-linked glycopeptide. *Nature Chemical Biology, 7*(2), 78-80.

[239] Otto, A., Bernhardt, J., Hecker, M., & Becher, D. (2012). Global relative and absoute quantitation in microbial proteomics. *Current Opinion in Microbiology, 15*, 364-372.

[240] Paik, S. H., Chakicherla, A., & Hansen, J. N. (1998). Identification and characterization of the structural and transporter genes for, and the chemical and biological properties of, sublancin 168, a novel lantibiotic produced by *Bacillus subtilis* 168. *Journal of Biological Chemistry, 273*(36), 23134-23142.

[241] Papadimitriou, K., Alegria, A., Bron, P. A., de Angelis, M., Gobbetti, M., Kleerebezem, M., . . . Kok, J. (2016). Stress physiology of lactic acid bacteria. *Microbiology and Molecular Biology Reviews, 80*(3), 837-890.

[242] Patel, V. j., Thalassinos, K., Slade, S. E., Connolly, J. B., Crombie, A., Murrell, J. C., & Scrivens, J. H. (2009). A comparison of labelling and label-free mass spectrometry-based proteomics approaches. *Journal of Proteome Reseach, 8*, 3752-3759.

[243] Percy, M. G., & Gründling, A. (2014). Lipoteichoic acid synthesis and function in gram-positive bacteria. *Annual Review of Microbiology, 68*, 81-100.

[244] Perez, R. H., Perez, M. T., & Elegado, F. B. (2015). Bacteriocins from lactic acid bacteria: A review of biosynthesis, mode of action, fermentative production, uses, and prospects. *International Journal of Philippine Science and Technology, 8*(2), 61-67.

[245] Piuri, M., Sanchez-Rivas, C., & Ruzal, S. M. (2004). Cell wall modifications during osmotic stress in *Lactobacillus casei*. *Journal of Applied Microbiology, 98*(1), 84-95.

[246] Ponnudurai, R., Kleiner, M., Sayavedra, L., Petersen, J. M., Moche, M., Otto, A., . . . Markert, S. (2017). Metabolic and physiological interdependencies in the *Bathymodiolus azoricus* symbiosis. *The ISME Journal, 11*, 463-477.

[247] Price, C. W., & Doi, R. H. (1985). Genetic mapping of *rpoD* implicates the major sigma factor of *Bacillus subtilis* RNA polymerase in sporulation initiation. *Molecular and General Genetics MGG, 201*, 88-95.

[248] Price, C. W., Fawcett, P., Cérémonie, H., Su, N., Murphy, C. K., & Youngman, P. (2001). Genome-wide analysis of the general stress response in *Bacillus subtilis*. *Molecular Microbiology, 41*(4), 757-774.

[249] Price, K. D., Roels, S., & Losick, R. (1997). A *Bacillus subtilis* gene encoding a protein similar to nucleotide sugar transferases influences cell shape and viability. *Journal of Bacteriology, 179*(15), 4959-4961.

[250] Proft, T., & Baker, E. N. (2009). Pili in grram-negative and gram-positive bacteria - structure, assembly and their role in disease. *Cellular and Moleuclar Life Sciences, 66*, 613-635.

[251] Pure Science Ltd. (2021, July 11). *Pure Science*. Retrieved from Pure Science: https://purescience.co.nz

[252] Rajagopal, M., & Walker, S. (2015). Envelope structures of gram-positive bacteria. In F. Bagnoli, & R. R., *Protein and Sugar Export and Assembly in Gram-positive Bacteria. Current Topics in Microbiology and Immunology* (Vol. 404, pp. 1-44). Cham: Springer.

[253] Ramos, J. L., Martinez-Bueno, M., Molina-Henares, A. J., Terán, W., Watanabe, K., Zhang, X., . . . Tobes, R. (2005). The TetR family of transcriptional repressors. *Microbiology and Molecular Biology Reviews, 69*(2), 326-356.

[254] Real, G., & Henriques, A. O. (2006). Localization of the *Bacillus subtilis murB* gene within the *dcw* cluster is important for growth and sporulation. *Journal of Bacteriology, 188*(5), 1721-1732.

[255] Ren, H., Biswas, S., Ho, S., van der Donk, W. A., & Zhao, H. (2018). Rapid discovery of glycocins through pathway refractoring in *Escherichia coli*. *ACS Chemical Biology, 13*, 2966-2972.

[256] Respicio, L., Nair, P. A., Huang, Q., Anil, B., Tracz, S., Truglio, J. J., . . . Slayden, R. A. (2008). Characterizing septum inhibition in *Mycobacterium tuberculosis* for novel drug discovery. *Tuberculosis, 88*(5), 420-429.

[257] Reyes, J., Panesso, D., Tran, T. T., Mishra, N. N., Cruz, M. R., Munita, J. M., . . . Arias, C. A. (2015). A *liaR* deletion restores susceptibility to daptomycin and antimicrobial peptides in multidrug-resistant *Enterococcus faecalis*. *The Journal of Infectious Diseases, 211*(8), 1317-1325.

[258] Riley, M. A., & Wertz, J. E. (2002). Bacteriocins: Evolution, ecology and application. *Annual Review of Microbiology, 56*, 117-137.

[259] Rismondo, J., Halbedel, S., & Gründling, A. (2019). Cell shape and antibiotic resistance are maintained by the activity of multiple FtsW and RodA enzymes in *Listeria monocytogenes*. *mBio, 10*(4), 1-17.

[260] Ritz, D., & Beckwith, J. (2001). Roles of thiol-redox pathways in bacteria. *Annual Review of Microbiology, 55*(1), 21-28.

[261] Roche. (2021, July 11). *Roche Diagnostics*. Retrieved from Roche Diagnostics: https://diagnostics.roche.com/global/en/about/about-roche-diagnostics.html

[262] Rogers, H. J., Perkins, H. R., & Ward, J. B. (1980). Biosynthesis of peptidoglycan. In H. J. Rogers, H. R. Perkins, & J. B. Ward, *Microbial Cell Walls and Membranes* (pp. 239-297). Dordrecht: Springer.

[263] Ross, A. C., & Vederas, J. C. (2011). Fundamental functionality: Recent developments in understanding the structure-activity relationships of lantibiotic peptides. *The Journal of Antibiotics, 64*, 27-34.

[264] Ruffert, S., Berrier, C., Krämer, R., & Ghazi, A. (1999). Identification of mechanosensitive ion channels in the cytoplasmic membrane of *Corynebacterium glutamicum*. *Journal of Bacteriology, 181*(5), 1673-1676.

[265] Samuelson, J. C., Chen, M., Jiang, F., Möller, I., Wiedmann, M., Kuhn, A., . . . Dalbey, R. E. (2000). YidC mediates membrane protein insertion in bacteria. *Nature, 406*, 637-641.

[266] Sandberg, A., Branca, R. M., Lehtiö, J., & Forshed, J. (2014). Quantitative accuracy in mass spectrometry based proteomics of complex samples: The impact of labeling and precursor interference. *Journal of Proteomics, 96*, 133-144.

[267] Sangubotla, R., & Kim, J. (2021). Advances in mass spectrometry for microbial proteome analysis. In B. Viswanath, *Recent developments in applied microbiology and biochemistry* (pp. 299-308). Academic Press.

[268] Santajit, S., & Indrawattana, N. (2016). Mechanism of antimicrobial resistance in ESKAPE pathogens. *BioMed Research International, 2016*, 1-8.

[269] Santos, J. A., & Lamers, M. H. (2020). Novel antibiotics targeting bacterial replicatve DNA polymerases. *Antibiotics, 9*(776), 1-14.

[270] Sassine, J., Sousa, J., Lalk, M., Daniel, R. A., & Vollmer, W. (2020). Cell morphology maintenance in *Bacillus subtilis* through balanced peptidoglycan synthesis and hydrolysis. *Scientific Reports, 10*, 1-14.

[271] Sauvage, E., Kerff, F., Terrak, M., Ayala, J. A., & Charlier, P. (2008). The penicillin-binding proteins: Structure and role in peptidoglycan biosynthesis. *FEMS Microbiology Reviews, 32*(2), 234-258.

[272] Schaefer, K., Matano, L. M., Qiao, Y., Kahne, D., & Walker, S. (2017). In vitro reconstitution demonstrates the cell wall ligase activity of LCP proteins. *Nature Chemical Biology, 13*, 396-401.

[273] Schirle, M., Bantscheff, M., & Kuster, B. (2012). Mass spectrometry-based proteomics in preclinical drug discovery. *Chemistry & Biology, 19*(1), 72-84.

[274] Schneider, E., & Hunke, S. (1998). ATP-binding-cassette (ABC) transport systems: Functional and structural aspects of the ATP-hydrolyzing subunits/domains. *FEMS Microbiology Reviews, 22*(1), 1-20.

[275] Schrumpf, B., Schwarzer, A., Kalinowski, J., Pühler, A., Eggeling, L., & Sahm, H. (1991). A functionally split pathway for lysine synthesis in *Corynebacterium glutamicum*. *Journal of Bacteriology, 173*, 4510-4516.

[276] Scopes, R. K. (1974). Measurement of protein by spectrophotometry at 205 nm. *Analytical Biochemistry, 59*(1), 277-282.

[277] Seki, T., Furumi, T., Hashimoto, M., Hara, H., & Matsuoka, S. (2019). Activation of extracytoplasmic function sigma factors upon removal of glucolipids and reduction of phosphatidylglycerol content in *Bacillus subtilis* cells lacking lipoteichoic acid. *Genes & Genetic Systems, 94*(2), 71-80.

[278] Seki, T., Mineshima, R., Hashimoto, M., Matsumoto, K., Hara, H., & Matsuoka, S. (2015). Repression of the activities of two extracytoplasmic function σ factors, σ^M and σ^V, of *Bacillus subtilis* by glucolipids in *Escherichia coli* cells. *Genes & Genetic Systems, 90*(2), 109-114.

[279] Sengupta, R., Altermann, E., Anderson, R. C., McNabb, W. C., Moughan, P. J., & Roy, N. C. (2013). The role of cell surface architechture of lactobacilli in host-microbe interactions in the gastrointestinal tract. *Mediators of Inflammation, 2013*, 1-16.

[280] Serrano, L. M., Molenaar, D., Wels, M., Teusink, B., Bron, P. A., de Vos, W. M., & Smid, E. J. (2007). Thioredoxin reductase is a key factor in the oxidative stress response of *Lactobacillus plantarum* WCFS1. *Microbial Cell Factories, 6*, 1-14.

[281] Shakil, S., Khan, R., Zarrilli, R., & Khan, A. U. (2008). Aminoglycosides versus bacteria – a description of the action, resistance mechanism, and nosocomial battleground. *Journal of Biomedical Science, 15*, 5-14.

[282] Shen, X.-L., Dong, H.-J., Hou, X.-P., Guan, W.-J., & Li, Y.-Q. (2008). FtsY affects sporulation and antibiotic production by WhiH in *Streptomyces coelicolor*. *Current Microbiology, 56*, 61-65.

[283] Shimizu, K. (2013). Main metabolism. In K. Shimizu, *Bacterial Cellular Metabolic Systems: Metabolic Regulation of a Cell System with 13c-Metabolic Flux Analysis* (pp. 1-54). Woodhead Publishing.

[284] Sievers, S. (2018). Membrane proteomics in gram-positive bacteria: Two complementary approaches to target the hydrophobic species of proteins. *Methods in Molecular Biology, 1841*, 21-33.

[285] Singh, J. K., Makde, R. D., Kumar, V., & Panda, D. (2007). A membrane protein, EzrA, regulates assembly dynamics of FtsZ by interacting with the C-terminal tail of FtsZ. *Biochemistry, 46*(38), 11013-11022.

[286] Singh, V., & Rao, A. (2021). Distribution and diversity of glycocin biosynthesis gene clusters beyond Firmicutes. *Glycobiology, 31*(2), 89-102.

[287] Solioz, M., Abicht, H. K., Mermod, M., & Mancini, S. (2010). Response of gram-positive bacteria to copper stress. *Journal of Biological Inorganic Chemistry, 15*, 3-14.

[288] Solis, N., & Cordwell, S. J. (2011). Current methodologies for proteomics of bacterial surface-exposed and cell envelope proteins. *Proteomics, 11*(15), 3169-3189.

[289] Soloviev, M. (2010). Peptidomics: Divide et impera. In M. Soloviev, *Peptidomics. Methods in Molecular Biology (Methods and Protocols)* (Vol. 615). Humana Press.

[290] Song, H., Lou, N., Liu, J., Xiang, H., & Shang, D. (2021). Label-free quantitative proteomic analysis of the inhibition effect of *Lactobacillus rhamnosus* GG on *Escherichia coli* biofilm formation in co-culture. *Proteome Science, 19*(4), 1-14.

[291] Stepper, J., Shastri, S., Loo, T. S., Preston, J. C., Novak, P., Man, P., . . . Norris, G. E. (2011). Cysteine *S*-glycosylation, a new post-translational modification found in glycopeptide bacteriocins. *FEBS Letters, 585*(4), 645-650.

[292] Stevens, M. J., Molenaar, D., de Jong, A., De Vos, W. M., & Kleerebezem, M. (2010). Sigma 54-mediated control of the mannose phosphotransferase system in *Lactobacillus plantarum* impacts on carbohydrate metabolism. *Microbiology, 156*, 695-707.

[293] Stingele, F., & Mollet, B. (1996). Disruption of the gene encoding penicillin-binding protein 2b (pbp2b) causes altered cell morphology and cease in exopolysaccharide production in *Streptococcus thermophilus* Sfi6. *Moleuclar Microbiology, 22*(2), 357-366.

[294] Stock, A. M., Robinson, V. L., & Goudreau, P. N. (2000). Two-component signal transduction. *Annual Review of Biochemistry, 69*, 183-215.

[295] Su, H.-N., Li, K., Zhao, L.-S., Yuan, X.-X., Zhang, M.-Y., Liu, S. M., . . . Zhang, Y.-Z. (2020). Structural visualization of septum formation in *Staphylococcus warneri* using atomic force microscopy. *Journal of Bacteriology, 202*(19), e00294-20.

[296] Swoboda, J. G., Campbell, J., Meredith, T. C., & Walker, S. (2010). Wall teichoic acid function, biosynthesis, and inhibition. *Chembiochem: A European Journal of Chemical Biology, 11*(1), 35-45.

[297] Swoboda, J. G., Meredith, T. C., Campbell, J., Brown, S., Suzuki, T., Bollenbach, T., . . . Walker, S. (2009). Discovery of a small molecule that blocks wall teichoic acid biosynthesis in *Staphylococcus aureus*. *ACS Chemical Biology, 4*(10), 875-883.

[298] Szklarczyk, D., Gable, A. L., Nastou, K. C., Lyon, D., Kirsch, R., Pyysalo, S., . . . von Mering, C. (2021). The STRING database in 2021: Customizable protein-protein networks, and functional characterization of user-uploaded gene/measurement sets. *Nucleic Acids Research, 49*(D1), D605-D612.

[299] Szurmant, H., Mohan, M. A., Imus, P. M., & Hoch, J. A. (2007). YycH and YycI interact to regulate the essential YycFG two-component system in *Bacillus subtilis*. *Journal of Bacteriology, 189*(8), 3280-3289.

[300] Taguchi, A., Welsh, M. A., Marmont, L. S., Lee, W., Sjodt, M., Kruse, A. C., . . . Walker, S. (2019). FtsW is a peptidoglycan polymerase that is functional only in complex with it cognate penicillin-binding protein. *Nature Microbiology, 4*, 587-594.

[301] Thakur, P., Gantasala, N. P., Choudhary, E., Singh, N., Abdin, M. Z., & Agarwal, N. (2016). The preprotein translocase YidC controls respiratory metabolism in *Mycobacterium tuberculosis*. *Scientific Reports, 6*, 1-14.

[302] The Gene Ontology Consortium. (2021). The Gene Ontology resource: Enriching a GOld mine. *Nucleic Acids Research, 49*, D325-D334.

[303] Thein, M., Sauer, G., Paramasivam, N., Grin, I., & Linke, D. (2010). Efficient subfractionation of gram-negative bacteria for proteomics studies. *Journal of Proteome Research, 9*(12), 6135-6147.

[304] Thermo Fisher Scientific. (2012, May 21). *Q Exactive Orbitrap Mass Spectrometers (MS)*. Retrieved from Thermo Fisher Scientific: https://www.thermofisher.com/nz/en/home/industrial/mass-spectrometry/liquid-chromatography-mass-spectrometry-lc-ms/lc-ms-systems/orbitrap-lc-ms/q-exactive-orbitrap-mass-spectrometers.html

[305] Thermo Fisher Scientific. (2019). *Pierce™ BCA Protein Assay Kit - Reducing Agent Compatible*. Retrieved from Thermo Fisher Scientific: https://www.thermofisher.com/order/catalog/product/23250

[306] Thermo Fisher Scientific. (2021, July 11). *Affymetrix*. Retrieved from Affymetrix: http://www.affymetrix.com/products/index.affx

[307] Thermo Fisher Scientific. (2021, July 11). *Fisher Bioreagents*. Retrieved from Fisher Scientific: https://www.fishersci.com/us/en/brands/IAOCLVV5/fisher-bioreagents.html

[308] Thermo Fisher Scientific. (2021, July 4). *Fisher Chemical*. Retrieved from Fisher Scientific: https://www.fishersci.com/us/en/brands/I8T3NQD9/fisher-chemical.html

[309] ThermoFisher Scientific. (2019, May). *Proteome Discoverer Software* . Retrieved from ThermoFisher Scientific: https://www.thermofisher.com/order/catalog/product/OPTON-30795

[310] Thibessard, A., Fernandez, A., Gintz, B., Leblond-Bourget, N., & Decaris, B. (2002). Effects of *rodA* and *pbp2b* disruption on cell morphology and oxidative stress response of *Streptococcus thermophilus* CNRZ368. *Journal of Bacteriology, 184*(10), 2821-2826.

[311] Throup, J. P., Koretke, K. K., Bryant, A. P., Ingraham, K. A., Chalker, A. F., Ge, Y., . . . Burnham, M. K. (2002). A genomic analysis of two-component signal transduction in *Streptococcus pneumoniae*. *Molecular Microbiology, 35*(3), 566-576.

[312] Tian, F. (2019). Stage division and development course and applications of the science and technology of lactic acid bacteria. In W. Chen, *Lactic Acid Bacteria: Omics and functional evaluation* (p. 4). Wuxi: Springer Nature Singapore Pte Ltd.

[313] Todorov, S. D., de Melo Franco, B. D., & Tagg, J. R. (2019). Bacteriocins of gram-positive bacteria having activity spectra extending beyond closely-related species. *Beneficial Microbes, 10*(3), 315-328.

[314] Treede, I., Jakobsen, L., Kirpekar, F., Vester, B., Weitnauer, G., Bechthold, A., & Douthwaite, S. (2003). The avilamycin resistance determinants AviRa andAviRb methylate 23S rRNA at the guanosine 2535 base and the uridine 2479 ribose. *Molecular Biology, 49*(2), 309-318.

[315] Tsirigos, K. D., Peters, C., Shu, N., Käll, L., & Elofsson, A. (2015). The TOPCONS web server for consensus prediction of membrane protein topology and signal peptides. *Nucleic Acids Research, 43*(W1), W401-W407.

[316] Typas, A., Banzhaf, M., Gross, C. A., & Vollmer, W. (2012). From the regulation of peptidoglycan synthesis to bacterial growth and morphology. *Nature Reviews Microbiology, 10*, 123-136.

[317] Uehara, A., Fujimoto, Y., Kawasaki, A., Kusumoto, S., Fukase, K., & Takada, H. (2006). *Meso*-diaminopimelic acid and *meso*-lanthionine, amino acids specific to bacterial peptidoglycans, activate human epithelial cells through NOD1. *The Journal of Immunology, 177*(3), 1796-1804.

[318] Umu, Ö. C., Bäuerl, C., Oostindjer, M., Pope, P. B., Hernández, P. E., Pérez-Martínez, G., & Diep, D. B. (2016). The potential of class II bacteriocins to modify gut microbiota to improve host health. *PLoS One, 11*(10).

[319] Univar Solutions. (2021, July 10). *Univar Solutions*. Retrieved from Univar Solutions: https://www.univarsolutions.com/product-categories

[320] Usachev, K. S., Yusupov, M. M., & Validov, S. Z. (2020). Hibernation as a stage of ribosome functioning. *Biochemistry Moscow, 85*, 1434-1442.

[321] van den Ent, F., Leaver, F., Bendezu, F., Errington, J., de Boer, P., & Löwe, J. (2006). Dimeric structure of the cell shape protein MreC and its functional implications. *Molecular Microbiology, 62*(6), 1631-1642.

[322] van Eijk, E., Wittekoek, B., Kuijper, E. J., & Smits, W. K. (2017). DNA replication proteins as potential targets for antimicrobials in drug-resistant bacterial pathogens. *Journal of Antimicrobial Chemotherapy, 72*(5), 1-10.

[323] Venugopal, H., Edwards, P. J., Schwalbe, M., Claridge, J. K., Libich, D. S., Stepper, J., . . . Pascal, S. M. (2011). Structural, dyanmic, and chemical characterization of a novel *S*-glycosylated bacteriocin. *Biochemistry, 50*, 2748-2755.

[324] Vershinina, O. A., & Znamenskaya, L. V. (2002). The pho regulons of bacteria. *Microbiology, 71*(5), 497-511.

[325] von Ballmoos, C., Wiedenmann, A., & Dimroth, P. (2009). Essentials for ATP synthesis by F_1F_0 ATP synthases. *Annual Review of Biochemistry, 78*, 649-672.

[326] Voyksner, R. D., & Lee, H. (1999). Investigating the use of an octupole ion guide for ion storage and high-pass mass filtering to improve the quantitative performance of electrospray ion trap mass spectrometry. *Rapid Communications in Mass Spectrometry, 13*(14), 1427-1437.

[327] VWR International. (2021, July 11). *Avantor delivered by VWR*. Retrieved from Avantor VWR: https://si.vwr.com/store/supplier/id/BALI/BDH+Prolabo

[328] Wang, H., Oman, T. J., Zhang, R., Garcia De Gonzalo, C. V., Zhang, Q., & van der Donk, W. A. (2014). The glycosyltranferases involved in thurandacin biosynthesis catalyzes both *O*- and *S*-glycosylation. *Journal of The American Chemical Society, 136*(1), 84-87.

[329] Wang, S. (2012). Bacterial two-component systems: Structures and signaling mechanisms. In C. Huang, *Protein Phosphorylation in Human Health* (pp. 439-466). Rijeka: InTech.

[330] Warner, D. F., Evans, J. C., & Mizrahi, V. (2014). Nucleotide metabolism and DNA replication. *Microbiology Spectrum, 2*(5).

[331] Weart, R. B., Lee, A. H., Chien, A. C., Haeusser, D. P., Hill, N. S., & Levin, P. A. (2007). A metabolic sensor governing cell size in bacteria. *Cell, 130*(2), 335-347.

[332] Weider, W., & Pelzer, H. (1964). Bagshaped macromolecules - A new outlook on bacterial cell walls. In F. F. Nord, *Advances in Enzymology and Related Areas of Molecular Biology* (pp. 193-232). USA: John Wiley & Sons, Inc.

[333] Weston, L. A., Bauer, K. M., & Hummon, A. B. (2013). Comparison of bottom-up proteomic approaches for LC-MS analysis of complex proteomes. *Analytical Methods, 5*, 4615-4621.

[334] Whitehead, H. R. (1933). A substance inhibiting bacterial growth, produced by certain strains of lactic streptococci. *Biochem J, 27*(6), 1793-1800.

[335] Wiedemann, I., Bottiger, T., Bonelli, R. R., Wiese, A., Hagge, S. O., Gutsmann, T., . . . Sahl, H.-G. (2006). The mode of action of the lantibiotic lacticin 3147 – a complex mechanism involving specific interaction of two peptides and the cell wall precursor lipid II. *Molecular Microbiology, 61*(2), 285-296.

[336] Wiedemann, I., Breukink, E., van Kraaij, C., Kuipers, O. P., Bierbaum, G., de Kruijff, B., & Sahl, H.-G. (2001). Specific bidning of nisin to the peptidoglycan precursor lipid II combines pore formation and inhibition of cell wall biosynthesis for potent antibiotic activity. *Journal of Biological Chemistry, 276*(3), 1772-1779.

[337] Wilson, D. N. (2009). The A-Z of bacterial translation inhibitors. *Critical Reviews in Biochemistry and Molecular Biology, 44*(6), 393-433.

[338] Winkler, M. E., & Hoch, J. A. (2008). Essentiality, bypass, and targeting of the YycFG (VicRK) two-component regulatory system in gram-positive bacteria. *Journal of Bacteriology, 190*(8), 2645-2648.

[339] Winther, A. R., Kjos, M., Stamsås, G. A., Håvarstein, L. S., & Straume, D. (2019). Prevention of EloR/KhpA heterodimerization by introduction of site-specific amino acid substitutions renders the essential elongasome protein PBP2b redundant in *Streptococcus pneumoniae*. *Scientific Reports, 9*(3681), 1-13.

[340] Wolff, S., Hahne, H., Hecker, M., & Becher, D. (2008). Complementary analysis of the vegetative membrane proteome of the human pathogen *Staphylococcus aureus*. *Mol & Cell Proteomics, 7*(8), 1460-1468.

[341] Wolff, S., Otto, A., Albrecht, D., Zeng, J. S., Büttner, K., Glückmann, M., . . . Becher, D. (2006). Gel-free and gel-based proteomics in *Bacillus subtilis*. *Molecular & Cellular Proteomics, 5*(7), 1183-1192.

[342] Wolfgang, M., Lauer, P., Park, H. S., Brossay, L., Hebert, J., & Koomey, M. (1998). PilT mutations lead to simultaneous defects in competence for natural transformation and twitching motility in piliated *Neisseria gonorrhoeae*. *Moleuclar Microbiology, 29*(1), 321-330.

[343] Wood, J. M. (2015). Bacterial responses to osmotic challenges. *Journal of General Physiology, 145*(5), 381-388.

[344] Wright, G. D. (2007). The antibiotic resistome: The nexus of chemical and genetic diversity. *Nature Reviews Microbiology, 5*, 175-186.

[345] Wu, C., Biswas, S., Garcia De Gonzalo, C. V., & van der Donk, W. A. (2019). Investigations into the mechanism of action of sublancin. *ACS Infectious Diseases, 5*, 454-459.

[346] Xaplanteri, M. A., Andreou, A., Dinos, G. P., & Kalpaxis, D. L. (2003). Effect of polyamines on the inhibition of peptidyltransferase by antibiotics: Revisiting the mechanism of chloramphenicol action. *Nucleic Acids Research, 31*(17), 5074-5083.

[347] Xiao, H., Sun, F., Suttapitugsakul, S., & Wu, R. (2019). Global and site-specific analysis of protein glycosylation in complex biological systems with mass spectrometry. *Mass Spec Rev, 38*(4-5), 356-379.

[348] Yasir, M., Dutta, D., & Willcox, M. D. (2019). Mode of action of the antimicrobial peptide Mel4 is independent of *Staphylococcus aureus* cell membrane permeability. *PLoS ONE, 14*(7), 1-22.

[349] Yosef, I., Bochkareva, E. S., Adler, J., & Bibi, E. (2010). Membrane protein biogenesis in Ffh- or FtsY-depleted *Escherichia coli*. *PLoS ONE, 5*(2), 1-7.

[350] Yoshida, H., Wada, A., Shimada, T., Maki, Y., & Ishihama, A. (2019). Coordinated regulation of Rsd and RMF for simultaneous hibernation of transcription apparatus and translation machinery in stationary-phase *Escherichia coli*. *Frontiers in Genetics, 10*, 1-15.

[351] Yoshikawa, M., Ito, A., Ishikawa, T., & Ikegami, Y. (2004). Drug resistance mediated by ABC transporters. *Gan To Kagaku Ryoho (Japanese Journal of Cancer and Chemotherapy), 31*(1), 1-6.

[352] Zeller, T., & Klug, G. (2006). Thioredoxins in bacteria: Functions in oxidative stress response and regulation of thioredoxin genes. *Naturwissenschaften, 93*, 259-266.

[353] Zhang, Y., Fonslow, B. R., Shan, B., Baek, M.-C., & Yates, J. R. (2013). Protein analysis by shotgun/bottom-up proteomics. *Chemical Reviews, 113*, 2343-2394.

[354] Zhu, W., Smith, J. W., & Huang, C.-M. (2010). Mass spectrometry-based label-free quantitative proteomics. *Journal of Biomedicine and Biotechnology, 2010*, 1-6.

7 Appendices

7.1 Protein concentrations

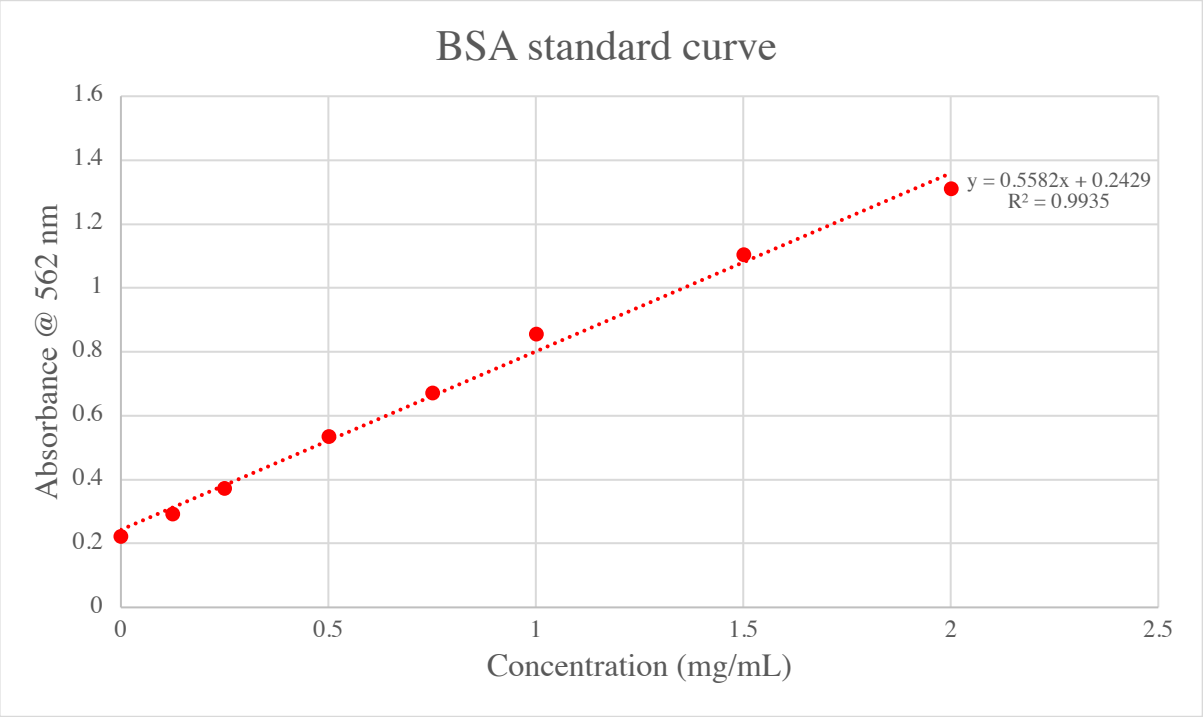

Figure 22: Standard curve used to determine protein concentrations of membrane and cytosolic fractions from *Lb. plantarum* ATCC 8014 cells. Seven BSA standards ranging from 0.125 mg/mL to 2 mg/mL were used to construct a protein standard curve. Membrane and cytosolic fraction from GccF-treated *Lb. plantarum* ATCC 8014 cells were prepared according to the manufacturer's instructions using a BCA protein assay kit and the absorbance was measured at 562 nm ($A_{562\ nm}$). The $A_{562\ nm}$ results were used to determine the protein concentrations of the membrane and cytosolic fractions (Appendix 7.2). The standard curve is representative of duplicate samples. Data points (*N*) = 8.

7.2 General stress proteins

Table 14: Proteins involved in the general stress response in gram-positive bacteria

Protein/protein family	Organism	Reference
Proteins that respond to non-specific/general stress		
Chaperone proteins, *e.g.* DnaJK, GroEL, ClpP, HtrA, GrpE	Various G+ve species	[248][241]
Gls24 and GlsB	*E. faecalis*	[241]
Universal stress proteins (Usp)	Various G+ve species	[138][241]
SigB (sigma factor B; σ^B)	Various low-GC G+ve species	[248]
One- and two-component systems (OCSs and TCSs)	Various G+ve species	[241]
Proteins that respond to metal stress		
Cop proteins (*e.g.* CopY, CopZ, CopA, CopB)	*E. hirae*	[287]
ZitR repressor	*S. pneumoniae*	[241]
SczA	*S. pneumoniae*	[241]
CsoR	*Mycobacterium tuberculosis*	[287]
ScaR regulator	Streptococci	[241]
YaiA, YtjD, LctO	*Lc. lactis*	[287]
CutC		[241]
Proteins that respond to heat stress		
CtsR regulator and CtsR repressor	*Lc. lactis*	[248][241]
Chaperone proteins (*e.g.* DnaK, GroEL/GroES, Clp proteins, DegP, sHSPs (FtsH, Lo18))	Various G+ve species	[241]
HrcA repressor	Various G+ve species	[241]

Proteins that response to oxidative stress		
YvyD	*B. subtilis*	[248]
PerR regulator	Various G+ve species	[241]
Clp proteins (*e.g.* ClpP and ClpC ATPase)	*B. subtilis*	[248]
Polyphosphate enzymes: Ppk, Ppx, GppA	Lactobacilli	[241]
NADH per-/oxidases, *e.g.* AhpCF, Npr, Tpx, Nox	Various G+ve species	[241]
Superoxide dismutase (SOD)	Various G+ve species	[241]
Glutathione (Gsh) and thioredoxin (Trx) proteins	Various G+ve species	[248][138][241]
PoxB	*Lb. plantarum*	[241]
Spx regulators: SpxA1 and SpxA2	Streptococci	[241]
Methionine sulfoxide reductase (MsrA2)	*Lb. plantarum*	[138]
MsrA and MsrB	*E. faecalis*	[241]
KatB and KatX (stationary phase catalases)	*B. subtilis*	[248]
HypR	*E. faecalis*	[241]
DNA-binding protein, Dpr/MrgA	*S. pneumoniae*, *B. subtilis*	[248][241]
Ers (enterococcal regulator of survival)	*E. faecalis*	[241]
AsrR (antibiotic and stress response regulator)	*E. faecium*	[241]
Proteins that respond to acid stress		
Glucose PEP-PTS	Various G+ve species	[241]
Clp proteins (*e.g.* ClpP, ClpE, ClpL, ClpX)	*Lb. delbrueckii*	[241]

Proteins that respond to acid stress		
Pyruvate oxidase (PO) and phosphate acetyltransferase	Lactobacilli	[241]
Asp1 and Asp2	*S. aureus, Lb. plantarum*	[138]
Proteins that respond to acid stress		
Phosphoglycerate kinase	*Lb. reuteri*	[189]
Pyruvate oxidase (POX) and P-acetyltransferase	*Lc. lactis*	[241]
Glutamate decarboxylase (GAD) pathways proteins: GAD, PLP-dependent enzyme, glutamate/GABA antiporter, GadR activator	*L. monocytogenes*	[241][33]
Peptidases PepO and PepC	*Lc. lactis*	[241]
Arginine deiminase (ADI) pathway proteins: ADI, cOTC and CK	*S. gordonii, Streptococcus rattus*	[241]
Histidine decarboxylase (HDC)	Lactobacilli	[241]
Agmatine deiminase (AgDI) pathway proteins: AguABC and D	Various G+ve species	[241]
SodA, AhpC, and Tpx	*Lc. lactis*	[138]
Aspartic acid decarboxylase pathway proteins: AspD and the Asp/Ala antiporter	Lactobacilli	[241]
Urease system proteins (*e.g.* UreI, UreABC, UreEFGH)	*S. thermophilus, Streptococcus salivarius, Lb. reuteri, Lb. fermentum*	[241]
TrxH and MsrA2	*Lb. plantarum*	[138]
ChoQS ABC transporter complex	*Lc. lactis*	[241]

Proteins that respond to alkaline stress		
ClpB chaperone	*Lb. plantarum*	[189]
AAA+ ATPases	*Lb. plantarum*	[189]
Ribonuclease HII	*Lb. plantarum*	[189]
Prolyl- and Tyrosyl-tRNA synthetases	*Lb. plantarum*	[189]
Glycolytic pathway proteins (*i.e.* enolase, phosphoglycerate kinase)	*Lb. plantarum*	[189]
CTP synthase	*Lb. plantarum*	[189]
Proteins that respond to nutrient metabolism stressors		
Sugar-PTS transporters	Various G+ve species	[241]
NAD(P)-dependent dehydrogenases (*e.g.* AldY, YdaD, GabD)	*B. subtilis*	[33]
DNA-binding protein, Dps	*B. subtilis*	[248]
BcaT and AraT	*Lc. lactis*	[241]
Proteins that respond to osmotic stress		
Serine/threonine kinase (Stk)	*S. pyogenes*	[241]
YfkE and YflA	*B. subtilis*	[248]
OpuA/BusA ABC transporter	*Lc. lactis, B. subtilis*	[248][241]
ChoS (of the ChoQS ABC transporter complex)	*Lc. lactis*	[241]
GroEL/GroES	*Lb. rhamnosus*	[241]
TetR family transcriptional regulators	Various G+ve species	[253]
YdbE and YdfC	*B. subtilis*	[248]
MurG and MurF	*Lc. lactis* subsp. *lactis*	[241]

Proteins that respond to various stressors		
StkP (Ser/Thr kinase)	Various G+ve species	[241]
cAMP receptors	Various G+ve species	[241]
CcpA	Various G+ve species	[241]
FNR regulators and FNR-like proteins	Various G+ve species	[241]
Rgg regulators	*S. pyogenes*	[241]
Glutamate decarboxylase (GAD) pathways proteins: GAD, PLP-dependent enzyme, glutamate/GABA antiporter, GadR activator	*L. monocytogenes*	[241][33]
Proteins that respond to antimicrobials		
IreK/IreP kinase/phosphorylase	*E. faecalis*	[241]
PBP transpeptidases	Various G+ve species	[241]
Sigma factors σ^W, σ^M, σ^V, σ^Y	*B. subtilis*	[162]
BceAB ABC transporter and BceRS regulator	*B. subtilis*	[241]
YsaBC	*Lc. lactis*	[241]
BlaRI/MecRI systems	Firmicutes	[162]
TCS09 and TCS12 (BceRS systems)	*Lb. casei, B. subtilis*	[162][241]
BcrR	*E. faecalis*	[162][241]
LiaRS/VanRS TCS	Firmicutes, Enterococci	[162][241]
CesFSR	*Lc. lactis*	[162][241]
β-lactamases	Various G+ve species	[162]

Proteins involved in cold shock		
Cold shock proteins (CSP; *e.g.* CspL, CspP, CspC, CspB, CspA)	*Lb. plantarum*	[197]
Xaa-Pr aminopeptidases	*Lb. plantarum*	[197]
Clp proteins (*e.g.* ClpP, ClpE, ClpL, ClpX)	*Lc. lactis, S. thermophilus*	[241]
Carbamoyl phosphate synthases	*Lb. plantarum*	[197]
C69 peptidases	*Lb. plantarum*	[197]
DnaK and GroEL	*Leuconostoc mesenteroides*, various G+ve species	[241]
Diaminopimelate decarboxylase	*Lb. plantarum*	[197]
sHSPs	Various G+ve species	[241]
Proteins involved in genotoxic stress (*e.g.* DNA damage)		
Y- and C-family SOS-induced error-prone polymerases	*S. uberis*	[241]
UvrA	*S. mutans, Lb. helveticus*	[241]
MutS and MutL	*Lc. lactis*	[241]
Smx nuclease	*S. mutans*	[241]
Proteins that respond to cell envelope stress		
MbrABRS system	*S. mutans*	[241]
CseABC-σ^B	*Streptomyces coelicolor*	[162]
LiaFSR	*B. subtilis*	[241]
CiaRH	*Streptococcus pneumoniae*	[162]

7.3 Method for manual normalisation of proteomic data

1. **Protein abundances were manually normalised in Microsoft Excel** [220] **using the following steps**:
    a. Divide 'abundance' by 'abundance count' for each protein per replicate (*i.e.* 'abundance value/count value'). This will generate a unique 'abundance/count' value for each protein per replicate (*e.g.* one protein identified in three replicates = three different 'abundance/count' values).
    b. Sum the 'abundance/count' values per replicate (in Excel, use the equation '= SUM (values a through z)'). This will generate a single number per replicate (R'n').
    c. Calculate the maximum summed value using the equation '= MAX (summed abundance/count values of 'R1','R2'.'R3')'.
    d. Calculate the multiplication factors for each replicate by dividing the 'max summed value' of all replicates by each replicates' 'summed value'.
    e. Multiply the original protein abundance value by the appropriate replicate multiplication factor to calculate the 'normalised abundance' per replicate.

2. **Significance was determined using the student T-tests to generate P-values. P-values less than or equal to 0.05 were considered significant**
    a. Calculate the average normalised abundance across replicates by using the Excel equation '= AVERAGE ('normalised abundance' values of 'R1'+'R2'+'R3')'. This will generate a single representative abundance value for each protein.
    b. Calculate the $\log_{10}$ value for each replicate using the 'normalised abundance' values calculated in part 1e (Excel equation: '= $\log_{10}$ ('normalised abundance value')').
    c. Use the T-test function in Excel to calculate the p-value of each protein across replicates ('= TTEST ('array1';'array2';2;1'). 'Array 1' and 'array 2' represent the array of samples to be compared (*e.g.* array 1 = untreated/control samples, array 2 = treated samples). Here they represent the three $\log_{10}$ values calculated in part 2b. The T-test will generate a single p-value representative of all replicates for each protein
    d. Custom sort the p-values from smallest to largest to determine which proteins are significant (below 0.05) or not (above 0.05).

3. **Volcano plots were created manually in Excel to observe differences in the pattern of up and down-regulated proteins**

a. Calculate the fold change of samples want to compare dividing the 'averaged normalised abundance' of the treated sample by the 'averaged normalised abundance' of the control/untreated sample.
b. Convert the fold change to $\log_2$ fold change using the equation '= $\log_2$ ('fold change' value)'.
c. Calculate the $-\log_{10}$ value of p-values using the equation '= $-\log_{10}$ (p-value)'.
d. Plot the $\log_2$ fold change values along the x-axis, and the $-\log_{10}$ p-values along the y-axis using the 'scatter plot' chart type in Excel.

7.4 Distribution plots of membrane proteins

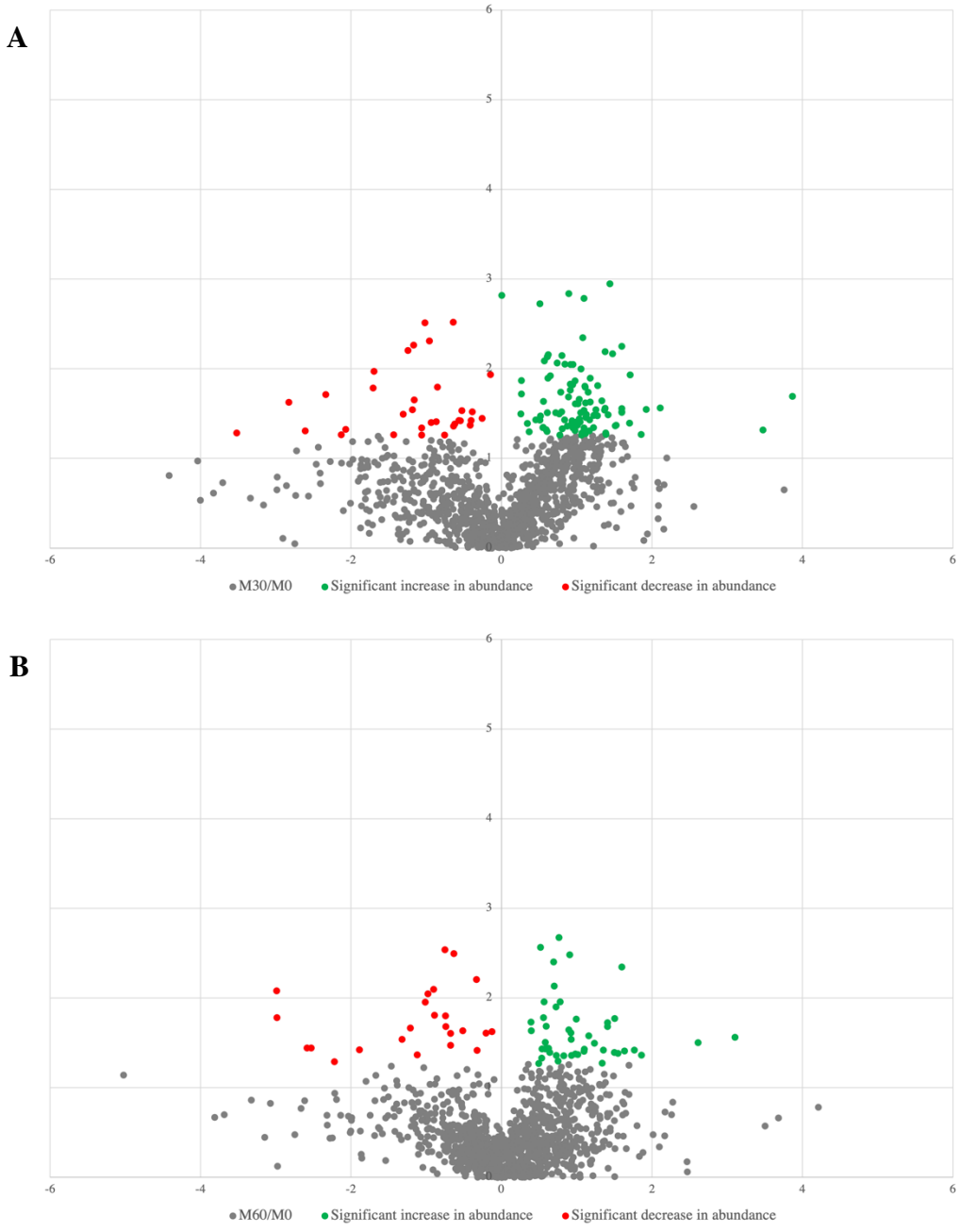

Figure 23: Distribution of proteins identified in the membrane fraction of *Lb. plantarum* ATCC 8014 cells following exposure to GccF. Volcano plot showing the changes in abundance of all proteins identified in the membrane fraction after 30 (**A**) and 60 minutes (**B**) of target cell exposure to GccF. Those with a significant increase in abundance are coloured green, and those with a significant decrease are coloured red. Proteins with a p-value ≤ 0.05 were considered significant, as determined by the manual normalisation method outlined in Appendix 7.3.

7.5 Distribution plots of cytosolic proteins

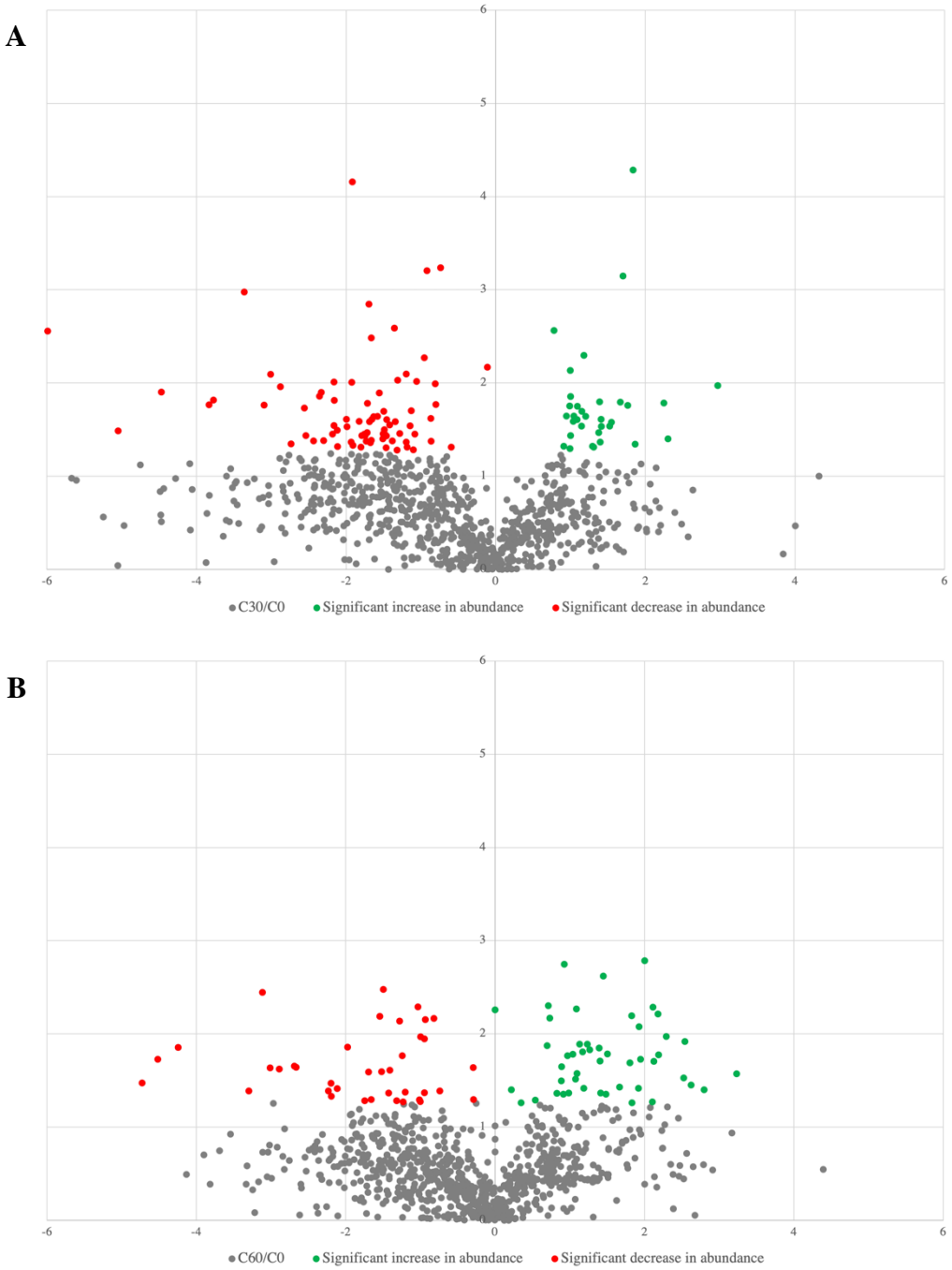

Figure 24: Distribution of proteins identified in the cytosolic fraction of *Lb. plantarum* ATCC 8014 cells following exposure to GccF. Volcano plot showing the changes in abundance of all proteins identified in the cytosolic fraction after 30 (**A**) and 60 minutes (**B**) of target cell exposure to GccF. Those with a significant increase in abundance are coloured green, and those with a significant decrease are coloured red. Proteins with a p-value ≤ 0.05 were considered significant, as determined by the manual normalisation method outlined in Appendix 7.3.

7.6 Selected proteins identified in the membrane fraction with the most statistically significant change in abundance

Table 15: Membrane proteins selected for in depth analysis and discussion

Accession #	Protein	Sequence coverage	PSMs	Unique peptides	MW (kDa)	Fold change*		
						T_{15}	T_{30}	T_{60}
Proteins with an increase in abundance								
ATQ34971.1+	universal stress protein	46	28	4	17.1	**18.903**	**14.567**	**8.573**
ATQ32803.1+	transcriptional regulator	45	28	5	16.3	**7.729**	**11.092**	18.485
ATQ34673.1+	ArsR family transcriptional regulator	41	15	3	12.6	**4.626**	**4.313**	4.468
ATQ32253.1+	Hsp20/alpha crystallin family protein	29	14	3	16	**4.444**	**2.179**	1.682
ATQ34661.1+	TetR/AcrR family transcriptional regulator	15	5	2	28.6	**3.398**	**3.021**	3.227
ATQ33039.1+	TetR/AcrR family transcriptional regulator	59	1545	10	21.6	**3.526**	1.918	1.605
ATQ32696.1+	UDP-glucose 4-epimerase GalE	20	23	4	36.1	2.026	**2.591**	**2.525**
ATQ32195.1+	6-pyruvoyl tetrahydropterin synthase	30	80	3	14	**2.242**	**2.517**	2.082
ATQ32284.1+	LacI family transcriptional regulator	10	7	2	37.9	**2.239**	**2.608**	3.478
ATQ33293.1+	HIT family protein	25	36	3	17	**2.972**	**3.251**	2.552
ATQ34700.1+	hypothetical protein CS400_13955	44	72	4	16.7	**2.346**	**3.782**	3.678
ATQ34678.1+	dihydropteroate synthase	36	127	11	43.4	**2.500**	**1.928**	1.790

ATQ34760.1+	MarR family transcriptional regulator	44	173	5	19.7	**2.553**	**1.965**	2.004
ATQ34155.1+	SAM-dependent methyltransferase	29	31	4	32.2	**2.396**	**0.444**	0.906
ATQ32219.1+	ArsR family transcriptional regulator	29	16	2	11.9	**2.850**	**2.873**	**3.022**
ATQ34718.1+	DUF488 domain-containing protein	35	30	4	14.4	**2.403**	**2.412**	**3.101**
ATQ34972.1+	PadR family transcriptional regulator	69	101	12	21.1	**2.248**	**2.848**	**3.396**
ATQ34761.1+	TetR/AcrR family transcriptional regulator	27	31	4	25.8	**2.734**	**3.617**	**3.628**
ATQ32252.1+	MarR family transcriptional regulator	32	61	3	17.6	**2.315**	**1.909**	1.687
ATQ34649.1	peptidase	16	37	3	25.2	**2.335**	**3.262**	2.694
ATQ33714.1	PhoH family protein	54	379	14	35.8	**2.085**	**1.710**	**1.973**
ATQ33505.1	DUF805 domain-containing protein	24	252	3	14.2	**2.143**	**1.788**	**1.712**
ATQ33098.1	acyltransferase	21	47	4	32.7	**2.063**	**2.250**	1.829
ATQ33376.1	OxaA precursor	11	118	3	34.2	2.063	**2.166**	**2.014**
ATQ32187.1	regulator	24	22	5	31.5	**2.035**	1.397	**1.314**
ATQ33291.1	foldase	42	1123	14	32.6	**1.945**	1.721	0.913
ATQ33784.1	glycosyltransferase	58	389	10	35.6	1.909	1.725	**1.614**
ATQ32443.1+	oxidoreductase	56	321	12	32.4	**1.832**	**1.421**	1.694
ATQ34616.1+	spermidine/putrescine ABC transporter ATP-binding protein	10	13	2	24	**1.864**	**1.747**	1.436

ATQ35029.1+	class I SAM-dependent methyltransferase	8	34	2	37.2	**1.925**	**1.886**	1.698
ATQ32679.1+	class I SAM-dependent methyltransferase	44	52	7	22.1	1.631	**2.162**	**2.920**
ATQ34515.1+	NAD(P)-dependent oxidoreductase	19	22	3	26.2	1.852	**2.089**	**2.651**
ATQ34242.1+	hydrolase	18	41	4	29.7	**1.995**	**1.999**	**1.494**
ATQ34083.1	alpha/beta hydrolase	51	277	9	31.7	**1.787**	**1.964**	**1.874**
ATQ33638.1	4-hydroxy-tetrahydrodipicolinate reductase	39	95	5	28.5	**1.756**	**2.420**	2.114
ATQ34741.1	alpha/beta hydrolase	35	122	8	35.5	**1.955**	**2.159**	1.667
ATQ33823.1+	iron-sulfur cluster biosynthesis family protein	40	34	5	14.5	**1.675**	**1.924**	2.411
ATQ33870.1+	TrkA family potassium uptake protein	9	43	3	24.3	1.535	**1.789**	**1.654**
ATQ34485.1+	AraC family transcriptional regulator	19	51	3	29.6	**1.713**	**1.519**	1.316
ATQ32747.1+	excinuclease ABC subunit UvrA	67	2270	52	105	**1.231**	1.249	**1.452**
ATQ34034.1+	uracil phosphoribosyltransferase	30	266	7	23	**1.367**	**1.267**	1.331
ATQ33889.1	penicillin-binding protein	15	48	9	77.2	**1.521**	**1.461**	1.246
ATQ34018.1	rod shape-determining protein RodA	27	114	6	44.5	**1.435**	**1.530**	1.373
ATQ32925.1	LytR family transcriptional regulator	54	777	17	37.7	**1.782**	**1.538**	1.303
ATQ32671.1	hydroxyacid dehydrogenase	7	9	2	36.3	**1.340**	1.176	**0.793**

ATQ32249.1	magnesium-transporting ATPase	51	1081	28	99.6	**1.440**	1.115	1.222
ATQ33108.1	aquaporin family protein	9	406	3	25.4	**1.598**	1.303	**1.496**
ATQ32636.1	PTS mannose family transporter subunit IID	65	2731	18	34.3	1.470	1.466	**1.309**
ATQ33426.1	osmoprotectant ABC transporter substrate-binding protein	53	520	14	34.8	1.288	**1.881**	0.531
ATQ32635.1	PTS mannose/fructose/sorbose transporter subunit IIC	38	1285	7	27.4	1.503	1.637	**1.857**
ATQ33843.1	FtsW/RodA/SpoVE family cell cycle protein	6	56	2	41.9	1.376	**1.721**	**1.650**
ATQ33987.1	rod shape-determining protein MreC	59	192	11	30.1	1.157	1.179	**1.770**
ATQ33803.1⁺	ribonuclease Z	68	724	18	34.2	**1.655**	1.636	1.052
ATQ32656.1⁺	DNA repair protein RadA	11	3	3	50	**1.688**	**1.743**	2.802
ATQ32530.1⁺	LemA family protein	72	1266	17	20.8	**1.739**	0.535	1.282
ATQ33279.1⁺	bifunctional 3,4-dihydroxy-2-butanone-4-phosphate synthase/GTP cyclohydrolase II	76	1233	24	43.6	**1.762**	1.342	1.142
ATQ33167.1⁺	glycosyltransferase	54	236	16	39.6	**1.251**	1.440	1.200
ATQ34573.1⁺	2,3-bisphosphoglycerate-dependent phosphoglycerate mutase	74	1301	15	26.1	**1.276**	1.937	1.256
ATQ34215.1⁺	dihydroorotase	71	664	14	45.4	**1.288**	1.634	2.135
ATQ33596.1⁺	CDP-glycerol--poly(glycerophosphate) glycerophosphotransferase	54	1023	30	72.6	**1.339**	1.153	1.003

ATQ33853.1+	branched-chain alpha-keto acid dehydrogenase subunit E2	50	473	16	46.6	**1.375**	1.255	1.038
ATQ33278.1+	riboflavin synthase	37	296	6	21.5	**1.386**	**1.289**	1.227
ATQ35161.1+	DUF1906 domain-containing protein (plasmid)	7	30	4	84.6	**1.394**	1.218	**1.695**
ATQ34892.1+	FAD-dependent oxidoreductase	71	519	20	44.3	0.920	**1.701**	1.053
ATQ34028.1+	ATP synthase subunit delta	77	534	14	20	1.670	1.647	**1.891**
ATQ33609.1+	DNA topoisomerase IV subunit A	62	1966	40	91.6	1.506	1.017	**1.541**
ATQ34658.1+	guanosine monophosphate reductase	17	108	4	35.4	1.330	**1.194**	**1.479**
ATQ34815.1+	galactokinase	60	1484	18	42.6	0.856	**1.200**	0.907
ATQ34730.1+	linear amide C-N hydrolase	59	62	9	36.2	1.053	**1.200**	**2.836**
Proteins with a decrease in abundance								
ATQ33988.1	rod shape-determining protein MreB1	66	1325	20	35.1	**0.263**	**0.141**	0.287
ATQ33447.1	signal recognition particle-docking protein FtsY	31	58	9	53.6	**0.607**	**0.306**	**0.507**
ATQ34819.1	PTS sugar transporter subunit IIA	42	801	16	71	**0.589**	0.327	0.500
ATQ32657.1	PIN/TRAM domain-containing protein	39	341	12	44.3	0.921	**0.755**	1.098
ATQ32753.1	YvcK family protein	14	18	3	36.6	0.843	**0.493**	**0.597**

ATQ32758.1+	RNA polymerase factor sigma-54	4	5	2	51.3	**0.260**	**0.087**	**0.173**
ATQ33109.1+	glycosyl transferase	42	280	17	45.7	**0.496**	**0.164**	0.380
ATQ32763.1+	enolase	81	8509	47	48	1.142	**0.370**	0.943
ATQ33984.1+	septum site-determining protein MinD	51	425	13	29.1	0.746	**0.447**	0.663
ATQ33655.1+	pyruvate kinase	90	5755	55	62.8	0.753	**0.514**	1.263
ATQ33348.1+	threonine--tRNA ligase	61	1829	30	73.8	0.998	**0.640**	1.007
ATQ32912.1+	asparagine synthetase B	71	862	27	73.1	0.583	0.321	**0.459**
ATQ32970.1+	DNA-directed RNA polymerase subunit alpha	75	1025	19	34.8	0.991	0.709	**0.625**
ATQ34070.1+	glucose-6-phosphate isomerase	68	2289	27	49.8	0.981	1.226	**0.700**

* Values highlighted in red are not significant. + Proteins identified as cytosolic proteins.

7.7 Selected proteins identified in the cytosolic fraction with the most statistically significant change in abundance

Table 16: Cytosolic proteins selected for in depth analysis and discussion

Accession #	Protein	Sequence coverage	PSMs	Unique peptides	MW (kDa)	Fold change*		
						T_{15}	T_{30}	T_{60}
Proteins with an increase in abundance								
ATQ33363.1	ribosome silencing factor	54	58	5	13	**10.952**	**7.809**	**9.408**
ATQ33208.1+	large conductance mechanosensitive channel protein MscL	58	57	5	14	**5.298**	**4.923**	**6.952**
ATQ33941.1	DUF948 domain-containing protein	39	53	3	15	**4.232**	**2.913**	3.812
ATQ33360.1	ribosome assembly RNA-binding protein YhbY	63	72	5	11.7	**3.670**	**4.743**	5.475
ATQ34034.1	uracil phosphoribosyltransferase	54	462	9	23	**3.469**	**3.567**	**4.326**
ATQ33118.1	hypothetical protein CS400_05310	25	12	4	24.3	**3.137**	**2.657**	2.781
ATQ32729.1	phosphate transport system regulatory protein PhoU	15	44	3	25.5	1.899	**2.872**	**2.729**

ATQ33361.1	nicotinate-nicotinamide nucleotide adenylyltransferase	45	101	5	24	**2.818**	**2.297**	**1.770**
ATQ34857.1	LacI family transcriptional regulator	10	6	2	35	**2.674**	**3.168**	3.247
ATQ33366.1	DNA-binding protein	36	55	4	20.7	**2.504**	**2.123**	**2.273**
ATQ34605.1+	amino acid ABC transporter permease	17	32	4	26.1	**2.412**	**2.627**	**2.406**
ATQ33378.1	RNA methyltransferase	34	17	5	27.6	**2.201**	**1.998**	1.809
ATQ34515.1	NAD(P)-dependent oxidoreductase	29	53	5	26.2	**2.200**	**2.475**	**2.108**
ATQ33908.1	GTP pyrophosphokinase	47	61	8	25.9	**2.168**	**2.209**	**2.124**
ATQ32669.1	50S ribosomal protein L10	38	33	5	17.9	**2.116**	**2.127**	3.069
ATQ33416.1	transcription antitermination factor NusB	36	103	4	15.7	**2.106**	**2.614**	3.488
ATQ33291.1	foldase	25	154	6	32.6	1.501	**2.061**	**2.190**
ATQ33924.1	metallophosphatase	22	26	3	23.4	**1.902**	**2.049**	**1.847**
ATQ32748.1	S-ribosylhomocysteine lyase	87	989	13	17.4	0.856	1.674	**1.896**
ATQ32782.1	UDP-N-acetylenolpyruvoylglucosamine reductase	39	254	8	32.3	**1.783**	**1.990**	**2.352**

ATQ32312.1	histidine phosphatase family protein	30	20	4	23.1	**1.599**	**1.922**	1.643
ATQ32425.1+	ABC transporter permease	13	21	3	31.7	**1.538**	**1.979**	**1.955**
Proteins with a decrease in abundance								
ATQ33988.1	rod shape-determining protein MreB1	29	59	7	35.1	**0.035**	**0.045**	**0.124**
ATQ34213.1	carbamoyl-phosphate synthase large subunit	45	365	30	115.6	**0.069**	**0.030**	0.493
ATQ32480.1	tryptophan--tRNA ligase	49	49	10	37.7	**0.115**	**0.016**	**0.044**
ATQ34764.1	glutamate decarboxylase	44	84	12	53.5	**0.126**	**0.262**	0.665
ATQ34023.1	UDP-N-acetylglucosamine 1-carboxyvinyltransferase	36	63	13	47.1	**0.143**	**0.073**	**0.053**
ATQ32895.1	aspartate--ammonia ligase	27	26	6	39	**0.181**	**0.070**	0.123
ATQ32332.1	dipeptidase	77	645	21	52.4	**0.181**	**0.351**	0.636
ATQ34982.1+	cell surface protein	5	340	2	39.6	**0.200**	**0.289**	0.535
ATQ32896.1	dipeptidase	76	1440	28	52.3	**0.210**	**0.339**	0.624
ATQ32763.1	enolase	85	8741	52	48	**0.222**	**0.313**	0.495
ATQ33984.1+	septum site-determining protein MinD	19	15	3	29.1	0.519	**0.223**	**0.500**

ATQ34852.1	6-phospho-beta-glucosidase	46	269	17	54.5	**0.230**	**0.172**	0.264
ATQ33512.1	dipeptidase	49	166	13	53.4	**0.232**	**0.362**	0.675
ATQ33762.1	DNA polymerase III subunit alpha	35	317	32	161.9	**0.237**	**0.223**	**0.343**
ATQ34874.1	phosphoketolase	15	170	7	89.7	**0.249**	**0.124**	**0.219**
ATQ32938.1	DNA-directed RNA polymerase subunit beta	76	6051	92	135.2	**0.270**	**0.317**	**0.434**
ATQ34093.1[+]	PTS N-acetylglucosamine transporter subunit IIABC	24	109	9	70.3	**0.273**	**0.436**	0.590
ATQ32518.1	serine--tRNA ligase	24	53	7	47.8	**0.279**	**0.301**	0.489
ATQ32719.1	protein translocase subunit SecA	33	187	20	89.5	0.237	**0.281**	**0.412**
ATQ33166.1	glycosyltransferase family 4 protein	45	112	10	44.2	**0.300**	**0.170**	**0.158**
ATQ34119.1	aspartate-semialdehyde dehydrogenase	74	346	17	38.3	**0.301**	**0.195**	**0.155**
ATQ33612.1	galactose mutarotase	39	131	7	32.6	**0.314**	**0.198**	**0.213**
ATQ33938.1	aminopeptidase P family protein	46	317	11	41.2	**0.320**	**0.220**	0.263
ATQ34815.1	galactokinase	71	5679	26	42.6	**0.337**	**0.266**	0.331
ATQ34158.1	pyruvate oxidase	57	195	20	64.2	**0.342**	**0.250**	0.350
ATQ33655.1	pyruvate kinase	97	14367	74	62.8	**0.346**	0.363	**0.316**
ATQ32881.1	peptidase	63	1686	41	93.9	0.280	**0.353**	**0.422**
ATQ34473.1	amidohydrolase	36	120	8	43	**0.370**	**0.528**	**0.566**
ATQ33991.1	valine--tRNA ligase	69	2568	55	101.5	0.296	**0.394**	**0.501**

ATQ32737.1	thioredoxin-disulfide reductase	52	200	13	33.4	**0.400**	**0.230**	**0.218**
ATQ34315.1	nucleoside hydrolase	54	436	10	35.3	**0.401**	**0.264**	**0.309**
ATQ33607.1	manganese-dependent inorganic pyrophosphatase	69	1283	16	33.6	**0.403**	**0.223**	**0.519**
ATQ33659.1	ATP-dependent chaperone ClpB	53	525	34	96.4	**0.403**	**0.202**	0.287
ATQ34042.1	mannose-6-phosphate isomerase, class I	64	634	15	35.9	**0.452**	**0.356**	**0.372**
ATQ33047.1	gfo/Idh/MocA family oxidoreductase	57	268	12	37.1	**0.490**	**0.402**	0.394
ATQ34657.1	adenylosuccinate synthetase	47	482	18	47.2	**0.496**	**0.316**	0.430
ATQ33228.1	excinuclease ABC subunit UvrA	41	407	22	82.4	**0.505**	**0.452**	0.614
ATQ32760.1	type I glyceraldehyde-3-phosphate dehydrogenase	98	17350	42	36.4	**0.546**	**0.480**	1.330
ATQ33634.1	thymidylate synthase	52	295	12	35.9	**0.590**	**0.304**	**0.298**
ATQ34214.1	carbamoyl-phosphate synthase small subunit	47	224	9	40	**0.675**	**0.516**	**0.519**

* Values highlighted in red are not significant. ⁺Proteins identified as membrane proteins.

7.8 Membrane proteins unique to the gel-free method

Table 17: Membrane proteins uniquely identified using the gel-free approach

Accession #	Protein	Sequence coverage %	PSMs	Unique Peptides	MW (kDa)
489736631	YlxR family protein	19	33	2	11.2
489741057	beta-hydroxyacyl-ACP dehydratase	47	46	5	15.1
489736758	cell division protein, SepF	11	22	2	15.3
499414817	helix-turn-helix domain-containing protein	24	39	4	15.5
489737349	F0F1 ATP synthase subunit epsilon	35	12	4	15.7
489739972	Asp23/Gls24 family envelope stress response protein	68	152	8	15.8
489736313	3-hydroxyacyl-ACP dehydratase FabZ	50	183	9	16
506305891	IS3 family transposase	14	3	2	16.1
489740348	peptide-methionine (R)-S-oxide reductase MsrB	13	6	2	16.3
489736143	6,7-dimethyl-8-ribityllumazine synthase	33	148	6	16.8
489736958	SsrA-binding protein SmpB	19	39	4	18.1
489741049	acyl-CoA thioesterase	13	4	2	18.6
489737344	F0F1 ATP synthase subunit B	32	9	4	18.7
489737959	LemA family protein	58	54	9	20.8
489737351	GNAT family *N*-acetyltransferase	16	17	3	21
489738074	NADP oxidoreductase	21	24	5	21

489737240	xanthine phosphoribosyltransferase	11	16	2	21.4
489738420	GTP cyclohydrolase I FolE	15	8	2	21.4
489736141	riboflavin synthase	32	167	5	21.5
489733725	ribosome-associated translation inhibitor RaiA	49	93	7	21.7
506305608	AAA family ATPase	31	25	4	22.1
489738043	signal peptidase I	64	116	11	23.3
502400138	helix-turn-helix domain-containing protein	40	92	9	23.9
499413507	ribose 5-phosphate isomerase A	14	20	2	23.9
489737439	2,3,4,5-tetrahydropyridine-2,6-dicarboxylate *N*-acetyltransferase	12	14	3	24.5
489736741	histidine phosphatase family protein	29	19	5	24.9
489736888	redox-sensing transcriptional repressor Rex	38	64	7	25.2
489740341	2-C-methyl-D-erythritol 4-phosphate cytidylyltransferase	13	12	4	25.9
489737958	class A sortase	20	28	4	26
489736755	DivIVA domain-containing protein	27	33	6	26.2
489739622	trehalose operon repressor	25	17	5	26.9
1274559665	enoyl-ACP reductase FabI	44	296	7	26.9
506305436	triose-phosphate isomerase	23	68	6	27
489737030	amino acid ABC transporter ATP-binding protein	49	54	9	27.4
489738482	ABC transporter ATP-binding protein	45	96	9	27.7
489738336	ParA family protein	20	12	4	27.8
489736908	phosphate ABC transporter ATP-binding protein	49	75	8	28

506306244	amino acid ABC transporter ATP-binding protein	49	134	12	28.1
502400226	peroxide stress protein YaaA	9	3	2	28.5
489738539	response regulator transcription factor	8	17	2	28.5
489737555	Cof-type HAD-IIB family hydrolase	13	19	3	28.7
489739528	glutamate 5-kinase	8	19	3	28.8
506305878	isoprenyl transferase	11	10	3	28.8
489737411	TIGR00282 family metallophosphoesterase	21	21	4	29.6
489737031	transporter substrate-binding domain-containing protein	42	115	12	29.9
506305421	acyl-ACP thioesterase	11	4	2	29.9
489736907	phosphate ABC transporter ATP-binding protein	28	103	8	30.4
489737935	pur operon repressor	23	52	6	30.5
489736597	SH3 domain-containing protein	18	9	4	30.9
499414036	acetyl-CoA carboxylase carboxyltransferase subunit beta	40	51	9	30.9
489737809	class II fructose-1,6-bisphosphate aldolase	64	490	17	30.9
506305962	amino acid ABC transporter substrate-binding protein	17	18	4	31.3
752446480	helix-turn-helix domain-containing protein	16	110	5	31.3
506305614	dTDP-4-dehydrorhamnose reductase	24	25	5	31.4
506305429	phosphate ABC transporter substrate-binding protein PstS family protein	38	325	9	31.5
489739912	TIGR00159 family protein	13	16	3	31.5

489740599	polysaccharide deacetylase family protein	20	15	4	31.6
499414043	SPFH domain-containing protein	10	9	2	31.7
506305278	helix-turn-helix transcriptional regulator	7	6	2	32
505192861	RluA family pseudouridine synthase	10	9	2	32.3
489736154	peptidylprolyl isomerase	64	522	19	32.6
506305989	NlpC/P60 family protein	16	11	5	32.9
489736316	ACP *S*-malonyltransferase	25	24	4	33.2
489739401	metal ABC transporter substrate-binding protein	13	8	3	33.9
505192486	KH domain-containing protein	36	15	6	34.2
489736584	GTPase Era	19	64	6	34.3
489738592	polyphosphate kinase 2 family protein	19	22	5	34.5
489737347	F0F1 ATP synthase subunit gamma	39	235	14	34.5
506305739	osmoprotectant ABC transporter substrate-binding protein	32	55	8	34.8
489740612	ABC transporter substrate-binding protein	25	13	7	35
489741866	ribose-phosphate diphosphokinase	18	13	5	35
489738397	GMP reductase	21	25	6	35.4
489736657	glycosyltransferase family 2 protein	23	52	6	35.6
489739752	ribose-phosphate diphosphokinase	39	217	11	35.9
506305538	Gfo/Idh/MocA family oxidoreductase	36	95	8	35.9
1024267468	catabolite control protein A	21	35	6	36.3

506305624	ATP-binding cassette domain-containing protein	27	42	6	36.6
489740349	LysR family transcriptional regulator	8	15	2	36.8
489736646	D-2-hydroxyacid dehydrogenase	61	762	25	37.2
506305747	phosphate acyltransferase PlsX	35	36	10	37.4
489739869	PhnD/SsuA/transferrin family substrate-binding protein	44	44	12	37.5
489737330	branched-chain amino acid aminotransferase	16	11	4	37.9
499414599	cell surface protein	32	44	6	38
506306332	LacI family DNA-binding transcriptional regulator	10	7	3	38.2
1140766229	ABC transporter substrate-binding protein	12	8	3	38.5
489739152	ABC transporter ATP-binding protein	36	110	14	39.7
489740188	membrane protein	29	72	10	40.1
489737409	recombinase RecA	36	81	10	40.6
489737826	ABC transporter ATP-binding protein	21	84	8	40.8
1248140241	peptide chain release factor 2	8	4	2	42
506305760	beta-ketoacyl-ACP synthase II	25	58	7	42.4
506305541	CamS family sex pheromone protein	51	387	17	42.6
506305884	hydroxymethylglutaryl-CoA synthase	7	2	2	42.7
489739828	phage major capsid protein	34	142	11	42.8
489737242	ATP-grasp domain-containing protein	38	81	9	42.8
489736950	phosphoglycerate kinase	66	571	27	42.8
506305283	acetate kinase	29	12	8	42.9
505453850	amidohydrolase	12	6	3	43

489737565	PDZ domain-containing protein	67	427	24	43.1
489740306	class I SAM-dependent RNA methyltransferase	13	9	5	43.1
489741910	serine hydrolase	45	214	15	43.3
489740295	pyridoxal phosphate-dependent aminotransferase	8	24	3	43.7
489737791	NAD(P)/FAD-dependent oxidoreductase	25	138	10	43.8
489737341	serine hydroxymethyltransferase	37	113	12	44.4
489740246	betaine/proline/choline family ABC transporter ATP-binding protein	65	307	23	44.4
489736217	endolytic transglycosylase MltG	68	519	32	44.7
489738456	GNAT family *N*-acetyltransferase	10	11	4	44.7
489740374	peptidase T	29	42	8	45.1
489738314	class I SAM-dependent methyltransferase	25	86	8	45.3
489742291	extracellular solute-binding protein	67	384	31	45.6
506305597	glycosyltransferase	25	58	10	45.7
489739137	NAD(P)/FAD-dependent oxidoreductase	34	98	11	47.6
489739900	phosphopyruvate hydratase	69	3067	36	48
506305994	NADH peroxidase	44	496	15	48.3
489736609	D-alanyl-lipoteichoic acid biosynthesis protein DltD	56	328	23	48.6
499414765	GHKL domain-containing protein	8	67	4	48.7
489739606	Na+/H+ antiporter NhaC	5	14	2	48.9
489738395	adenylosuccinate lyase	7	32	3	49
489741592	trigger factor	26	70	13	49.4
489736727	dihydrolipoyl dehydrogenase	19	46	9	49.9

489742117	hypothetical protein	24	34	7	50.1
489739850	C1 family peptidase	25	50	8	50.2
506305572	phage major capsid protein	20	56	8	50.4
489737348	F0F1 ATP synthase subunit beta	66	1800	31	50.8
489741198	dipeptidase PepV	11	17	3	50.8
489737982	L,D-transpeptidase family protein	13	17	5	51.1
489740644	HlyC/CorC family transporter	24	23	8	51.7
489737102	C69 family dipeptidase	37	301	16	52.3
489741119	NADP-dependent phosphogluconate dehydrogenase	39	203	17	52.9
506305826	S41 family peptidase	47	222	19	53.2
506306333	UDP-glucose--hexose-1-phosphate uridylyltransferase	35	214	12	54.3
489737346	F0F1 ATP synthase subunit alpha	45	1337	27	54.6
506306269	cardiolipin synthase	21	62	7	55.7
489737845	ABC transporter permease/substrate-binding protein	19	28	8	55.8
489740418	D-alanine--poly(phosphoribitol) ligase subunit DltA	5	39	2	56.1
489737835	multicopper oxidase domain-containing protein	14	31	3	56.8
506306422	cell surface protein	15	22	5	56.8
489739960	glutamine-hydrolysing GMP synthase	23	95	11	57.4
489739138	peptide chain release factor 3	29	78	12	59.5
489737947	CTP synthase	62	541	30	59.7
506306104	ATP-binding cassette domain-containing protein	11	25	5	60.2

505193008	peptide ABC transporter substrate-binding protein	68	1169	40	60.3
506305746	DAK2 domain-containing protein	30	80	11	60.7
489739896	peptide ABC transporter substrate-binding protein	60	974	40	61
489740010	acetolactate synthase AlsS	26	149	13	61.2
506306154	ABC transporter ATP-binding protein	20	37	10	62.8
489742487	phosphoenolpyruvate--protein phosphotransferase	24	61	10	63.1
489742025	phospho-sugar mutase	14	32	7	63.5
489737382	septation ring formation regulator EzrA	7	7	3	64.5
506306047	FtsX-like permease family protein	8	11	4	66.2
489736892	APC family permease	12	74	9	67.2
489736682	PTS fructose transporter subunit IIC	20	263	15	68.5
489737327	ABC transporter ATP-binding protein	9	9	4	70
506306297	copper-translocating P-type ATPase	5	11	3	72.2
506305812	ribitolphosphotransferase	34	126	19	72.6
654308906	Stk1 family PASTA domain-containing Ser/Thr kinase	17	28	8	74.6
489736765	PASTA domain-containing protein	12	18	8	77.2
489740138	LTA synthase family protein	31	230	23	79
503120561	class 1b ribonucleoside-diphosphate reductase subunit alpha	13	57	8	82.1
506306023	cell wall hydrolase	3	8	2	82.1

506305660	excinuclease ABC subunit UvrA	15	40	9	82.4
506306336	alpha-galactosidase	4	2	2	83.7
489736601	bifunctional (p)ppGpp synthetase/guanosine-3',5'-bis(diphosphate) 3'-pyrophosphohydrolase	3	12	2	86.2
489739958	AAA family ATPase	12	69	9	87.9
499414403	phosphoketolase family protein	6	18	5	88.7
506305457	Xaa-Pro dipeptidyl-peptidase	13	14	7	91.5
506305386	cation-translocating P-type ATPase	35	153	24	95.2
506305249	cation-transporting P-type ATPase	37	125	19	99.6
506305955	YfhO family protein	16	71	13	114.7
506306039	carbamoyl-phosphate synthase large subunit	16	41	11	115.6
506306144	LPXTG cell wall anchor domain-containing protein	3	13	3	118.3
506305312	MMPL family transporter	4	21	4	137.7

7.9 Proteins that lack an assigned function

Table 18: Proteins that lack an assigned function beyond that identified by PD

Accession #	PD generated protein ID	Sequence coverage	PSMs	Unique peptides	MW (kDa)	Fold change		
						T_{15}	T_{30}	T_{60}
Membrane proteins								
ATQ34649.1	Zinc-dependent peptidase	16	37	3	25.2	**2.335**	**3.262**	2.694
ATQ33505.1	DUF805 domain-containing protein	24	252	3	14.2	**2.143**	**1.788**	**1.712**
ATQ34741.1	alpha/beta hydrolase	35	122	8	35.5	**1.955**	**2.159**	1.667
ATQ34083.1	alpha/beta hydrolase	51	277	9	31.7	**1.787**	**1.964**	**1.874**
ATQ33098.1	alpha-beta hydrolase	21	47	4	32.7	**2.063**	**2.250**	1.829
Cytosolic proteins								
ATQ33366.1	DNA-binding protein	36	55	4	20.7	**2.504**	**2.123**	**2.273**
ATQ34605.1	L-cysteine ABC transporter permease	17	32	4	26.1	**2.412**	**2.627**	**2.406**
ATQ34515.1	SDR-family NAD(P)-dependent oxidoreductase	29	53	5	26.2	**2.200**	**2.475**	**2.108**
ATQ33924.1	Metallo-phosphoesterase	22	26	3	23.4	**1.902**	**2.049**	**1.847**

7.10 Propidium iodide (PI) fluorescence microscopy

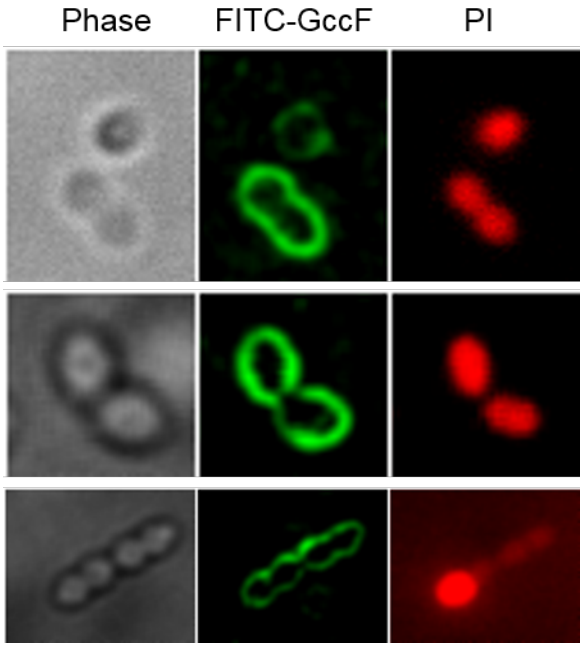

Figure 25: Localisation of GccF at the cell membrane of *Lb. plantarum* ATCC 8014 cells. *Lb. plantarum* ATCC 8014 cells treated with fluorescein isothiocyanate (FITC) labelled GccF (centre column; green). The nucleus was stained with propidium iodide (right column; red) showing the cell membrane to be permeable. Interestingly, the cells were still viable and could be revived by the addition of free-GlcNAc. Image provided by Associate Professor Gillian E. Norris as a personal communication (unpublished data).

7.11 Microscopy images

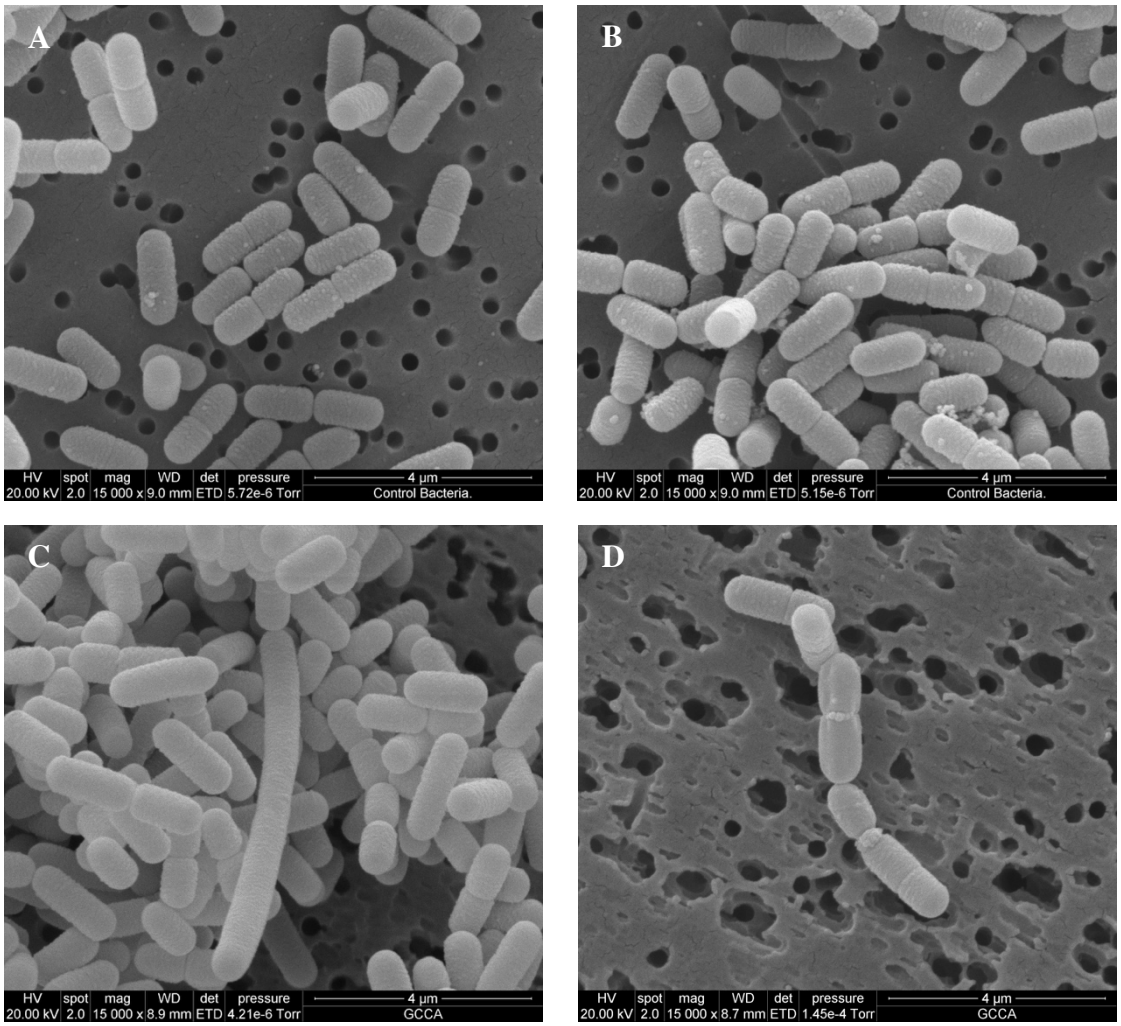

Figure 26: Comparison of GccF-treated and untreated *Lb. plantarum* ATCC 8014 cells. Microscopy images showing changes in cell morphology between control and GccF-treated *Lb. plantarum* ATCC 8014 cells. **(A and B)** Control *Lb. plantarum* ATCC 8014 cells showing normal growth morphology with obvious septum formation and complete cell division. **(C and D)** GccF-treated *Lb. plantarum* ATCC 8014 cells showing cell elongation (C) and chains of unseparated daughter cells (D). Images provided by Associate Professor Gillian E. Norris as a person communication (unpublished data).

7.12 Gene ontology (GO) terms

Table 19: BLAST2GO [122] **analysis of the proteins with the most significant change in abundance**

Accession #	Protein description	GO IDs	GO terms
		Membrane proteins	
ATQ34093.1	PTS GlcNAc transporter, **PTS18CBA**	P: GO:0009401 P: GO:0016310 P: GO:0034219 P: GO:1901264 F: GO:0008982 F: GO:0015572 F: GO:0016301 F: GO:0103111 C: GO:0005886 C: GO:0016021 C: GO:0019866	P: PEP-dependent sugar PTS system; P: phosphorylation; P: carbohydrate transmembrane transport; P: carbohydrate derivative transport; F: protein-phospho-His-sugar phosphotransferase activity; F: GlcNAc transmembrane transporter activity; F: kinase activity; F: D-glucosamine PTS permease activity; C: plasma membrane; C: integral component of membrane; C: organelle inner membrane
ATQ33843.1	FtsW/RodA/SpoVE family cell cycle protein, **FtsW**	P: GO:0051301 F: GO:0008955 C: GO:0016021	P: cell division; F: peptidoglycan glycosyltransferase activity; C: integral component of membrane
ATQ34018.1	Rod shape-determining protein, **RodA**	P: GO:0008360 P: GO:0051301 C: GO:0016021	P: regulation of cell shape; P: cell division; C: integral component of membrane
ATQ33208.1	Large-conductance mechanosensitive channel protein, **MscL**	P: GO:0034220 F: GO:0008381 C: GO:0005887	P: ion transmembrane transport; F: mechanosensitive ion channel activity; C: integral component of plasma mem.
ATQ33889.1	PASTA domain-containing protein, **PBP2b**	F: GO:0008658 C: GO:0016021	F: penicillin binding; C: integral component of membrane
ATQ32925.1	**LCP** family protein	C: GO:0016021	C: integral component of membrane
ATQ33987.1	Rod shape-determining protein, **MreC**	P: GO:0008360	P: regulation of cell shape

Accession #	Protein description	GO IDs	GO terms
		Membrane proteins	
ATQ33108.1	Aquaporin family protein, **GlpF4**	P: GO:0055085 F: GO:0015267 C: GO:0005886 C: GO:0016021	P: transmembrane transport; F: channel activity; C: plasma membrane; C: integral component of membrane
ATQ33376.1	Membrane protein insertase, **YidC**	P: GO:0015031 P: GO:0090150 F: GO:0032977 C: GO:0005886 C: GO:0016021	P: protein transport; P: establishment of protein localisation to membrane; F: membrane insertase activity; C: plasma membrane; C: integral component of membrane
ATQ32187.1	Two-component system regulatory protein, **YycI**	C: GO:0016021	C: integral component of membrane
ATQ32425.1	ABC transporter permease, **TagG**	P: GO:0055085 C: GO:0043190	P: transmembrane transport; C: ABC transporter complex
		Cytosolic proteins	
ATQ33638.1	4-hydroxytetrahydro-dipicolinate reductase, **DapB**	P: GO:0009089 P: GO:0019877 F: GO:0008839 F: GO:0016726 F: GO:0050661 F: GO: 0051287 C: GO:0005737	P: lysine biosynthetic process *via* diaminopimelate; P: diaminopimelate biosynthetic process; F: 4-hydroxy-tetrahydrodipicolinate reductase; F: oxidoreductase activity, acting on CH or CH_2 groups, NAD or NADP as acceptor; F: NADP binding; F: NAD binding; C: cytoplasm
ATQ34034.1	Uracil phosphoribosyl-transferase, **Upp**	P: GO:0006223 P: GO:0009116 P: GO:0044206 F: GO:0000287 F: GO:0004845 F: GO:0005525	P: uracil salvage; P: nucleoside metabolic process; P: UMP salvage; F: magnesium ion binding; F: uracil phosphoribosyl-transferase activity; F: GTP binding
ATQ33988.1	Rod shape-determining protein, **MreB1**	P: GO:0008360 F: GO:0005524 C: GO:0005737	P: regulation of cell shape; F: ATP binding; C: cytoplasm

Accession #	Protein description	GO IDs	GO terms
		Cytosolic proteins	
ATQ33447.1	Signal recognition particle-docking protein, **FtsY**	P: GO:0006614 F: GO:0005525	P: signal recognition particle-dependent co-translational protein targeting to membrane; F: GTP binding
ATQ32657.1	PIN/TRAM domain-containing protein, **PilT**	No GO ID	No GO terms
ATQ33363.1	Ribosome silencing factor, **RsfS**	P: GO:0008033 P: GO:0017148 P: GO:0042256 P: GO:0090071 F: GO:0046872 C: GO:0005737	P: tRNA processing; P: negative regulation of translation; P: mature ribosome assembly; P: negative regulation of ribosome biogenesis; F: metal ion binding; C: cytoplasm
ATQ32782.1	UDP-*N*-acetylmuramate dehydrogenase, **MurB**	P: GO:0007049 P: GO:0008360 P: GO:0009252 P: GO:0051301 P: GO:0071555 F: GO:0008762 F: GO:0071949 C: GO:0005737	P: cell cycle; P: regulation of cell shape; P: peptidoglycan biosynthetic process; P: cell division; P: cell wall organisation; F: UDP-*N*-acetylmuramate dehydrogenase activity; F: FAD binding; C: cytoplasm
ATQ34023.1	UDP-*N*-acetylglucosamine 1-carboxyvinyltransferase, **MurA2**	P: GO:0007049 P: GO:0008360 P: GO:0009252 P: GO:0019277 P: GO:0051301 P: GO:0071555 F: GO:0008760 C: GO:0005737	P: cell cycle; P: regulation of cell shape; P: peptidoglycan biosynthetic process; P: UPD-*N*-acetylgalactosamine biosynthetic process; P: cell division; P: cell wall organisation; F: UDP-*N*-acetylglucosamine 1-carboxyvinyl-transferase activity; C: cytoplasm
ATQ33166.1	Glycosyltransferase family 4 protein, **UgtP**	F: GO:0016757	F: glycosyltransferase activity

Accession #	Protein description	GO IDs	GO terms
		Cytosolic proteins	
ATQ32737.1	Thioredoxin-disulfide reductase, **TrxB1**	P: GO:0019430 F: GO:0004791 C: GO:0005737	P: removal of superoxide radicals; F: thioredoxin-disulfide reductase activity; C: cytoplasm
ATQ32426.1	ABC transporter ATP-binding protein, **TagH**	P: GO:0015777 P: GO:0055085 F: GO:0005524 F: GO:0015438 F: GO:0016787 C: GO:0005886 C: GO:0016021	P: teichoic acid transport; P: transmembrane transport; F: ATP binding; F: ABC-type teichoic acid transporter activity; F: hydrolase activity; C: plasma membrane; C: integral component of membrane
ATQ33714.1	PhoH family protein, **PhoH**	F: GO:0005524	F: ATP-binding

Abbreviations: GO, gene ontology; **P**, biological process; **F**, molecular function; **C**, cellular component; **GlcNAc**, *N*-acetylglucosamine; **PTS**, phosphotransferase system; **PEP**, phosphoenolpyruvate; **His**, histidine; **mem**, membrane; **PASTA**, penicillin-binding and Ser/Thr kinase-associated; **ATP**, adenosine triphosphate; **UMP**, uridine monophosphate; **GTP**, guanosine triphosphate; **ABC**, ATP-binding cassette; **PIN**, PilT N-terminus; **TRAM**, TRM2 and MiaB.

7.13 Raw proteomic data

Link 1: Membrane data

file:///Users/user/Documents/MembraneOnly_ProteomicData_TStephens2021.xlsx

Link 2: Cytosol data

file:///Users/user/Documents/CytosolOnly_ProteomicData_TStephens2021.xlsx